Determinants of global color-based attention: insights from electromagnetic brain recordings in humans

Dissertation

zur Erlangung des akademischen Grades

doctor rerum naturalium
(Dr. rer. nat.)

genehmigt durch die Fakultät für Naturwissenschaften
der Otto-von-Guericke-Universität Magdeburg

von   Mandy Viktoria Bartsch, M.Sc.

geb. am 13.11.1985 in Lübeck

Gutachter: Prof. Dr. med. Jens-Max Hopf

                       Prof. em. Steven A. Hillyard, Ph.D.

eingereicht am: 15.12.2014

verteidigt am: 24.11.2015

I dedicate this work to my parents Alfred and Sabine Bartsch.

In memory of my grandmother Erika Proeber and

my grandaunts Ruth Bartsch and Christel Bork.

Ob tuum fatum vola, pectoris sequere sonum.

Si ipsum te superes demum solutus eris.

Volo, accipiter, volo!

(from 'Duos Accipitres' by M.V. Bartsch)

"Exploration of the human brain is of the utmost intellectual interest: the whole humanity depends on our minds."

(M. Hämäläinen et al., 1993, p. 415)

Acknowledgements

First and foremost I would like to thank my supervisor *Jens-Max Hopf*, who gave me the opportunity to do incredible interesting research on feature-based attention (although it was supposed to explicitly not end up with color) and who spent an outrageous amount of time on the discussion of the data (from data acquisition to data analysis to rather philosophical questions concerning the data interpretation). Furthermore, this thesis would not have been possible without...

> ➢ ... the help of *the MEG team* (Special thanks belongs to *Steffi Bachmann* for her invaluable help with participant recruitment and data aquisition and to *Stefan Knape* who was always there to revive the MEG or otherwise rescue my data).

> ➢ ... technical support from *Michael Scholz* (who provided and patiently explained (multiple times) a bunch of EEG/MEG analysis tools), *Hans-Jürgen Warmbold* (who kept the computers alive, spent nights on my broken notebook and helped to arrange the installation of missing hard and software) and *Mircea Ariel Schönfeld* (who funded important parts of my technical equipment and who should also be mentioned for fruitful research discussions especially including poster presentations).

> ➢ ... my friendly and helpful colleagues. Special thanks goes to "Do it in Matlab" *Hendrik Strumpf* who helped me a lot with the initial stimulus design and all kinds of Matlab-related scripts, to *Anja Rautzenberg* who spent countless hours in front of my screen discussing artifact rejection, data analysis, ERP/ERMF waveforms, and life in general and to *Sarah Donohue* who spent an immense amount of time and effort on the discussion of my data and proofreading of my manuscript including this sentence.

Besides my friendly colleagues, an essential amount of mental support was provided by my family (my parents *Sabine and Alfred Bartsch* and my brother *Philipp Bartsch*), my partner *Marcel Genzmehr* and my horse *Franziska*. They supported me all the time regardless of the outcome and almost without asking me when I'm going to finish (at least Franziska did not). My parents as well as my partner deserve my deepest gratitude as they suffered the most.

Table of contents

List of tables

List of figures

List of abbreviations

ACC	Anterior Cingulate Cortex
BOLD	Blood Oxygenation Level–Dependent (response)
EEG	ElectroEncephaloGram/Graphy
EOG	ElectroOculoGram
EPSP	Excitatory PostSynaptic Potential
ERMF	Event-Related Magnetic Field
ERP	Event-Related Potential
fMRI	functional Magnetic Resonance Imaging
FOA	Focus Of Attention
FSGM	Feature-Similarity Gain Model
GCBA	Global Color-Based Attention
GFBA	Global Feature-Based Attention
IPSP	Inhibitory PostSynaptic Potential
LOC	Lateral Occipital Complex
LVF	Left Visual Field
MEG	MagnetoEncephaloGram/Graphy
MNI	Montreal Neurological Institute
MST	Medial Superior Temporal (visual area)
MT	Middle Temporal (visual area)
PET	Positron Emission Tomography
PSP	PostSynaptic Potential
rANOVA	repeated measures ANalysis Of VAriance
RSVP	Rapid Serial Visual Presentation
RF	Receptive Field
RVF	Right Visual Field
SEM	Standard Error of the Mean
SN	Selection Negativity
SOA	Stimulus-Onset Asynchrony
SP	Selection Positivity
SQUID	Superconducting Quantum Interference Device
SSVEP	Steady-State Visual Evoked Potential
VO-1/2	two visual hemifield maps in the Ventral Occipital cortex cluster
pT	picoTesla

Summary

It is well-known that attention to features is not limited to the spatial focus of attention (FOA), but can operate throughout the whole visual field in a spatially global way. For example, attending to the color red somewhere in a visual scene can cause the selection of red all over the visual field even at locations that are completely unattended. While many studies have demonstrated this kind of global feature-based attention (GFBA), there is also a number of experiments, in which attention to features remained confined to the spatial FOA. This raises the question, which factors actually render feature-based attention to work in a spatially global manner.

The following work addresses this issue and will challenge a recent hypothesis according to which feature competition in the FOA is crucial for effects of GFBA to arise. To this end, a series of experiments combining electro- and magnetoencephalographic brain recordings was conducted in human observers focusing onto the determinants of global color-based attention (GCBA). To assess effects of GCBA, the subjects performed a color/shape discrimination of a target object in the in the left visual field, while task-irrelevant color probes were simultaneously presented outside the FOA in the unattended right visual field. The brain response to the unattended probes (event-related potentials/ event-related magnetic fields) could then be analyzed as a function of whether the probe's color matched or did not match the currently-attended target color. The first out of five experiments served to characterize the electromagnetic correlates of GCBA under conditions of color competition in the FOA. It revealed a sequence of modulations in ventral extrastriate visual cortex propagating through the cortical hierarchy from higher to lower tier areas. Specifically, an early maximum at 200ms arising in more anterior-lateral occipito-temporal regions was found to be followed by a later maximum at 280ms originating in more posterior-medial early visual areas. The second experiment ruled out the possibility that low level stimulus differences accounted for the observed effects. The third experiment finally demonstrated that the modulation sequence of GCBA arises without a competing color in the FOA. A fourth experiment showed that early parts of GCBA appear even for task-relevant colors that are not contained in the target object and hence not even present in the FOA. A fifth experiment demonstrated that both early and late effects of GCBA were eliminated when the subjects performed a simple onset-detection of the target without selecting its color or shape.

The reported experiments together suggest that early parts of GCBA index an internal template of task-relevant colors ('color template matching') while later parts reflect selection processes related to target discrimination ('discrimination matching'). Importantly, GCBA did not require color competition in the FOA, but rather depended on the active discrimination of the colored target.

Zusammenfassung

Determinanten globaler farbbasierter Aufmerksamkeit: Einblicke mittels elektromagnetischer Ableitungen am Menschen

Es ist bekannt, dass merkmalsbasierte Aufmerksamkeit nicht auf den räumlichen Aufmerksamkeitsfokus beschränkt ist, sondern auf dem gesamten visuellen Feld agieren kann. Infolgedessen kann das Richten der Aufmerksamkeit auf die Farbe Rot irgendwo innerhalb einer visuellen Szenerie zu einer Selektion von Rot im gesamten visuellen Feld führen, d.h. auch an Orten, die vollkommen unbeachtet sind. Während diese Art der globalen Merkmalsselektion ('global feature based attention', GFBA) bislang in vielen Studien dokumentiert wurde, sind auch einige Experimente bekannt, in denen die merkmalsbasierte Aufmerksamkeit auf den räumlichen Aufmerksamkeitsfokus begrenzt blieb. Dies führt zu der Frage, welche Faktoren tatsächlich zu einem räumlich ungebundenen globalen Agieren der Merkmalsselektion führen.

Die vorliegende Arbeit versucht, diese Faktoren zu identifizieren, wobei sie insbesondere eine kürzlich vorgeschlagene Hypothese überprüft, nach der Merkmalskompetition innerhalb des räumlichen Aufmerksamkeitsfokus für das Auftreten von Effekten der GFBA ist. Zu diesem Zweck wurde eine Reihe von elektro- und magnetoenzephalographischen Hirn-Ableitungen an Menschen durchgeführt, um Determinaten globaler farbbasierter Aufmerksamkeitsselektion ('global color-based attention', GCBA) zu identifizieren. Um Effekte der GCBA untersuchen zu können, wurde ein experimentelles Design entwickelt, bei dem die Versuchspersonen eine Farb-/Form Diskriminationsaufgabe im linken visuellen Feld (LVF) durchführten, während zeitgleich im unbeachteten rechten visuellen Feld (RVF) aufgabenirrelevante Farbstimuli (sog. 'probes') präsentiert wurden. Die Analyse der durch die unbeachteten 'probes' ausgelösten Hirnantworten (ereigniskorrelierte Potentiale/ ereigniskorrelierte magnetische Felder) ermöglichte es, das räumlich globale Wirken der Farbselektion zu untersuchen. Hierzu wurden die Hirnantworten zu 'probes' einer aufgabenrelevanten Farbe mit den Hirnantworten zu 'probes' einer aufgabenirrelevanten Farbe verglichen.

Das erste von insgesamt fünf Experimenten diente dazu, die elektromagnetischen Korrelate der GCBA unter Bedingungen der Farbkompetition im Aufmerksamkeitsfokus zu charakterisieren. Hierzu wurde den Versuchspersonen für 300 ms ein Kreis im LVF präsentiert, der aus zwei verschiedenfarbigen Hälften bestand (Zielfarbe und Distraktorfarbe). Die Aufgabe war es, zu entscheiden, ob die konvexe Seite des in der Zielfarbe gehaltenen Halbkreises nach links oder nach rechts wies. Während die Zielfarbe innerhalb einzelner Experimentalblöcke konstant war, nahm der Farbstimulus im RVF ('probe') in jedem Durchgang zufällig eine von insgesamt drei möglichen Zielfarben an. GCBA Modulationen wurden berechnet, indem die Hirnantworten zu 'probes', die nicht der Zielfarbe entsprachen ('non-match'), von Hirnantworten zu 'probes' in der Zielfarbe ('match') subtrahiert wurden. Die gefundenen GCBA Modulationen bestanden aus einer frühen und einer späten Phase, die die Areale des ventralen extrastriären visuellen Kortex

in umgekehrter hierarchischer Reihenfolge durchliefen (von hierarchisch höher zu hierarchisch niedriger gelegenen Regionen). Das frühe Modulationsmaximum um 200ms befand sich im weiter anterior-lateral gelegenen okzipito-temporalen Kortex, während das spätere Maximum um 280ms weiter posterior-medial in frühen visuellen Arealen auftrat. Da physikalische Unterschiede zwischen den verglichenen Versuchsbedingungen ('match' und 'non-match') bestanden, wurde ein zweites Experiment durchgeführt, das kontrollieren sollte, ob die beobachtete Modulationssequenz allein durch diese sensorischen Unterschiede hervorgerufen werden kann oder ob ihr tatsächlich farbbasierte Aufmerksamkeitsprozesse zugrunde liegen. Hierzu wurde – zusätzlich zu den farbigen Stimuli im rechten und linken visuellen Feld – zentral ein achromatischer Buchstabenstrom präsentiert. Da die zuvor gefundenen Modulationssequenzen nur auftraten, wenn die Versuchspersonen ihre Aufmerksamkeit auch auf die farbigen Stimuli richteten, nicht aber, wenn sie sich auf die Buchstaben konzentrierten, konnte bestätigt werden, dass es sich bei den Modulationen um echte Aufmerksamkeitseffekte handelte. Das dritte Experiment zeigte, dass die Wegnahme der zweiten farbigen Halbkreishälfte im LVF, d.h., des kompetitierenden Farbdistraktors im Aufmerksamkeitsfokus, die GCBA Modulationen nicht eliminierte. Ein einfarbiger Halbkreis im Aufmerksamkeitsfokus genügte, um die Modulationssequenz mit früher und später Phase hervorzurufen. Das vierte Experiment ging noch einen Schritt weiter und demonstrierte, dass frühe Anteile der GCBA Modulation auch durch Farben hervorgerufen werden konnten, die zwar aufgabenrelevant waren, aber nicht im beachteten LVF präsentiert wurden. Hierzu wurden die Versuchspersonen instruiert, während eines Experimentblockes auf zwei verschiedene Zielfarben gleichzeitig zu achten, von denen bei jeder Stimuluspräsentation nur jeweils eine im LVF gezeigt wurde. Unbeachtete Farbstimuli im RVF, die der tatsächlich präsentierten Zielfarbe entsprachen, riefen die bekannte GCBA Modulation mit früher und später Phase hervor, während unbeachtete Farbstimuli, die die andere, gerade nicht im LVF erscheinende Zielfarbe, aufwiesen, lediglich zu frühen GCBA Modulationen führten. Das fünfte Experiment zeigte schließlich, dass weder frühe noch späte GCBA Modulationen auftraten, wenn die Versuchspersonen schnellstmöglich das Erscheinen der zweifarbigen Kreise aus dem ersten Experiment per Tastendruck anzeigen mussten, ohne deren Farbe oder Form zu diskriminieren.

Die durchgeführten Experimente legen nahe, dass die der globalen Farbselektion zugrundeliegende Modulationssequenz aus einer frühen und einer späten Phase besteht, bei der die frühe Phase einen Abgleich mit einem internen Set von relevanten Farben darstellt ('color template matching'), während die späte Phase einen auf dem farbigen Zielobjekt durchgeführten Diskriminationsprozess reflektiert ('discrimination matching'). Weder die frühe noch die späte Phase der GCBA hingen hierbei von der Anwesenheit eines kompetitierenden Farbdistraktors im Aufmerksamkeitsfokus ab.

Outline

The first chapter will introduce and discuss concepts and types of visual attention (spatial, object-based, feature-based) with a particular focus on global feature-based attention (GFBA) and its possible determinants. The second chapter reviews basic principles and the instrumentation of electromagnetic brain recordings. The third chapter describes the approach to data aquisition and data analysis. The fourth chapter will provide – in separate sections – the motivation, methods, results, and discussion of each of the conducted experiments. The fifth chapter summarizes the main findings, and the sixth chapter offers a general discussion of the experiments in the context of the relevant literature. The seventh chapter finally will deal with open questions and describe possible future experiments to address them.

1. Introduction

The present work aims at investigating the underlying mechanisms of global feature-based attention. The introduction sets out to first present the types of attention, then focuses on feature-based attention and the feature-similarity gain model proposed by (Treue & Martínez Trujillo, 1999). After establishing a theoretical framework, the current research questions are formulated.

1.1. Visual attention – concepts and theories

The visual system plays a central role in the uptake and processing of information in the surrounding environment. Even though the brain areas involved in visual information processing represent a large part of the primate cortex – about 50% in the macaque monkey and 20-30% in the human (Van Essen, 2004), the processing capacity for visual information is limited (e.g., Broadbent, 1958). According to computational considerations at the complexity level Tsotsos (2011), the problem is not simply the mere amount of sensory input, but rather the fact that each component of a perceived stimulus can be matched to multiple objects and scenes in memory leading to a vast amount of combinatorial possibilities, for which coding becomes intractable. The incoming flood of visual information, therefore, needs mechanisms that constrain and disambiguate the input to a processable amount of information relevant for behavior. Such mechanisms are referred to as selective visual attention:

Attention is the process by which the brain controls and tunes information processing.

(Tsotsos, 2011, p. 10)

The locus of attentional selection

Many different theories have been put forward to explain at which stage of the information processing stream attentional selection operates. Broadbent (1958) stated in his 'filter model' that perception is a limited process with attentional selection taking place before the stimuli are fully perceived. Based on a rudimentary analysis of the physical properties of incoming stimuli, an attentional filter decides which of them are relevant and further processed and which are irrelevant and filtered out ('early selection'). Broadbent's theory was refined by Treisman's 'attenuation model' (Treisman, 1969) favoring an early selection filter that attenuates irrelevant signals instead of completely blocking them, such that they can still undergo further processing if they pass a certain threshold. Other researchers like Deutsch and Deutsch (1963), Norman (1968) or MacKay (1973) suggested that attentional selection occurs after the full, automatic and unlimited perception of all stimuli and only after perception it would be decided which stimuli will then enter memory ('late selection'). The 'perceptual load theory' (Lavie & Tsal, 1994; Lavie,

1995) finally provided a compromise between early and late selection views: the perceptual load of the relevant information determines the occurrence of early or late selection and thus, how much of the irrelevant information will be processed. Whenever the relevant information exhausts the available attentional capacity early selection takes place, if resources are left, then processes of late selection will occur. However, irrespective of the precise locus or nature of the attentional selection process all models agree on the fact, that out of all stimuli provided by the environment only a few will be finally selected and stored in the memory. As a logical consequence, stimuli have to compete for the available visual processing capacity to reach consciousness, which will be discussed in the following section.

Competition of stimuli for attentional resources – biased-competition theory and saliency maps

The competition of stimuli for limited attentional resources has been supported by numerous behavioral, electrophysiological, and neuroimaging studies (reviews: Desimone & Duncan, 1995; Reynolds & Chelazzi, 2004; Beck & Kastner, 2005). A well-known theory that attempts to describe the neuronal mechanisms underlying competition of stimuli in the visual field is the so-called *'biased-competition' model* (Desimone & Duncan, 1995). It postulates that objects, which are simultaneously present in the visual field, compete for neuronal responses in the visual cortex. This competition is then biased by task-dependent *top-down* control mechanisms – e.g., attending to a certain location more than to another – or via *bottom-up* stimulus-driven factors – e.g., whether a stimulus is novel or larger, brighter, faster moving, etc. – (for a review on top-down and bottom-up mechanisms in biasing competition, see Beck & Kastner, 2009). A prominent computational attempt at understanding bottom-up stimulus-driven factors is the 'saliency map' model of Koch and Ullman (1985), that was first purely conceptual, but later computationally implemented by Niebur and Koch (1996) and further refined by Itti et al. (1998) and Itti and Koch (2001). The 'saliency map' model describes the item saliency as a measure of its difference in physical properties (like color, motion, orientation, etc.,) from its surround. After all physical feature contrasts are represented in one topographic 'saliency' map, attention is then assumed to shift serially from location to location following a rank order of saliency. However, the orienting of attention is not solely determined by exogenous bottom-up saliency, but also by endogenous top-down factors (i.e., the task at hand). For instance, according to the feature-similarity gain model of Treue and Martínez Trujillo (1999), the top-down saliency of stimuli can be biased because of their similarity with behaviorally relevant target features (see detailed discussion in section 1.2.3.). Another mechanism causing a competitive advantage of features by virtue of the fact that they are part of the attended object will be described in section 1.2.2. ('integrated competition hypothesis': Duncan et al., 1997).

1.2. Types of visual attention

Visual attention can operate at the level of spatial locations, whole objects or it can be directed to certain feature values like the color red. The following sections will describe these three main types of attentional selection.

1.2.1. Spatial attention

Numerous psychophysical, electromagnetic or fMRI studies in humans, as well as single-unit recordings in monkeys, have demonstrated that attention can be directed to a certain location in visual space, which is referred to as 'spatial attention' (e.g., Posner, 1980; Moran & Desimone, 1985; Mangun & Hillyard, 1991; Heinze et al., 1994; Luck et al., 1997). Single-unit recording studies have shown that neurons in extrastriate visual cortex enhance their firing rates when the spatial focus of attention is directed inside the cell's receptive field (e.g., Luck et al., 1997). Likewise, fMRI studies in humans documented enhanced responses in visual cortex areas retinotopically corresponding with the attended location in space (e.g., Tootell et al., 1998). The direction of spatial attention can be accompanied by eye movements ('overt' attention), but it can also work independently of them, i.e., outside the currently fixated location ('covert' attention) as first demonstrated by von Helmholtz (1896). The spatial focus of attention has been likened to a *spot- or searchlight*, where the processing of information is facilitated within its beam, leading to enhanced detectability and discriminability of targets (e.g., James, 1890; Shulman et al., 1979; Posner et al., 1980; Crick, 1984; Downing, 1988). A prime example for demonstrating faster target detection within the spatial focus of attention is the 'Posner cuing paradigm': If a spatial cue indicates the position where the target is highly likely to appear, target detection at that position (spatial cue valid) is much faster compared to a target at an uncertain position (no spatial cue presented) or a target at an unexpected position (spatial cue invalid) (Posner, 1980; Posner et al., 1980). Importantly, while subjects maintain a central fixation, attention can be oriented to the peripheral location of the expected target by both endogenous cues (e.g., a central arrow pointing to that peripheral location) or exogenous cues (e.g., a brightening of a peripheral box in which the target will appear) (Posner & Cohen, 1984). Extending notions of Posner's initial fixed spotlight model, the 'zoom-lens' model assumed that the size of the spotlight can change flexibly depending on the current task-demands (C. W. Eriksen & St James, 1986). While it has been assumed that attention drops gradually with increased eccentricity from its focus (Downing & Pinker, 1985; C. W. Eriksen & St James, 1986), newer models derived from computational modeling and magnetoencephalographic brain recordings in humans suggest a 'center-surround' or 'Mexican hat' profile: The processing of stimuli is highest within the focus of attention, suppressed in a narrow zone surrounding the attended location and again increased for more distant stimuli (Hopf et al., 2006; Tsotsos, 2011)

ERP/ERMF correlates of spatial attention

Event-related potential (ERP) experiments using Posner's experimental design (for an explanation of the ERP technique see section 2.2) revealed that the performance increments observed for validly versus invalidly cued targets are reflected by amplitude enhancements of early ERP components (P1/N1) at occipital and parietal recording sites contralateral to the visual hemifield of target presentation (Mangun et al., 1987; Mangun & Hillyard, 1991). The fact that P1/N1 amplitude enhancements were typically observed without significant shifts in latency or altered field distributions, was taken to indicate that these amplitude modulations index changes of sensory gain of the visual input at early stages of visual processing (Hillyard et al., 1998). While the P1 modulation turned out to reflect location selection per se, the N1 modulation seemed to relate to subsequent stimulus discrimination processes (Mangun & Hillyard, 1991; Vogel & Luck, 2000; Hopf et al., 2002). ERP studies proposed that the generator of the P1 is localized in lateral occipital extrastriate visual cortex, while the posterior N1 modulation arises from lateral occipital-temporal cortex regions (Mangun, 1995). Combined imaging studies (EEG/PET; EEG/fMRI) confirmed sources in the fusiform gyrus and middle occipital gyrus for focusing attention to a certain location in space (Heinze et al., 1994; Mangun et al., 1997; Di Russo et al., 2003).

1.2.2. Object-based attention

Theories of object-based attention propose that attention is not only bound to specific locations or features, but that attention can select entire objects for preferential processing (for reviews see Kanwisher & Driver, 1992; Driver & Baylis, 1998; Scholl, 2001). Indeed, effects of object-based selection have been reported in numerous studies including single-unit recordings in monkeys (e.g., Roelfsema et al., 1998; Fallah et al., 2007; Wannig et al., 2007; Katzner et al., 2009) as well as psychophysical, fMRI or electromagnetic (EEG/MEG) studies in human observers (e.g., Duncan, 1984; Egly et al., 1994; Valdes-Sosa et al., 1998; O'Craven et al., 1999; Blaser et al., 2000; Schoenfeld et al., 2003; Melcher et al., 2005; Sohn et al., 2005; Boehler et al., 2011). For example, Roelfsema et al. (1998) observed enhanced firing rates for V1 neurons when their receptive field encompassed a segment of the currently-attended target curve but not a distractor curve. Object-based selection effects were also reported for more complex stimuli (O'Craven et al., 1999). Using fMRI, the authors showed that subjects' attention to one out of two spatially transparently superimposed pictures (house and face) led to selectively enhanced brain responses in the corresponding cortical modules (fusiform face area for faces, parahippocampal place area for houses), suggesting that these objects could be distinctly attended and processed.

The 'same object advantage' as an index of object-based attention

Much of the research in support of object-based attention builds on the so-called 'same-object advantage'. Specifically, subjects are better at reporting two features of the same object as

compared to reporting two features which belong to different objects (Duncan, 1984; Baylis & Driver, 1993). This effect is seen even when the different objects are superimposed and the features occupy the same spatial location (e.g., Duncan, 1984). Another influential experimental design showing the 'same-object advantage' has been developed by Egly et al. (1994). In their experiment the subjects had to detect the onset of a square at one out of four different locations, with two locations belonging to one rectangle and the other two locations belonging to another rectangle. One location was precued (75% valid) before the onset of the luminance change. Interestingly, the performance costs (prolonged reaction times) at equidistant invalidly cued locations were reduced, if those locations were part of the cued rectangle as compared to being part of the uncued rectangle. Despite the elegance of the respective experimental approach, the study of Egly et al. (1994) confounds the comparison of location and object cues by simultaneously altering the physical stimuli (see Figure 1.1A). In general, it is very challenging to design an experiment that can separate object-based attention from feature- or space-based effects. For example, the experimental design of Duncan (1984) does not rule out an explanation of the 'same-object advantage' in terms of spatial or spatial-frequency effects (Lavie & Driver, 1996) (see Figure 1.1B). A more convincing experimental design, avoiding such confounds when showing the 'same-object advantage' was first developed by Valdes-Sosa et al. (1998). The authors used two sets of differently colored moving dots to create two perfectly superimposed transparent surfaces which served as objects (see Figure 1.1C). They showed that the simultaneous judgments of the speed and direction of linear dot translations were more accurate when both concerned the same surface than when they had to be performed on different surfaces. Another innovative design that ruled out any contribution of spatial attention and prevented target selection on the basis of some constant featural difference between objects was developed by Blaser et al. (2000). In their study, the authors superimposed two Gabor patches that dynamically changed over time in color, orientation and spatial frequency, but could still be tracked by the subjects as separate objects. When the subjects were asked to discriminate discontinuities in the changes of two features (like color and orientation 'jumps'), they were significantly better when those discontinuities belonged to the same Gabor compared to different Gabors, replicating again the 'same-object advantage'.

Importantly, the selection of features belonging to the same attended object occurs automatically and irrespective of the features' task-relevance. For example, single-unit recordings in monkeys found that the firing rates of motion direction-sensitive MT neurons were not only modulated when monkeys attended to the motion direction of a moving random dot pattern, but also when they attended to its color, a feature that is not specifically represented in area MT (Katzner et al., 2009). Such object-mediated processing of task-irrelevant features has also been reported in many psychophysical, fMRI and electromagnetic (EEG/MEG) studies in humans (O'Craven et al., 1999; Schoenfeld et al., 2003; Melcher et al., 2005; Sohn et al., 2005; Boehler et al., 2011; Schoenfeld et al., 2014).
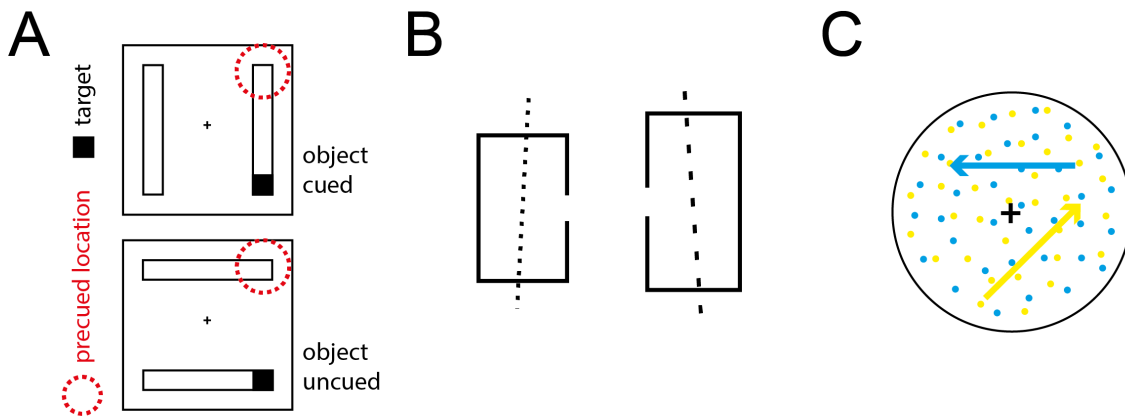
Figure 1.1. Stimulus designs to investigate object-based attention. **(A)** Egly et al. (1994) cuing task. The subjects had to detect the onset of a square that could appear at each end of the rectangles. Effects of object-based attention were assessed by comparing reaction times to the square onsets as a function of whether they were inside the precued or inside the uncued rectangle. Although the spatial relationship of the precued location and the target position were identical in the example displayed here, the rectangles' orientations differed between the conditions. **(B)** Two possible stimuli of Duncan (1984). They consisted of a box (small or large) with a gap (right or left) and a line (dotted or dashed) struck through it that was tilted (clockwise or counterclockwise). Subjects were better at reporting two features when they belonged to the same object (e.g., gap position and size of the box) compared to when the features belonged to different objects (e.g., gap position and line texture). However, the two features belonging to the line (texture and fine orientation) were closest in space (defined across the same spatial locations) and available at high spatial frequencies, while gap position and box size resembled rather low-frequency features. **(C)** Valdes-Sosa et al. (1998) used two sets of moving differently colored dots (e.g., blue and yellow) to create two perfectly superimposed transparent surfaces sliding across each other. The subjects were asked to judge the speed and the direction of linear dot translations with the two judgements (speed and direction) being made either on the same or on different surfaces.

Feature binding and the integrated competition hypothesis

To produce the above reported object-based selection effects, the visual system has to define which parts of the visual input refer to one and the same object. A number of elementary selection operations including perceptual grouping (e.g., common motion, good continuation, common color) and segmentation of the visual scene may be important here (e.g., Driver, 1996). Interestingly, these mechanisms also work for objects defined by subjective illusory contours or objects that are partly occluded (Moore et al., 1998). With the *integrated competition hypothesis* account Duncan et al. (1997) provide a possible explanation of how the different features of an object are bound together to form an integrated object representation. Multiple sensory and motor, cortical and subcortical brain subsystems are assumed to be concurrently activated to access the different properties (like color, size, and motion) and the action implications of an object. Within many if not most of these subsystems, object-bound activations compete for representation as suggested by the 'biased competition' model (Desimone & Duncan, 1995), see section 1.1 above. The competition is then integrated across all subsystems representing the

different object features in a joint fashion, so that the winning object in one subsystem entails a competitive advantage of all its other features in the other subsystems. This model accounts perfectly for the finding that attending to a feature of an object automatically entails the selection of all other features of that object, even though they might be completely task-irrelevant.

ERP/ERMF correlates of object-based attention

Correlates of the 'same object advantage'

Using a modified version of the previously described cuing task of Egly et al. (1994), Martínez et al. (2006) investigated the relationship between space- and object-based attention in a combined ERP and fMRI study. They specifically compared object-selective effects (target at invalidly cued location belonging to the cued vs. a different object) to effects of spatial attention (targets at cued vs. uncued locations). They found that object-based selection lacks the P1 (80-128ms) enhancement characteristic for spatial attention. However, both types of attention shared a posterior contralateral N1 (160-196ms) enhancement, generated in the middle occipital gyrus in or near the lateral occipital complex (LOC). The latter is a cortical region known to be involved in the encoding and segmentation of objects (Grill-Spector, 2003). Thus, Martínez et al. (2006) suggested that the allocation of spatial attention might include an object-selective component acting at the discriminative stage of the N1, which is in line with the hypothesis that object-selection is mediated by spatial attention mechanisms (Weber et al., 1997).

Correlates of task-irrelevant object features

A number of EEG/MEG experiments have explicitly focused on the neural correlates of object-mediated selection for task-irrelevant features (e.g., Schoenfeld et al., 2003; Boehler et al., 2011; Schoenfeld et al., 2014). For example, Schoenfeld et al. (2014) used transparent motion surfaces in an ERMF study to compare object-based selection of task-relevant and task-irrelevant feature changes (dot motion and color). They found enhanced ERMF responses to color and motion that arose in V4 and human MT, respectively. Task-relevant feature changes, however, preceded task-irrelevant feature changes by 60-65ms. Notably, it has been shown, that ERP modulations reflecting the object-based selection of a task-irrelevant color are not confined to the attended object, but can also appear in unattended objects in case they share that irrelevant color (Boehler et al., 2011). These modulations suggest that feature-based attention operates in a global way – a property more thoroughly discussed in the next section (1.2.3).

1.2.3. Feature-based attention and its spatially global nature

Attention has the ability to not only select certain positions in space or entire objects for preferential processing – as described in the sections 1.2.1 and 1.2.2 above, it can also be directed to non-spatial features such as shape, color or motion direction. This is commonly referred to as

feature-based attention. The ability to select items merely based on their features like color, motion, orientation, size, or spatial frequency, is apparently an important prerequisite for guiding the selection of a target object among irrelevant distractors (Shih & Sperling, 1996; Moore & Egeth, 1998; Wolfe & Horowitz, 2004).

Aside from its importance for guiding attention towards target items, feature-based attention can also improve the perception of targets sharing an attended feature as shown by psychophysical experiments with moving stimuli. Speed increments are better detected if they affect dots moving in the attended direction (T. Liu et al., 2007; White & Carrasco, 2011) and the motion direction of moving dots can be better discriminated with regard to a reference direction, if the subjects are precued to the upcoming reference direction before stimulus onset (Ling et al., 2009). In addition to these behavioral performance benefits, neuroimaging studies in humans revealed that attention to a certain feature (color, motion or shape) not only increases the sensitivity to detect changes of the attended feature, but it is also accompanied by an enhanced neural activation of extrastriate cortex areas specialized for processing that feature (e.g., increased blood-flow in a MST-like area for attention to motion) as first shown by (Corbetta et al., 1990, 1991). Subsequent neuroimaging studies confirmed effects of feature-based attention in specialized cortical areas like enhanced responses in human MT+ when attending to motion or enhanced responses in color selective areas like V4 when attending to color (e.g., Beauchamp et al., 1997; O'Craven et al., 1997; Chawla et al., 1999; Saenz et al., 2002; Schoenfeld et al., 2003).

Separating feature-based attention from spatial selection

Since attended features are typically presented at attended spatial locations, it is not trivial to separate feature-based from spatial attention effects. Attention to features could act by increasing the gain for the attended feature value in a location-independent manner, or it could operate by guiding the spatial focus of attention to locations where this feature value is present. Andersen et al. (2009) addressed this question with an elegant steady-state visual evoked potential (SSVEP) study. Subjects had to attend to one of two overlapping flickering random dot kinematograms (red: 10Hz, blue: 12Hz) with the dots unpredictably changing positions after each flicker cycle (10-12Hz). Although the spatial tracking of individual dots and hence the focusing of spatial attention to a certain dot group was rendered impossible, the authors still found the SSVEP amplitudes to be enhanced for the currently-attended color. This finding provided strong evidence that attention to color does not rely on a mediation by spatial attention, but is rather consistent with a location-independent signal enhancement process. However, the random dot kinematograms (diameter: 12.78° visual angle) were presented at the attended location an thus within the subjects' spatial focus of attention. Thus, although the selection of dots of a certain color did not rely on a spatial tracking within the attended area, the feature enhancement processes could still be restricted to the attended part of the visual field.

The spatially global nature of feature-based attention

That feature-based attention is "spatially global", i.e., not bound to a certain location in space (referred to as *global feature-based attention*, GFBA), was shown in experiments that tested attention effects at remote locations outside the spatial focus of attention. These experiments included single-unit recordings in monkeys (e.g., Motter, 1994; Treue & Martínez Trujillo, 1999; McAdams & Maunsell, 2000; Martinez-Trujillo & Treue, 2004; Bichot et al., 2005; review: Maunsell & Treue, 2006) as well as psychophysical studies (e.g., Rossi & Paradiso, 1995; Sàenz et al., 2003; T. Liu & Hou, 2011; T. Liu & Mance, 2011; White & Carrasco, 2011) and fMRI or electromagnetic (EEG/MEG) studies in human observers (e.g., Saenz et al., 2002; Hopf et al., 2004; Serences & Boynton, 2007; Zhang & Luck, 2009; Jehee et al., 2011; Bondarenko et al., 2012; Andersen et al., 2013).

A typical way to investigate GFBA is to assess the influence of a spatially unattended stimulus on the behavioral performance and/or brain response as a function of whether it contains a feature that matches the currently-attended feature located elsewhere in the visual field Saenz et al. (2002); (e.g., Zhang & Luck, 2009; Bondarenko et al., 2012). For example, Saenz et al. (2002) had subjects attend to either a certain motion direction or color in one visual field, while they assessed the BOLD response to a stimulus in the other visual field that could either match or not match the attended feature. They found that in visual cortex areas (striate and extrastriate cortex) the responses to stimuli in the unattended hemifield were enhanced when they shared the color or motion direction currently attended in the other visual hemifield. Thus, paradigms such as that of Saenz et al. (2002), permit the assessment of the brain's response to stimuli that are not contained in the spatial focus of attention and therefore provide a measure of feature selection at unattended locations. The fact that visual fields are primarily represented in the contralateral hemisphere is an important feature of such experimental design. It is the basis for separating the brain response to stimuli presented in the attended and stimuli presented in the unattended hemifield. That is, stimuli in the LVF should elicit responses in the right hemisphere and stimuli in the RVF should give rise to responses in the left hemisphere due to the contralateral retinotopic organization of the visual cortex (e.g., Sereno et al., 1995).

A uniform enhancement of selected features across the visual field

Some psychophysical studies used orientation (tilt) or motion aftereffects as a measure of GFBA at unattended spatial locations in the same or the opposite hemifield relative to the attended target. They found a constant spread of feature-based attention both within and across visual hemifields (T. Liu & Hou, 2011; T. Liu & Mance, 2011). Surprisingly, these psychophysical studies also revealed that effects of GFBA could be observed at remote locations that had not been visually stimulated. Specifically, tilt or motion aftereffects were observed at locations where no stimulus at all was presented during the previous adaptation period (Arman et al., 2006; T. Liu & Hou, 2011; T. Liu & Mance, 2011). This observation was further confirmed by Serences and Boynton (2007) who performed a pattern classification analysis on fMRI data enabling them to infer the currently-attended motion direction from brain responses to a

contralateral unstimulated region of space. That is, although the spatial receptive field of the selected brain region did not encompass the currently-attended stimulus, the activity pattern of this brain region was systematically modulated by feature-based attention as indexed by an above-chance classification of the currently-attended motion direction.

Remarkably, the global selection of features seems to spread uniformly across the visual field even when the current task demands would favor a spatially restricted feature selection. Andersen et al. (2013) reported a clear performance decrement accompanied by a cancellation of the response selectivity of attended and unattended colors when subjects simultaneously attended in each visual hemifield to a color that had to be ignored in the opposite hemifield (e.g., LVF: attend blue, ignore red; RVF: attend red, ignore blue). Instead of a hemifield-specific response enhancement (LVF: blue enhanced; RVF: red enhanced), the SSVEP amplitudes of the two opposing colors were equally high at both locations (uniform enhancement across the visual field for both colors) showing no selectivity of one of the colors in either visual hemifield. Thus, the uniform enhancement of the selected colors across the visual field could not be overcome by task demands, even if it caused an impairment in the behavioral performance.

A potential neuronal mechanism underlying GFBA: the feature-similarity gain model (FSGM)

In spite of the fact that there is a wealth of literature on the global spread of feature-based attention, the question still remains as to what neural mechanisms actually underlie global feature selection. To clarify this issue, Martinez-Trujillo and Treue compared effects of spatial and feature-based attention in the motion sensitive middle temporal visual area (MT) of macaque visual cortex (Treue & Martínez Trujillo, 1999; Martinez-Trujillo & Treue, 2004). In their experiments, moving stimuli (coherently moving random dot patterns) were simultaneously presented in both visual hemifields with one stimulus inside and one outside the receptive field (RF) of a MT neuron. Spatial attention was manipulated by having the monkey attend to the motion stimulus either inside or outside of the RF. Feature-based attention was assessed as a function of the match between the motion direction attended outside the RF and the motion-direction preference of the neuron recordings were made from. Importantly, both spatial attention and feature-based attention modulated the responses of MT neurons in a multiplicative fashion without changing their underlying response properties. Specifically, the tuning curves of the MT neurons – reflecting their sensitivity to different orientations of motion direction – were multiplicatively scaled with no systematic sharpening or widening. Directing spatial attention inside the RF enhanced the response of the MT neuron to all motion directions (multiplication with the same factor), as did attending to a motion direction outside the RF that matched the neuron's preferred motion direction. Notably, the modulations of spatial and feature-based attention worked in an additive manner. Furthermore, Martinez-Trujillo and Treue (2004) found the feature-based modulations of the neuron's firing rate to range from neuronal enhancement (attention to preferred direction) to neuronal suppression (attention to anti-preferred direction). These observations together led to the 'feature-similarity gain model' (FSGM) that was first proposed by Treue and Martínez Trujillo (1999). The FSGM is an attention

model that unifies spatial and non-spatial attentional effects by treating both as features of the relevant target (hence, similarity might be based on spatial location or any other feature):

> *[...] the up or downregulation of the gain of a sensory neuron reflects the similarity of the features of the currently behaviourally relevant target and the sensory selectivity of the neuron along all target dimensions.*

Note, that the FSGM predicts that the sensory gain of a neuron is not determined by the similarity between the attended stimulus and the stimulus inside the RF, but between the attended stimulus and the neuron's feature preferences.

The FSGM also provides a possible explanation at the neural population level of how the cortical representation of stimuli might be altered by feature-based attention: Attending to a certain feature will enhance the response to neurons that are tuned to this feature and decrease the response of neurons tuned to opposite features resulting in a selectively enhanced representation of stimuli containing features similar to the currently-attended one. Importantly, only the spatial but not the non-spatial feature-similarity requires the neuron's RF to encompass the attended stimulus, while the RFs of neurons modulated by features such as the attended color or motion direction do not have to include the attended stimulus location by virtue of the spatially global nature of feature-based attention. Nevertheless, it should be kept in mind that the FSGM was derived from single-unit recordings and thus the mechanisms of GFBA could be more complex on the neuronal population level. Instead of a mere multiplicative scaling mechanism as observed for single cells, feature-based attention might actually alter the neural representation of feature space on the population level thereby enabling the visual system to dynamically separate relevant from irrelevant features by increasing the distance between them (Zirnsak & Hamker, 2010).

ERP/ERMF correlates of feature-based attention

Selection Negativity/Positivity

There are many ERP studies on feature-based attention showing that stimuli elicit a broad negative ERP deflection when they match the currently-attended feature value (e.g., a certain color or orientation). This modulation is known as *selection negativity (SN)* (reviewed in: Hillyard & Anllo-Vento, 1998). The SN is best observed in waveform differences, that is by subtracting ERP waveforms of stimuli with unattended feature values (e.g., a green stimulus under 'attend red' conditions) from ERP waveforms elicited by stimuli with the currently-attended feature value (e.g., a green stimulus under 'attend green' conditions). The SN has been reported for numerous features including color (Hillyard & Münte, 1984; Wijers et al., 1989; Anllo-Vento & Hillyard, 1996; Anllo-Vento et al., 1998), motion direction (Anllo-Vento & Hillyard, 1996), orientation (Harter & Guido, 1980; Kenemans et al., 1993), and spatial frequency (Harter & Previc, 1978; Kenemans et al., 1993; Baas et al., 2002). The SN typically onsets between

140-200ms poststimulus (depending on the experimental setup and the relative discriminability of attended and unattended features) and persists for 200ms or longer. The SN tends to be largest over the posterior regions of the scalp, with the scalp topography differing for individual feature types. For color it arises more contralateral at occipito-temporal sites compared to motion where the SN appears more symmetrical and at temporal and parietal sites (Anllo-Vento & Hillyard, 1996). The SN has often been reported to be accompanied by an anterior *selection positivity (SP)* either within the SN time range or with a slightly earlier onset (e.g., Wijers et al., 1989; Kenemans et al., 1993; Anllo-Vento & Hillyard, 1996; Anllo-Vento et al., 1998; Baas et al., 2002).

Importantly, the SN, which served as an index of feature-based attention, was elicited by stimuli presented in the attended visual hemifield, but was substantially reduced or absent for distant stimuli in the opposite, unattended hemifield (Hillyard & Münte, 1984; Wijers et al., 1989; Anllo-Vento & Hillyard, 1996). This led Hillyard and colleagues to propose that target feature selection is hierarchically contingent on the spatial selection of the target (Hillyard & Münte, 1984). Figure 1.2 illustrates the stimulus designs of respective ERP studies.

Correlates of global feature-based attention: task-relevant features

In contrast to initial observations (Hillyard & Münte, 1984; Wijers et al., 1989; Anllo-Vento & Hillyard, 1996), there is a growing number of EEG and MEG studies that have documented neural correlates of feature-based attention rather consistent with a global location-independent selection process (e.g., Hopf et al., 2004; Zhang & Luck, 2009; Andersen et al., 2011; Boehler et al., 2011; Bondarenko et al., 2012; Stoppel et al., 2012; Andersen et al., 2013). For example, Zhang and Luck (2009) had subjects continuosly attending to random dot groups of a particular color in one visual hemifield while color probes were flashed in the other unattended hemifield. When the probes matched the currently-attended color, they elicited an early contralateral occipital enhancement of the *P1 component* (80-130ms). Notably, this P1 enhancement was observed when the subjects had to select the dot group with the attended color when it was mixed with a group of distractor dots drawn in a different color. The P1 enhancement was, however, eliminated when the dots drawn in the attended color were shown in isolation.

In line with the previously reported selection negativities at attended locations, global effects of feature-based attention were also observed in the time-range of the *N1/N2 component* (Hopf et al., 2004; Bondarenko et al., 2012; Stoppel et al., 2012). Bondarenko et al. (2012) assessed effects of global attention to orientation. They found that task-irrelevant orientation probes presented in the unattended visual hemifield gave rise to an enhanced N1 (150-200ms) and N2 (230-330ms) when they matched the currently-attended orientation target in the opposite hemifield. The N1/N2 enhancements were observed at parieto-occipital electrode sites contralateral to the unattended probes, and a subsequent current source localization analysis yielded an underlying cortical current origin in the posterior lateral and ventral occipital cortex. The earlier N1 modulation could be localized anterolateral relative to the later N2 modulation which was found to arise slightly more posterior and ventral. While the N1 modulation turned out to reflect a

match of the probe's orientation with task-relevant orientations, the N2 modulation scaled with the sensory similarity of the probe and the actually presented target. The modulation sequence observed by Bondarenko et al. (2012) nicely fits previous observations of feature selection in visual search (Hopf et al., 2004). Hopf et al. (2004) reported negative-polarity ERP modulations in the time range between 140-190ms and 200-290ms after stimulus onset in response to target-defining features in search distractors. That is, enhanced negativities were elicited contralateral to irrelevant distractors that matched the currently relevant orientation irrespective of their location relative to the target (within the same hemifield as the target or in the opposite hemifield). Those N1/N2 modulations were localized to originate from ventral occipito-temporal cortex. In a combined ERP/ERMF study on feature attention to motion direction Stoppel et al. (2012) found no modulation of the N1, but a N2 amplitude effect (210-310ms) that scaled, like in (Bondarenko et al., 2012), with the similarity between the motion directions of the unattended probe and that of the spatially attended target: ERP/ERMF amplitudes contralateral to the unattended probe were more negative for motion directions matching more closely the target's direction. Stoppel et al. (2012) localized these global motion-based attentional effects to the lateral middle occipito-temporal cortex, most likely representing area V5/hMT, a cortex region known to be motion-sensitive (e.g., Beauchamp et al., 1997; O'Craven et al., 1997).

Correlates of global feature-based attention: task-irrelevant features

All the previously-described ERP/ERMF studies on global feature-based attention (Hopf et al., 2004; Zhang & Luck, 2009; Bondarenko et al., 2012; Stoppel et al., 2012) investigated the spread of the attended orientation, motion direction or color across the visual field. A notable extension of these observations was provided by Boehler et al. (2011). These authors reported correlates of global feature-based attention even for a completely task-irrelevant color, provided this color was contained in the target object. Specifically, the ERP response contralateral to an unattended object showed a positive enhancement (270-500ms) over the lateral occipital cortex when this unattended object contained a color that was task-irrelevant, but happened to be part of the attended search target in the opposite visual hemifield. Apparently, this kind of global feature-based attention, referred to as *irrelevant feature effect (IFE),* is mediated by object-based attention (see 1.2.2), which illustrates the inherent difficulty of separating correlates of feature-based attention from those of object-based attention.
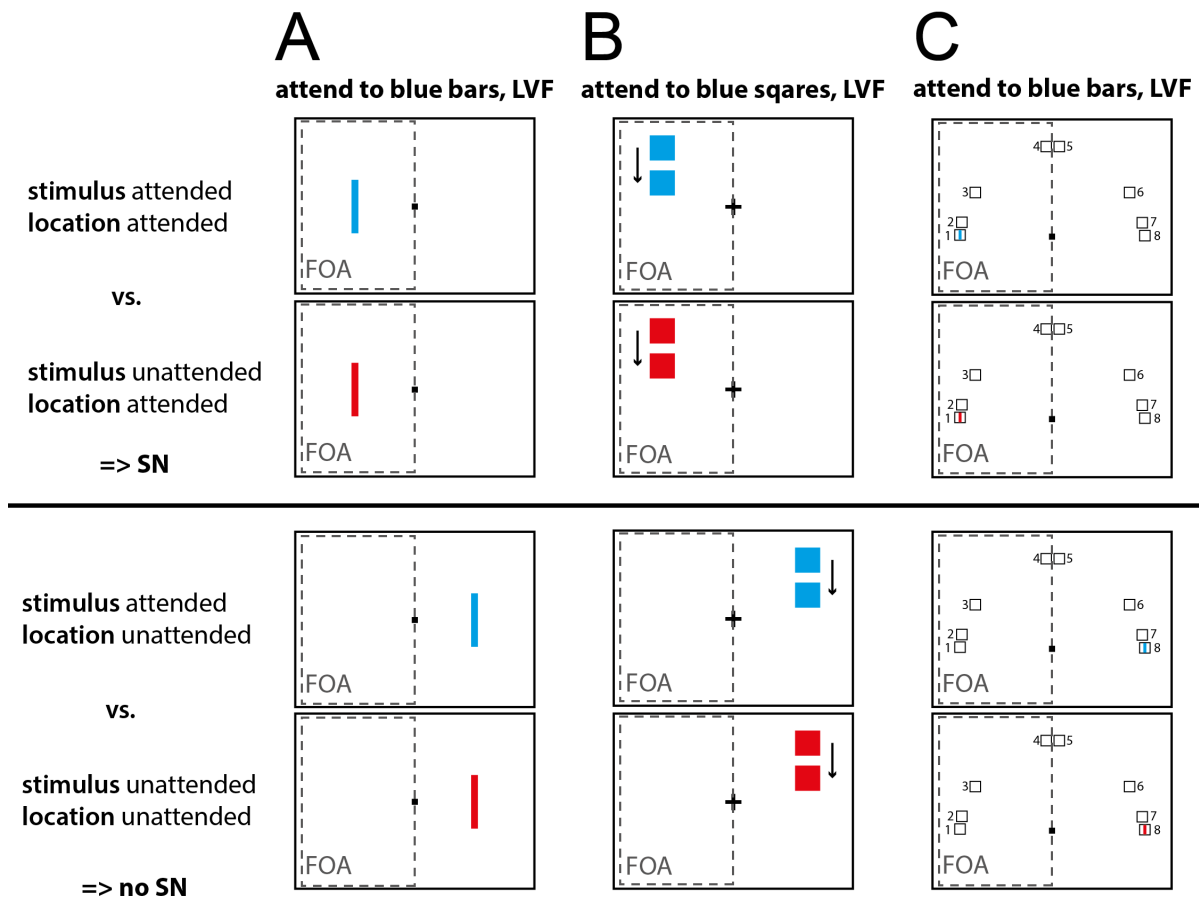
Figure 1.2. Stimulus designs of studies investigating the SN. All of the designs shown here **(A-C)** reported effects of selection negativity when comparing attended to unattended stimuli presented within the attended hemifield **(upper rows)**, but did not find such effects of feature-based selection for stimuli presented outside the spatial FOA in the unattended hemifield **(lower rows)**. **(A)** Stimulus design of Hillyard and Münte (1984), location-easy experiment. Red or blue bars were randomly presented either to the left or right of fixation. The subjects were to attend to bars of a certain color (here: blue) in one visual hemifield (here: LVF) and report the occasional occurance of shorter bars (targets, here: short blue bars in the LVF). **(B)** Stimulus design of Anllo-Vento and Hillyard (1996). The stimuli consisted of a pair of subsequently flashed squares (SOA: 50ms) producing the perception of a single moving square. The pairs of red or blue squares were presented to the RVF or LVF in random order. The subjects' fixation remained on the central cross while they attended in one visual hemifield (here: LVF) either to a certain motion direction (horizontal or vertical) or to a certain color (here: blue). The targets were infrequent pairs of squares separated by a longer SOA (150ms) appearing as a rapid sequence of two square presentations or as a slower movement of a single square (here: blue squares in the LVF separated by 150ms). **(C)** Stimulus design of Wijers et al. (1989). Eight possible stimulus locations were arranged as a half circle around the fixation dot (here indicated by squares). The subjects had either to attend to one of the most lateral locations (location 1 or 8, focused attention condition) or to simultaneously attend to all four possible locations within one hemifield (locations 1-4 or 5-8, divided attention condition). In both cases they were to report the onset of a bar of a certain color (here: blue) at the attended location(s) (here shown: divided attention conditon, attend to locations 1-4 in the LVF).

1.3. Motivation of the current work

The current thesis uses electromagnetic brain recordings (EEG/MEG) in human observers to study a remarkable property of feature-based attention, namely that it operates throughout the whole visual field without being bound to the spatial focus of attention (referred to as global feature-based attention [GFBA]). Dovetailing with evidence from single-unit recordings in monkeys as well as psychophysics and fMRI in humans (e.g., Motter, 1994; Rossi & Paradiso, 1995; Treue & Martínez Trujillo, 1999; McAdams & Maunsell, 2000; Saenz et al., 2002; Sàenz et al., 2003; Martinez-Trujillo & Treue, 2004; Bichot et al., 2005; review: Maunsell & Treue, 2006; Serences & Boynton, 2007; Jehee et al., 2011; T. Liu & Hou, 2011; T. Liu & Mance, 2011; White & Carrasco, 2011), there is a growing number of electromagnetic studies documenting correlates (ERP, ERMF, SSVEP) of global feature-based attention (Hopf et al., 2004; Zhang & Luck, 2009; Andersen et al., 2011; Boehler et al., 2011; Bondarenko et al., 2012; Stoppel et al., 2012; Andersen et al., 2013). Nonetheless, earlier ERP studies found feature-based attention to be contingent on prior spatial selection (Hillyard & Münte, 1984; Wijers et al., 1989; Anllo-Vento & Hillyard, 1996), a dependency speaking against a spatially global mode of operation. Hence, the critical question arises as to why the former but not the latter studies found feature-based attention to operate outside the spatial focus of attention. Obvious issues to be considered in this framework arise from the fact that there are substantial differences in the experimental design. Those are described in the following.

First, Hillyard and Münte (1984); Wijers et al. (1989); Anllo-Vento and Hillyard (1996) presented all items either in the attended or unattended visual hemifield (cf. Figure 1.2 in the previous section). Hence, they tested the effects of feature-based attention in the unattended hemifield when the attended feature was actually not presented in the spatial focus of attention. In studies reporting effects of GFBA (Hopf et al., 2004; Zhang & Luck, 2009; Andersen et al., 2011; Boehler et al., 2011; Bondarenko et al., 2012; Stoppel et al., 2012; Andersen et al., 2013) the target feature is typically presented in and outside the FOA. Thus, the actual presence of the attended feature in the spatial FOA might be crucial for GFBA to arise.

Second, Hillyard and Münte (1984); Wijers et al. (1989); Anllo-Vento and Hillyard (1996) presented feature values always in isolation without any competing feature values. It is well-known that attentional modulations are typically largest when stimuli compete within a neuron's receptive field (Moran & Desimone, 1985; Chelazzi et al., 1993; Luck et al., 1997; Reynolds et al., 1999; Treue & Maunsell, 1999; Reynolds & Chelazzi, 2004; J. Lee & Maunsell, 2010). Likewise, behavioral performance benefits due to GFBA were found to be clearly reduced when eliminating feature competition within visual hemifields (Sàenz et al., 2003). In line with these obervations, Zhang and Luck (2009) reported ERP correlates of GFBA that were contingent on the simultaneous presence of competing feature-values in the FOA. Hence, feature-competition might be necessary for feature-bassed attention to work in a global manner. Specifically, GFBA may depend on the simultaneous presence of competing feature values in the FOA .

Finally, of note, all of the ERP experiments that missed to find effects of GFBA had very short stimulus durations with items being presented only for 32-60ms (Hillyard & Münte, 1984; Wijers et al., 1989) or consisting of two sequentially 33ms presentations with onsets separated by 50-150ms (Anllo-Vento & Hillyard, 1996). The experiments reporting electromagnetic correlates of GFBA, in contrast, usually used long stimulus durations of at least 700ms (Hopf et al., 2004; Andersen et al., 2011; Boehler et al., 2011; Bondarenko et al., 2012; Andersen et al., 2013). Another stimulus design that gave rise to effects of GFBA included continuous representations of the attended feature, during which features were briefly probed (100-200ms) in the unattended visual hemifield (Zhang & Luck, 2009, experiment 1a/b; Stoppel et al., 2012). Hence, in studies that reported effects of GFBA, the subjects viewed the attended feature for much longer time periods than in studies that did not find effects of GFBA. Thus, stimulus duration could be a critical factor determining GFBA. Although the role of stimulus duration is not explicitly addressed in the current experimental series the stimulus presentations (300ms) were selected to be well above the short durations used by Hillyard and Münte (1984); Wijers et al. (1989); Anllo-Vento and Hillyard (1996).

Taken together there might be two possible factors that are crucial for GFBA to arise that will be addressed in the following work:

> factor 1)   the presence of the attended feature in the spatial FOA
> factor 2)   the presence of competing feature values in the spatial FOA

The current thesis is particularly motivated by the results of a recent ERP study that addressed factor 2) by testing effects of global attention to color with and without a second competing color being presented at the attended location (Zhang & Luck, 2009). The authors reported an early occipital enhancement of the P1 component contralateral to unattended probes when those probes matched the target color. Importantly, this P1 effect was present under conditions of color competition, but completely abolished when only one color at a time was present in the FOA. While this observation is supported by behavioral data (Sàenz et al., 2003), and generally in line with attention effects being maximal under conditions of stimulus competition (Moran & Desimone, 1985; Chelazzi et al., 1993; Luck et al., 1997; Reynolds et al., 1999; Treue & Maunsell, 1999; Reynolds & Chelazzi, 2004; J. Lee & Maunsell, 2010), there are studies in humans (EEG/MEG) (Bondarenko et al., 2012; Stoppel et al., 2012), and in monkeys (e.g., McAdams & Maunsell, 2000; Martinez-Trujillo & Treue, 2004) reporting effects of GFBA without any competition of feature values at the attended location. However, the studies reporting GFBA in the absence of feature competition did usually not include an experimental condition where feature competition was present. A direct comparison of effects of GFBA with and without competing feature values was therefore not possible. The current experimental series tries to fill this gap by providing a direct comparison between the effects of global color selection with and without color competition in the spatial focus of attention.

To preview the observations, experiment 3 will reveal that effects of GFBA do not depend on the simultaneous presence of different feature values in the focus of attention. Accordingly,

further experiments were designed with the aim to pinpoint the actual determinants that are crucial for GFBA to arise. Respective experiments will also permit to test the aforementioned factor 1). An overview summarizing the objectives of the current work and how they will be addressed with the reported experiments will be provided below.

Aim of the current work

The current experimental series was designed to characterize electromagnetic correlates of global color-based attention (GCBA) and to determine which factors actually render color selection a spatially global operation. The reported experiments addressed the following specific questions:

Question 1)   What are the electromagnetic correlates (ERP/ERMF) of GCBA when performing a color/shape discrimination task?

Question 2)   Does GCBA depend on the competition of color values in the FOA?

Question 3)   Does GCBA depend on the physical presence of the attended color in the FOA?

Question 4)   Does GCBA depend on the discrimination of the target in the FOA?

Experiments 1 and 2 serve to characterize the electromagnetic indices of global color-based selection when performing a color/shape discrimination task (Question 1). Experiment 3 addresses Question 2) by comparing effects of GCBA with and without competing color values in the spatial FOA. Experiment 4 addresses Question 3) by testing the effects of GCBA for task-relevant colors that are absent from the target presented in the FOA. Experiment 5 provides data pertinent to Question 4) by instructing the subjects to perform a simple onset-detection of the targets irrespective of their color, thereby preempting the need to discriminate to the colored targets.

Prediction 1)   According to previous findings for attention to orientation and motion (Hopf et al., 2004; Bondarenko et al., 2012; Stoppel et al., 2012), GCBA should be indexed by modulations of the ERPs/ERMFs in the N1/N2 time range. (experiment 1, 2)

Prediction 2)   If GCBA depends on color competition in the FOA, GCBA modulations should be absent or at least substantially reduced without a competing distractor color in the FOA. (experiment 3)

Prediction 3)   If GCBA is bound to the presence of the attended color in the FOA, it should be absent for a task-relevant color that is not contained in the FOA. (experiment 4)

Prediction 4)   If GCBA requires the discrimination of the target in the FOA, it should be eliminated when performing a simple onset-detection task where the need to discriminate the colored target is abolished. (experiment 5)

2. Fundamentals of brain activity recording

The current chapter focuses on the basic principles of recording the electromagnetic brain activity in human observers using electroencephalography (EEG) as well as magnetoencephalography (MEG) (section 2.1), followed by a short description of the event-related potential (ERP) and event-related magnetic field (ERMF) techniques (section 2.2).

2.1. EEG/MEG recordings of electromagnetic brain activity

Electroencephalography (EEG) as well as magnetoencephalography (MEG) are techniques which allow the non-invasive investigation of the neuronal activity of the human brain. Specifically, they record extracranial electric potentials (EEG) or magnetic fields (MEG) with sensors placed directly on or close to the scalp. Both techniques provide a high temporal resolution on the order of milliseconds. While EEG requires electrodes placed on the scalp, the MEG sensors are located inside a helium-filled dewar, which is placed as close as possible to the head. Coupled to magnetic pick-up coils the MEG sensors contain superconducting quantum interference devices (SQUIDs) that were introduced by Zimmerman et al. (1970). SQUIDs are able to detect very small magnetic fields by using quantum mechanic effects in a superconducting loop which turn the magnetic flux produced by the brain into measurable voltage values as described by M. Hämäläinen et al. (1993). The following sections will describe how the measured electromagnetic activity is generated in the brain and discuss how well it can be localized with EEG and MEG.

Neurophysiological background of electromagnetic brain activity

The voltage fluctuations and magnetic fields that can be measured on the head surface are created by neuronal postsynaptic potentials (PSPs) in the cortex, whose superimpositions sum up to slowly fluctuating potentials that can be measured at a macroscopic level (Hubbard et al., 1969; Creutzfeldt & Houchin, 1974). Figure 2.1 illustrates how an excitatory PSP causes a directed intracellular ('primary') current thereby generating an electric field with returning volume ('secondary') currents and hence leading to a neuronal dipole structure. The electric intracellular currents induce magnetic fields oriented perpendicularly to them, according to the 'right-hand rule': if you wrap the right hand around the electrical current flow with the thumb of the right hand pointing in the motion direction of the positively charged ions, the fingers indicate the direction of the magnetic flux. Importantly, only synchronous activities of parallelly-oriented neurons with dendrites along the predominant direction lead to a macroscopically observable current dipole at a distant recording site. This so-called *'open field' configuration* is found in pyramidal neurons in the neocortical layers. In contrast, electric activities in inhomogeneous cell clusters with radially spreading dendrites, such as spiny stellate neurons in neocortical layers, cancel each other, which is referred to as a *'closed field' configuration* (Lorente de Nó, 1947). However, the current-dipole moments of measurable

cortical generators are are generally on the order of 10 nA m (e.g., M. Hämäläinen et al., 1993) and computational estimates assume that this requires approximately 50,000 cortical pyramidal neurons to be synchronously active (with layer V and II/III pyramidal cells being presumably the major contributors to EEG and MEG signals) (Murakami & Okada, 2006). Subcortical sources, on the other hand, are less likely to be detected by EEG and MEG for several reasons. First, the signal strength of both the electric and the magnetic field decreases with the square of the distance to the underlying current source (inverse-square law of Coulomb and inverse-square force law of Biot-Savart). This clearly limits the contribution of deeper structures to the signal measured on the head surface (Elbert, 1993; Hillebrand & Barnes, 2002). Second, the often irregular neuronal structure of subcortical structures like the thalamus and reticular formation leads to the above described 'closed field' situation with randomly oriented primary currents cancelling each other. However, and rather controversially, there are also studies reporting activity in deep brain structures at the diencephalic level, the thalamus, the amygdala or the hippocampus (Ribary et al., 1991; Volkmann et al., 1996; Tesche, 1997; L. Liu et al., 1999; Timmermann et al., 2003; Cornwell et al., 2008; Riggs et al., 2009).

Spatial resolution

There are substantial differences concerning the limits on spatial resolution between electric and magnetic fields. The main sources for the electromagnetic field giving rise to the MEG and EEG are directed intracellular currents (see Figure 2.1), which can in good approximation be described as dipoles (Okada, 1982; de Munck et al., 1988). Those dipoles are located in the macroscopically rather homogeneous intracranial space and the emerging magnetic fields are only marginally influenced by the different volume conductivities of cerebrospinal fluid, skull and skin. The different volume conductivities have therefore not to be taken into account for the analysis of MEG data (M. S. Hämäläinen & Sarvas, 1989). In contrast, the corresponding electric field gets strongly affected by the inhomogeneities of the volume conductor as it blurs at the border of different layers of tissue (e.g., Nunez, 1981; Luck, 2005). Hence, the source localization for the electric fields measured by EEG is complicated by the resulting signal distortion, and it is difficult to compensate for this even if anatomically realistic head models implementing the geometry and conductivity of the different volume compartments are taken into account. Furthermore the EEG signal requires a stable connection between the electrodes and the skin and can be greatly influenced by potential drifts due to impedance changes at the scalp/electrode contact (e.g., due to perspiration). Since the MEG signal is neither distorted by different tissue conductivities nor influenced by factors like skin or bone conductivity, it overall provides a higher spatial resolution, which can theoretically reach 2-3mm for cortical sources under most favorable circumstances (Yamamoto et al., 1988). However, small head movements in the MEG device (the human head is placed below the MEG sensors, and can only be partially fixated by items such as foam pads) usually limit the achievable spatial resolution. Taken together, although the spatial resolution of MEG might be better than that of EEG, both often end up with a resolution in the centimeter rather than in the millimeter range.

Environmental noise

The recorded electromagnetic fields are fairly small (EEG: µV range; MEG: 50-500ft), so that environmental sources of electric/magnetic noise like induced voltage changes by AC line current (50 or 60Hz) or video monitors (50-120Hz refresh rate) would considerably influence the measured signal. In principle, any large external electric source can induce fluctuations of the measured magnetic and electric field. In addition, disturbing external magnetic fields emerge by opening or closing metal doors in the vicinity of the recording booth. When recording the EEG, the potential of the active electrode is measured against that of a reference electrode, such that external noise that is equally strong at both recording sites should cancel out. The choice of a reference site, however, influences the EEG data as there is no completely electrically neutral site on the head (Luck, 2005, pp. 101-112: Active and Reference Electrodes). For example, if the reference electrode picks up parts of the effect that should be measured, these parts will not be seen in all the other channels that are referenced against that electrode, and if there is strong muscle activity near the reference site, it will contribute to the signal of all other electrodes. Fortunately, these problems are not encountered when recording MEG, since the MEG signal (magnetic field strength) can be measured without reference. However, MEG measurements encounter a huge signal-to-noise problem: The neuromagnetic signal is up to 10^{-9} times smaller than the earth's magnetic field (25-65µT), so that an expensive magnetically shielded recording chamber is required. To compensate for the remaining environmental magnetic noise additional reference sensors are required. Those are placed further away from the subject's head so that they do not pick up the brain's magnetic field, but detect external fields from distant noise sources. But even if the environmental noise can be minimized, there is still significant magnetic noise produced by physiological sources like the human heart, skeletal muscles or eye-movements that has to be dealt with (M. Hämäläinen et al., 1993).

Field distributions and source localization

When interpreting MEG and EEG data, it is important to keep in mind, that the magnetic and electric field distributions that emerge from the same current source will be orthogonal to each other as illustrated in Figure 2.3. Another principal difference between the brain's electric and magnetic field is that the latter is typically dominated by current sources that are tangential to the cortex surface. While the EEG electrodes are sensitive to the electric fields of both radially and tangentially oriented dipoles, the magnetometer coils of the MEG sensors, that are typically oriented tangentially to the head surface, can only measure magnetic flux orthogonal to them as elicitied by tangential but not radial sources (see Figure 2.2). Notably, mathematic calculations show that when considering the human head as a spherically symmetric conductor, a radial current dipole would not be able to produce a magnetic field outside the head anyway (Sarvas, 1987). Thus, while the EEG is sensitive to both the tangential sources in the sulci and the radial sources of the cerebral gyri, the signal of the MEG is dominated by the activity of the tangential sources of the cerebral sulci. However, it should be mentioned, that the MEG is not completely blind to gyral sources as shown by Hillebrand and Barnes (2002). Specifically, they used MRI-

extracted cortical surfaces to construct all possible single source elements (equivalent current dipoles) and analytically compute the proportion of neocortex that is detectable by a whole-head MEG system. Hillebrand and Barnes (2002) found that only very thin strips (~2mm) at the crests of gyri (and the troughs of sulci) have a low detection probability, while gyral sources located towards the sulcal walls possess a large enough tangential component to remain visible for MEG sensors. According to their analyses, even dipoles that are almost radial – forming an angle with the radius of 17° – can have a detection probability of more than 70%. In contrast, Hillebrand and Barnes (2002) found that the detection probability of sources depended highly on their distance to the MEG sensors, which led to the conclusion that source depth rather than source orientation limits the sensitivity of the MEG to activity in the cortex. Despite the differences in the extracranially recorded electric and magnetic fields, both can be used to reconstruct the current source and thus localize the activated cortex site. While it is easy to calculate the field distribution on the head evoked by given intracranial current sources (provided source locations, orientations and the conductivity profile of the volume conductor is known), deriving the current sources from a given field distribution represents a far more complicated problem. According to Helmholtz (1853), there is no unique solution as an infinite number of possible sets of sources can account for the same field distribution. This is referred to as the *‘electromagnetic inverse problem’*. Detailed knowledge about the volume compartments, appropriate a priori assumptions about cortex geometry and suitable source models such as current dipoles or current-distribution models using special estimation techniques like the minimum norm approach (M. S. Hämäläinen & Ilmoniemi, 1984; Fuchs et al., 1999) are necessary to render the inverse problem solvable and reconstruct the anatomical sources underlying the measured electromagnetic brain activity.
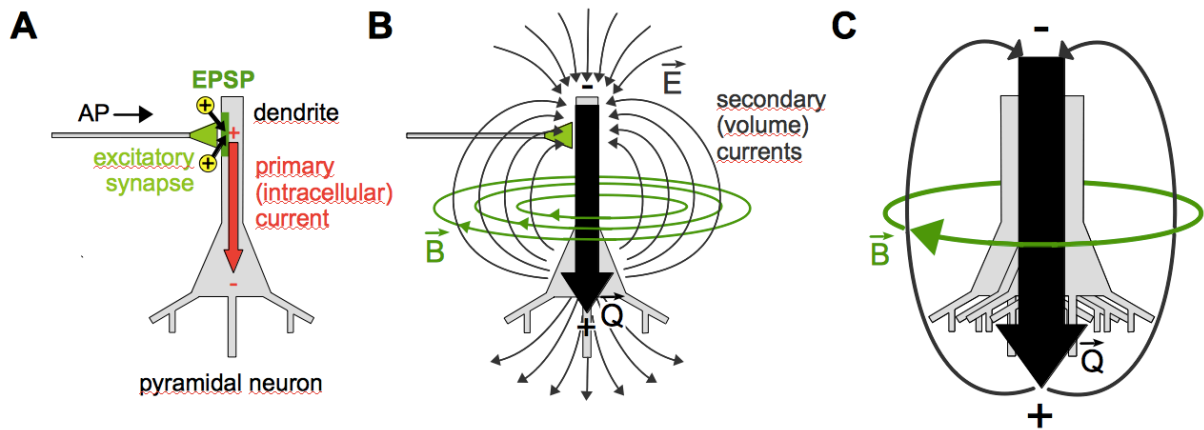
Figure 2.1. EPSP giving rise to a neuronal dipole structure. (A) If an action potential (AP) arrives at an excitatory synapse at the apical dendrite of a pyramidal neuron, the ionic influx of positively charged sodium ions depolarizes the postsynaptic membrane (excitatory postsynaptic potential, EPSP) leading to the so-called primary current inside the neuron (red arrow). **(B)** A neuronal dipole structure ($\vec{Q}$, black) is created with extracellular "secondary" or "volume currents" closing the circuit of the electric field ($\vec{E}$, dark grey). According to the 'right-hand rule' (see text) the primary current induces perpendicular to the electrical current flow a magnetic field ($\vec{B}$, green). **(C)** Synchronous activity of a group of ~50.000 aligned neurons gives rise to a macroscopic dipole that can be detected on the head surface by EEG and MEG.
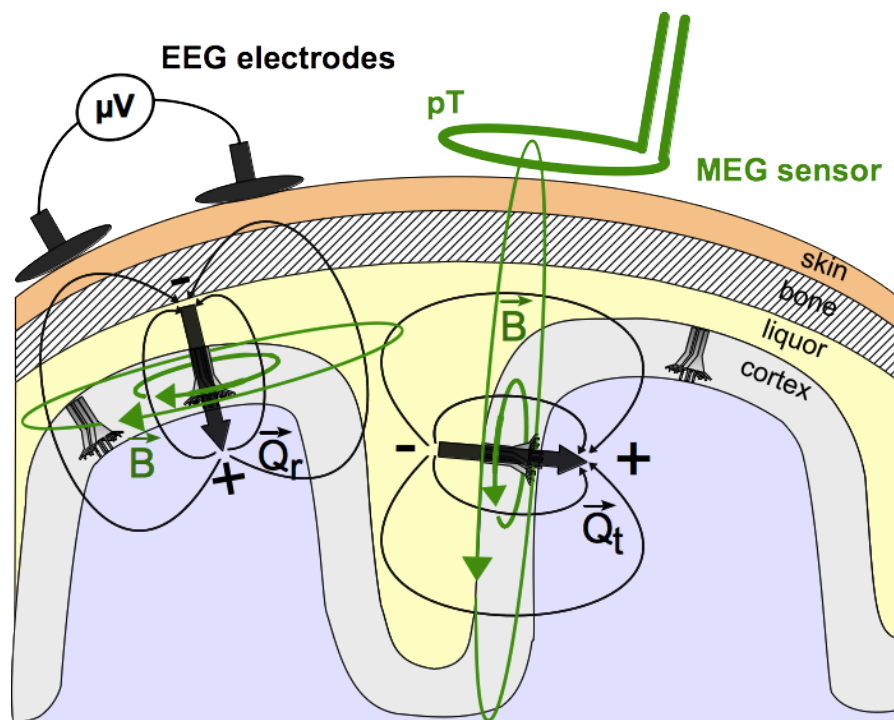
Figure 2.2. Detection of cortical dipoles by EEG electrodes and MEG sensors. In principle, MEG sensors can only detect dipoles with a component tangential to the cortex surface ($\vec{Q_t}$). The magnetic field lines of a radial dipole ($\vec{Q_r}$) do not invade the pickup coil of the MEG sensor. In contrast, the electrical fields (dark grey lines) caused by both dipole types spread through the tissues (volume conduction) towards the head surface, such that the EEG electrodes are sensitive to both tangential and radial dipoles.
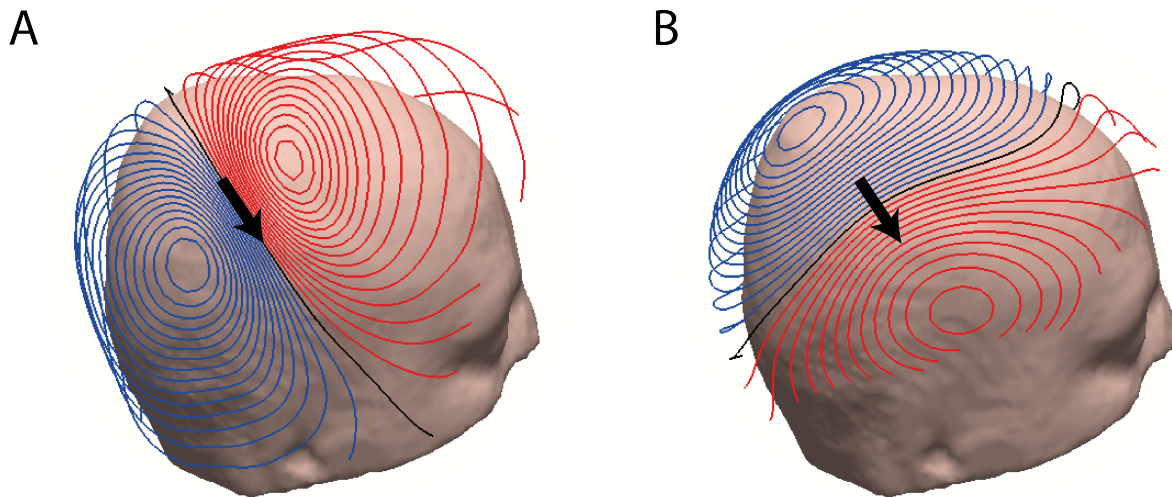
Figure 2.3. Electric and magnetic field distributions. The magnetic **(A)** and electric **(B)** field distributions elicited by the same tangential dipole (black arrow) were simulated using Curry Neuroimaging Suite 7.0.6 SBA (Neuroscan, Charlotte, NC, USA) and a four-compartment model (brain, cerebrospinal fluid, skull, scalp) to approximate the human head. The field distributions detected by MEG and EEG are mutually orthogonal to each other.

2.2. Event-related potentials (ERPs) and event-related magnetic fields (ERMF)

Every sensory, cognitive, or motor event is associated with neuronal activity. Those electric potentials, that display a stable temporal relationship to a definable reference event are called event-related potentials or ERPs (cf. Vaughan, 1969). The corresponding event-related magnetic fields are referred to as ERMF. Unfortunately, the neuronal activity evoked by a single event is fairly small compared to the ongoing background activity of the brain like spontaneous alpha rhythm or physiological noise like heartbeats, eye movements or the contraction of skeletal muscles. In fact, the magnetic fields evoked by sensory stimulation are typically in the range of several tens or hundreds of fT, while the amplitude of the alpha rhythm is about 1-2 pT and the contraction of the cardiac muscle can even reach signal strengths of several tens of pT (M. Hämäläinen et al., 1993). Nevertheless, the event-related activity can be extracted from electromagnetic brain recordings by repeating the event multiple times and averaging the measured brain responses afterwards. A detailed overview of the ERP methodology is provided by Luck (2005). The averaged event-related signal consists of a series of voltage (or magnetic field strength) deflections, which are referred to as components or peaks. In the ERP those components are commonly named after their polarity (P: positive deflection, N: negative deflection) and ordinal temporal position in the waveform (P1 before P2). Each component is associated with certain latencies and field distributions, which can be modality-dependent (e.g., auditiory stimuli evoke different P1s than visual stimuli). Furthermore, the components can be modulated by attentional processes. Spatial attention to a stimulus leads to higher P1 and N1

amplitudes (Mangun & Hillyard, 1991; Anllo-Vento, 1995 ; Mangun, 1995; Hillyard & Anllo-Vento, 1998), with the initial P1 reflecting the spatial selection of the stimulus and the subsequent N1 modulation indexing its discrimination (Mangun & Hillyard, 1991; Vogel & Luck, 2000; Hopf et al., 2002) (see Figure 2.4 A). Figure 2.4 B/C provides a direct comparison of ERP and ERMF waveforms simultaneously evoked by the same visual stimulus. While for the given example, both waveforms at the chosen sensor sites show a comparable modulation sequence with curve deflections of the same polarity within similar time ranges, this similarity is by far no common phenomenom. The electric and the magnetic field of a given cortical activation can differ substantially. An activation successively moving across gyri and sulci will lead to signal changes that vary over time individually for EEG and MEG (cf. section 2.1 above). Thus, the signature of a given effect typically varies dramatically for the ERP and ERMF, not only with respect to the field distribution and waveform polarity, but often also with regard to its precise time course.

For a detailed description of ERP/ERMF correlates of spatial, object- or feature-based attention see sections 1.2.1 - 1.2.3.
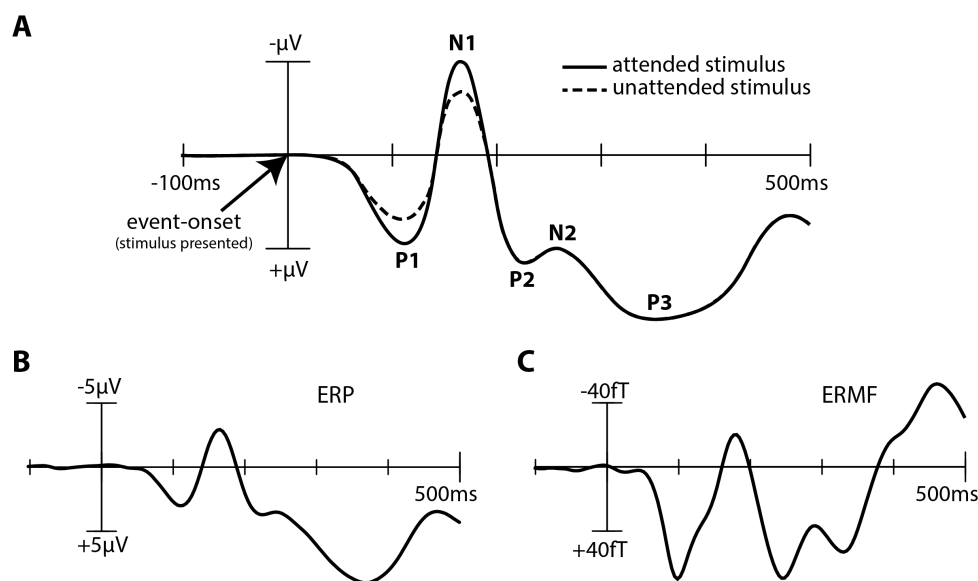
Figure 2.4. ERP and ERMF waveforms. **(A)** Schematic illustration of an event-related potential (ERP) evoked by the presentation of a visual stimulus, which could be either spatially attended (solid line) or unattended (dashed line). The components enhanced by spatial attention (P1, N1) as well as subsequent components (P2, N2, P3) are labelled according to the ERP convention. **(B/C)** The event-related response elicited by a visual stimulus in an attention experiment (average of ~500 presentations of the same stimulus) simultaneously recorded with EEG and MEG. The ERP at a parietal electrode **(B)** and the corresponding event-related magnetic field (ERMF) at a parietal MEG sensor **(C)** were evoked by the same visual stimulus. EEG electrode and MEG sensor were in close proximity. Though the signal can vary substantially for EEG and MEG (see text), the waveforms displayed here show a comparable modulation sequence with curve deflections in similar time ranges.

Caveats / Limitations

Because the signal-to-noise ratio improves with the square root of the trial number, the signal has to be averaged over a large amount of stimulus presentations. That is, to reduce the noise by 50 percent, the number of trials has to be quadrupled. Furthermore, the amount of trials that is necessary to examine an ERP/ERMF component, depends on its size and whether the signal is averaged over several subjects ('grand average'). According to Luck (2005) an ERP experiment dealing with a medium-sized component like the N2 needs approximately 10-20 subjects with each being presented a given stimulus about 150 times. Note that when averging signals across several subjects, it is important to consider that these 'grand averages' usually display smaller amplitudes compared to measurements of single subjects and that the onset and offset of an effect are determined by the fastest and slowest brain responses of individual subjects and not by the mean on- and offset of the effect. Most importantly, when interpreting the change of a certain ERP/ERMF component it should always be kept in mind that the different components overlap with each other (e.g., an increase in the N1 amplitude can lead to a decrease of the P1 amplitude) and that different combinations of the components can sum up to the very same ERP or ERMF waveform. Thus, if components in temporal proximity are modulated in an experiment, it is often impossible to tell which specific component is actually enhanced or reduced. Hence, the factors influencing other components than the one of interest should be kept constant. Since early components like the P1 are influenced by physical stimulus properties like brightness or contrast (Regan, 1989), these properties should not differ across the experimental conditions unless they are the object of investigation. Hence, *always compare ERPs elicited by the same physical stimuli, varying only the psychological conditions* ('*The Hillyard Principle*', Luck, 2005, p. 97).

The last issue that should be mentioned in this section concerns the meaningfulness of the polarity of an observed ERP/ERMF modulation. It would be helpful if the polarity of the ERP or ERMF modulation would reflect whether the underlying process refers to a neuronal enhancement or to a neuronal suppression. Unfortunately, the polarity of the observed ERP deflections gives actually no information about the nature of the underlying neuronal process. Whether one records a negativity or positivity at the scalp surface is determined by the location and orientation of the intracerebral current source and hence, depends on the cortical folding and if the postsynaptic potentials that give rise to the observed surface signals (cf. 2.1) arise at more apical or more basal sites of the pyramidal neurons (see illustration in Figure 2.5).
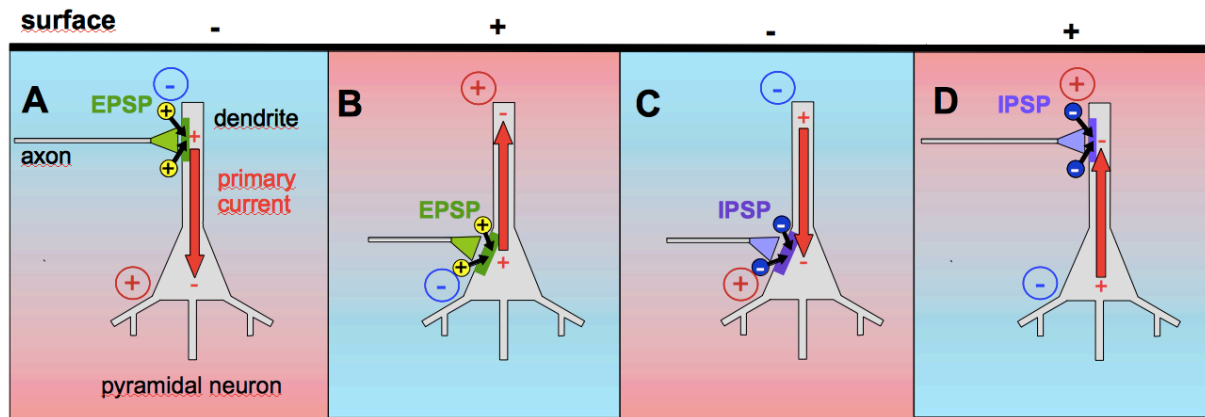
Figure 2.5. Schematic illustration of PSPs arising at apical or basal sites of a pyramidal neuron. **(A/B)** The influx of positively charged sodium ions resulting in an excitatory postsynaptic potential (EPSP) leads to a more negative extracellular environment near the site of the EPSP and a more positive environment at distant sites. **(C/D)** The influx of negatively charged chloride ions giving rise to an inhibitory postsynaptic potential (IPSP) leads to the external cellular environment becoming more positively charged. The polarity observed at the cortical surface (and the direction of the intracellular current determining the direction of the magnetic fields observed in the MEG) depends not only on the type of PSP (excitatory/inhibitory), but also on whether the PSP arises at distal apical sites **(A/D)** or at more proximal basal sites (e.g., the soma) **(B/C)**. Thus, the polarity at the cortical surface or the direction of the observed magnetic field provides ambiguous information about the nature of the underlying neuronal (excitatory/inhibitory) processes.

3.   Materials and Methods

3.1.   General stimulus design and color calibration

All of the reported experiments share the same general stimulus design, which will be described below. Experiment-specific modifications of stimuli and task will be reported individually in the respective methods sections.

General stimulus design

All of the stimuli were designed to assess effects of global color-based selection outside the spatial focus of attention. As illustrated in Figure 3.1, they consisted of a central fixation cross, a bicolored to-be-attended target circle in the left visual field (LVF) and a task-irrelevant unicolored probe circle simultaneously presented in the unattended right visual field (RVF). The circles and the fixation cross were created using MATLAB (MathWorks Inc., Natick, MA, USA) and smoothened with a standard Gaussian filter (mean: 0,0; standard deviation: 1) to prevent sudden luminance changes at the edges. Both circles had a diameter of 3.1° (visual angle) and their respective centers were placed 3.1° below and 4.9° lateral to the fixation cross. Subjects covertly attended to the target on the left while their fixation remained constantly on the central cross. The circle in the LVF was composed of two differently-colored half circles with one half circle always drawn in the target color – defined at the beginning of each experimental block – and the other half circle drawn in a randomly changing distractor color. The subjects were instructed to exclusively attend to the bicolored circle in the LVF and ignore the task-irrelevant probe in the RVF. The task was to report whether the curved section of the half circle drawn in the target color faced to the left or to the right. With the subjects' attention being focused onto the target in the LVF, the brain response to the color probe in the unattended RVF was analyzed as a function of whether the probe color matched the attended color in the LVF, thereby providing a measure of color-based attention outside the spatial focus of attention.

Importantly, the distractor color of the bicolored target circle never matched the simultaneously presented probe color. This was done to prevent the distractor color from interfering with global effects of target color selection. As recently shown with a similar stimulus setup in visual search, a color which is completely task-irrelevant but part of the attended object (like the distractor color) is biased even in other unattended objects (like the color probe in the RVF) (irrelevant feature effect (IFE): Boehler et al., 2011). Therefore a match of distractor and probe color could lead to an unwanted modulation of the measured probe response.
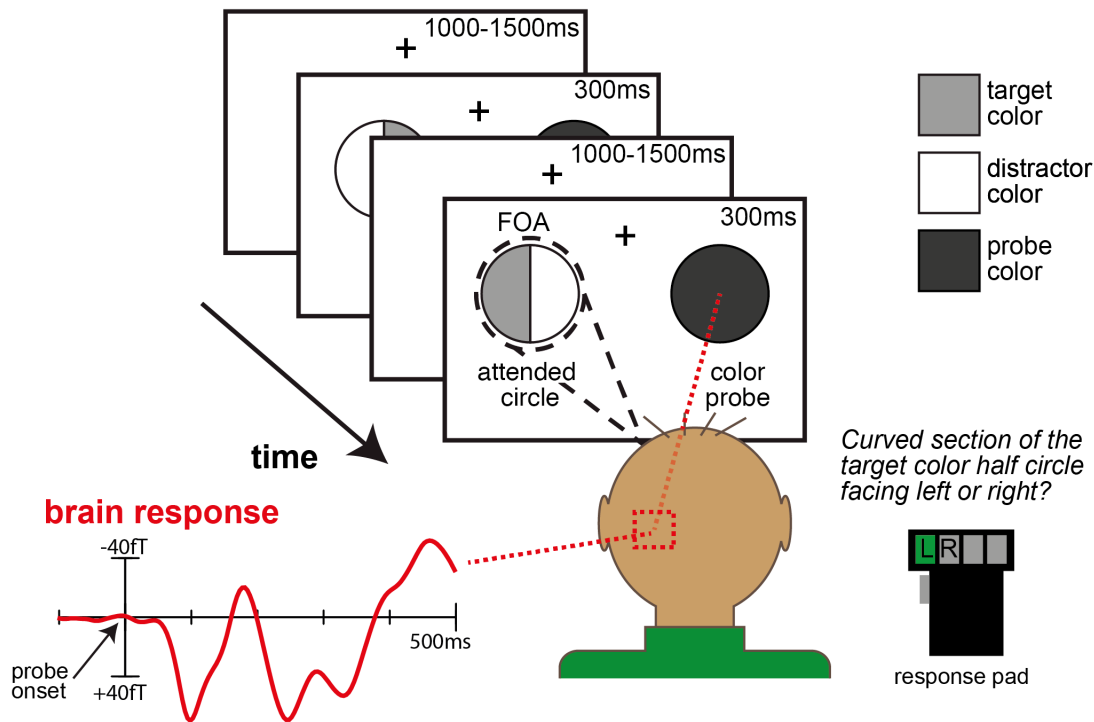
Figure 3.1. General stimulus design. While fixation remained on the central cross, subjects covertly attended to the circle in the left visual field and reported with a button press whether the curved section of the half drawn in the target color faced to the left or right (left: index finger, right: middle finger). The time between the stimulus onsets (stimulus-onset asynchrony, SOA) was varied from 1300-1800ms (rectangular distribution). The simultaneously presented color probe in the right visual field was completely task-irrelevant and never attended. To assess color selection outside the spatial focus of attention, the brain response to the probe (shown here: event-related magnetic response at a selected sensor site) was analyzed as a function of whether it matched the target color presented in the LVF. Note that due to the contralateral retinotopic organization of the visual cortex stimuli in the right visual field are presented in the left hemisphere and vice versa (e.g., Sereno et al., 1995).

Calibration of stimulus colors

To avoid confounding global color-based selection with differences in perceived luminance, the colors used in experiments 1, 2, 3 and 5 (red, magenta, blue, green, yellow, grey) were psychophysically matched prior to the first experiment based on heterochromatic flicker photometry (B. B. Lee et al., 1988). Specifically, one color (here: red) served as the reference background color on which two squares (1.6° visual angle height, 0.34° below and 6.33° left and right to the fixation cross) of the to-be-adjusted color were presented at a 15Hz flicker rate. While the luminance value of the squares' color changed from high to low and vice versa, three experienced subjects had to define the calibration point at which the perceived flicker of the squares – and therefore the luminance difference to the red background – was minimal. The results were averaged across the selected subjects and the resulting color values were subsequently used throughout all sessions of experiment 1, 2 ,3 and 5. Since an additional color

(cyan) was introduced in experiment 4, the whole procedure was repeated in five experienced subjects prior to that experiment. The luminance of the psychophysically matched colors was determined photometrically with the Luminance meter LS-110 (Minolta Camera Co., LTD Osaka, Japan) yielding an average luminance of 44.0 cd/m^2 for all of the used colors (excluding the dark background grey and the fixation cross white). Throughout all experiments the background color of the screen was set to a dark grey (8.3 cd/m^2), while the fixation cross was drawn in a well distinguishable white (120 cd/m^2). The RGB values as well as the luminance values of all colors are summarized in Table 3.1.

Table 3.1. RGB and luminance values. Listed are all the RBB and luminance values of all the colors that were used in the reported experiments.

Color	Experiment	RGB values			Luminance
		R	G	B	[cd/m^2]
Red	1-5	200	000	000	40,5
Magenta	1-3,5	160	000	160	32,0
	4	148	000	148	27,2
Blue	1-3,5	000	000	209	12,5
	4	000	000	165	8,0
Yellow	1-3,5	099	099	000	53,5
	4	105	105	000	59,5
Green	1-3,5	000	127	000	69,0
	4	000	122	000	63,0
Grey	1-3,5	091	091	091	49,0
	4	098	098	098	55,0
Cyan	4	000	113	113	59,0
Dark Grey	1-5, background	040	040	040	8,3
White	1-5, fixation cross	150	150	150	120

3.2. Subjects

All the subjects that took part in the reported experiments were students of the University of Magdeburg. They gave informed consent and were financially compensated for their participation (6 EUR per hour). The participants had normal or corrected-to-normal vision and were all right-handed with the exception of one left-handed participant who took part in experiment 5. All experiments were approved by the ethics board oft the University of

Magdeburg and conducted according to the regulations of the Declaration of Helsinki. Twenty-one subjects (14 females, mean age 25.8) participated in Experiment 1, nineteen (15 females, mean age 26.6) participated in Experiment 2, twenty-two (16 females, mean age 25.9) participated in Experiment 3, twenty-five (15 females, mean age 25.3) participated in Experiment 4 and twenty (13 females, mean age 25.8) participated in Experiment 5.

3.3. Data acquisition

General Procedure

After the EEG cap was placed on the head and it was ensured that the subject was wearing clothing that was free of metal, the subject was positioned below the MEG dewar in a dimmed magnetically shielded recording chamber (μ-metal, Vacuumschmelze, Hanau, Germany), as shown in Figure 3.2. To stabilize the subject's head position within the MEG dewar, foam pads were placed between head and dewar. The program Presentation (Neurobehavioral Systems Inc., Albany, CA) was used to coordinate the presentation of the stimuli, which were back-projected by an LCD projector (DLA-G150CLE, COVILEX GmbH, Magdeburg, Germany) from the outside of the recording chamber onto a partly transparent screen (COVILEX GmbH, Magdeburg, Germany) placed inside the chamber at a viewing distance of 1.0m. The subjects responded with the right hand to the stimuli using a LUMItouch response system (Photon Control Inc., Burnaby, DC, Canada), providing separate buttons for the response alternatives. The magnetically-shielded chamber stayed closed for the duration of the recording session, during which verbal communication was provided by an intercom system. The subjects were monitored via a video surveillance system which displayed the head on a monitor in the control room. The electroencephalogram (EEG) and magnetoencephalogram (MEG) were simultaneously recorded throughout the whole experimental session. EEG and MEG signals were both band-pass filtered online DC-to-50Hz – a range optimal to record ERPs. Specifically, frequencies above 30Hz are typically of no interest in cognitive ERP experiments, such that noise above 30Hz produced by e.g., line current or monitor refresh rates can be filtered out (Luck, 2005, p. 113). Data were digitized for storage with a sampling rate of 254,31Hz. A detailed description of the EEG/MEG recording parameters is provided below in the respective sections.

EEG

The electroencephalogram (EEG) was recorded using a 32-electrode cap (Easycap, Herrsching, Germany) with plastic adapters allowing to mount sintered silver/silver chloride electrodes. As illustrated in Figure 3.3A, those were placed according to the international extended 10-20-system (American Electroencephalographic Society, 1994). An electrode at the right mastoid served as reference during the recording. Activity recorded at the left mastoid served to rereference the data offline to the weighted mean of the left and right mastoid. Specifically, as described by Luck (2005, pp. 107-108) the subtraction of half of the amplitude of the left mastoid

signal from the recorded data leads to an average mastoids reference derivation combining left with right mastoid algebraically. To control for eye-movements, the following three additional electrooculogram (EOG) electrodes were attached to the skin: left and right to the eyes (at the outer canthi) for bipolar horizontal EOG derivation, and below the right eye for a unipolar derivation of the vertical EOG. The impedances between the scalp and the electrode were kept below 5kΩ at all electrode positions by pretreating the skin with the abrasive electrolyte gel Abralyt light (Easycap, Herrsching, Germany). The latter was also filled into the plastic adapters to establish the contact between electrodes and head surface. The EEG signal was amplified using a Synamps amplifier system (NeuroScan, El Paso, TX).

MEG

The magnetoencephalogram (MEG), was recorded with a 248-sensor BTI Magnes 3600 whole-head magnetometer system (4D Neuroimaging, San Diego, CA, USA). A set of built-in reference coils was used to cancel environmental magnetic noise online (Robinson, 1989). To obtain the spatial relationship of MEG sensors, electrodes and the subject's head position, individual anatomical landmarks (nasion, left and right preauricular point) as well as five localizer coils placed at standardized positions on the EEG cap (near inion, vertex, nasion, left and right pre-auricular points) were digitized three-dimensionally prior to data recording using the 3Space Fastrak System (Polhemus, Colchester, VT, USA). In addition, all electrode locations were digitized. The position of the localizer coils relative to the MEG dewar was determined at the beginning of each experimental session. Figure 3.3 B provides a 2D map of the MEG sensor layout and Figure 3.3 C/D illustrates the spatial arrangement of the electrodes and MEG sensors on the subject's head.
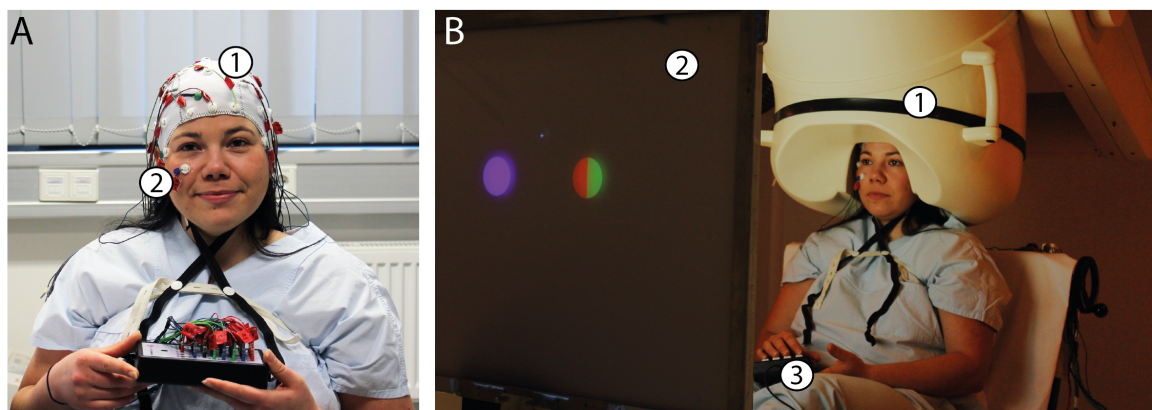
Figure 3.2. **Experimental procedure. (A)** Subject dressed in metal-free clothes with mounted electrode cap (1) and additional electrodes below the right eye as well as at the outer canthi of both eyes for eye-movement monitoring (2). **(B)** The subject was placed below the MEG dewar (1) in a dimmed magnetically shielded recording chamber, viewed the stimuli on the screen (2) and answered the task-specific questions using a response pad (3).
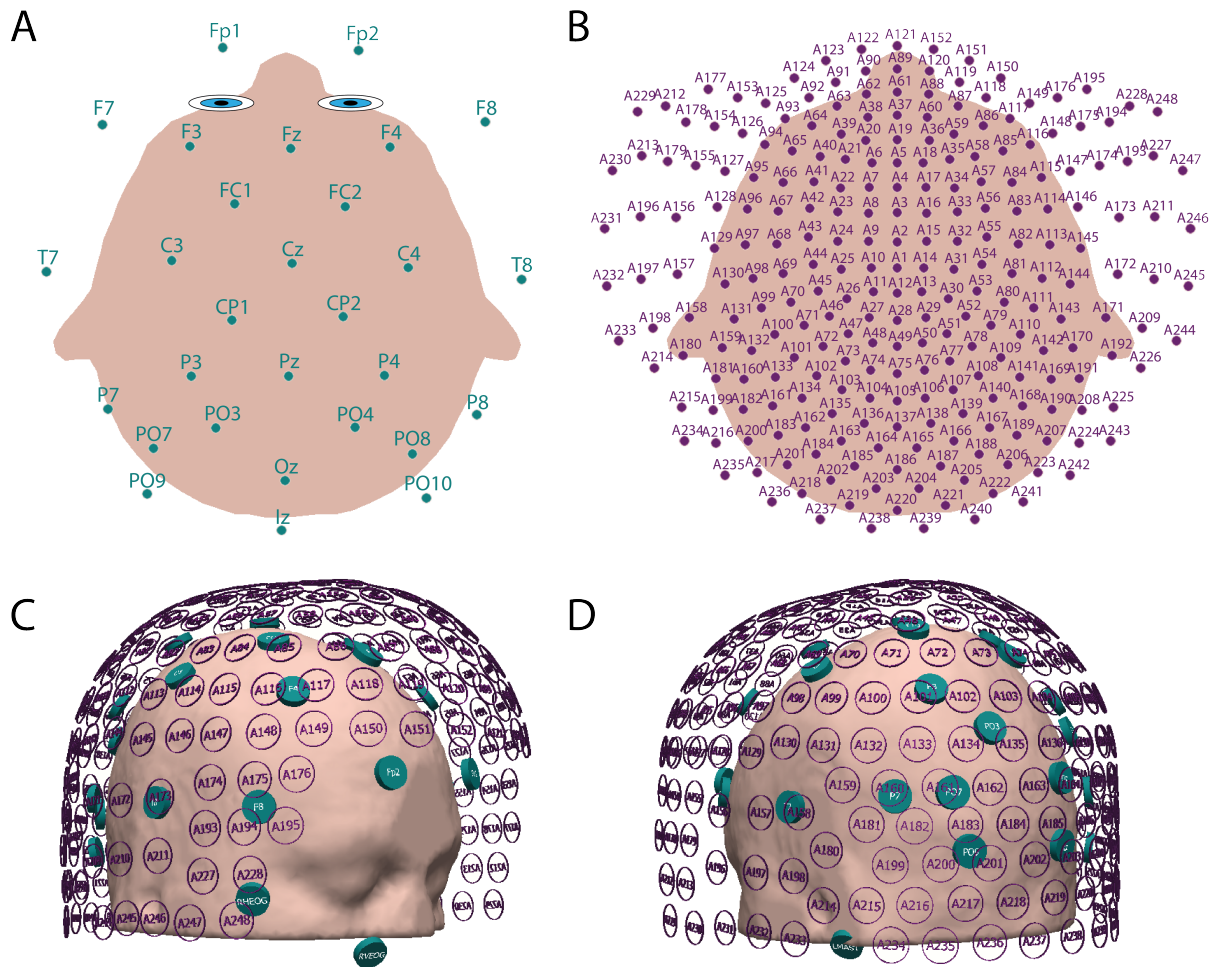
Figure 3.3. Spatial arrangement of electrodes and MEG sensors. The two and three-dimensional head shapes and sensor layouts were obtained by adapting pictures created with Curry 7 Neuroimaging Suite (Compumedics Neuroscan USA Ltd.). The upper panels show two-dimensional maps of the electrode positions (EOG and mastoid reference electrodes not included) **(A)** as well as the MEG sensor positions **(B)**. A bigger and therefore more easily read version of the two-dimensional MEG sensor map is provided in the Supplementary (section S.3, Figure S.**5**.). The lower panels display a frontal **(C)** and a rear view **(D)** of the three-dimensional sensor layout of electrodes (green) and MEG sensors (purple) as used for EEG and MEG recording. The head position within the MEG dewar could individually vary, which was corrected for by the repositioning procedure explained in 3.4.2.

Artifact rejection

After EEG/MEG data acquisition, trials with incorrect responses were removed including early anticipatory responses (< 200ms) and delayed responses (> shortest possible SOA). For the RSVP task of experiment 2, the response could be prepared prior to the query, such that all responses were accepted that were given after the presentation of the last letter and before 800ms. The remaining correct responses were then subjected to an offline artifact rejection using Magnetic Source Imaging (Biomagnetic Technologies Inc., San Diego, USA). Epochs were eliminated when peak-to-peak amplitude measures exceeded a specific threshold. The size of the

artifacts (esp. eye-blinks, muscle tension and alpha rhythm) in relation to physiological noise and ongoing background brain activity differed considerably between subjects. Furthermore, artifacts could be more prominent in the EEG (e.g., muscle tension near the reference electrode) or in the MEG (e.g., heartbeats or environmental magnetic disturbances). The thresholds were therefore determined individually for each subject separately for the EEG (including the EOG) and MEG in the following way: The raw data of each subject were visually inspected and the thresholds were adjusted iteratively until all major artifacts both in EEG and in MEG were removed. Overall this led to 4-16% trial rejection with the threshold values ranging between 1.7 to 3.4 $\times 10^{-12}$ T for the MEG (mean: 2.5×10^{-12} T) and 60 to 130µV for the EEG (mean: 90µV). Of note, epochs were removed separately for EEG and MEG, such that an epoch containing only magnetic noise (e.g., sensors disturbances) was removed from the MEG data, but could be preserved in the EEG data. If a single sensor of the MEG showed longer lasting severe disturbances during the measurement or delivered no signal at all, it was interpolated by the signal of its surrounding neighbours.

3.4. Data analysis

The following sections describe the data analysis of the recorded EEG, MEG and behavioral data.

3.4.1. Event-related potentials/ magnetic fields

For primary data analysis, ERPs as well as ERMFs were epoched from -200 before to 700ms after stimulus onset. All trials belonging to the same experimental condition were averaged within individual subjects. Each target and probe color combination (e.g., target red, probe blue) served as a separate condition subsequently collapsed over specific colors for further data analysis (e.g., probe color matching target color). To yield 'grand averages' the data of each experimental condition was additionally averaged across all subjects that took part in the experiment. For MEG data, the individual datasets were aligned before computing the 'grand average' to account for differences in the subjects' head positions with respect to the MEG sensory array (see section 3.4.2, Grand average analysis: Alignment of individual head positions). The resulting ERP/ERMF waveforms were plotted from -100 to 500ms using the Event-related Potential Software Sytem ERPSS (Event-Related Potential Laboratory, University of California San Diego, La Jolla, CA, USA). Before visualization waveforms were smoothed in the temporal domain with a Gaussian filter ("gauss.l.2.0", time domain standard deviation of 2 sample points). Smoothing was applied exclusively for plotting purposes.

Statistical validation

To validate the amplitude differences between conditions in the ERP and ERMF waveforms, functions based on ERPSS (Event-Related Potential Laboratory, University of California San

Diego, La Jolla, CA, USA) were used to perform a time-sample by time-sample sliding window t-test (window width: 30ms) in the time range between 0 and 500ms after stimulus onset on the unfiltered waveforms. To correct for multiple comparisons (Bonferroni correction), the number of independent hypotheses being tested was estimated by the number of independent variance components in the data. The general idea behind this approach was motivated by Guthrie and Buchwald (1991, p. 241) where the amount of autocorrelation of the data was taken into account for testing the statistical significance of difference potentials. The processes underlying the ERP/ERMF generation will have some degree of statistical continuity because of high correlation between consecutive time samples (autocorrelation). Importantly, the number of independent hypotheses decreases with the amount of autocorrelation in the data. Accordingly, the amount of statistically independent variance components and not the number of time samples tested should be taken to define the degree of the Bonferroni correction. To derive the number of independent variance components in the tested time range, for each experiment a matrix containing the waveforms of the reported experimental conditions (time series of amplitude values) of all subjects at all selected sensor sites was created. Its correlation matrix over time samples (variables) was subjected to an eigenvalue decomposition. The number of eigenvalues > 1 (that is, variance components explaining more than one time sample) was taken as the level of independent variance in the data. The significance level was then corrected for multiple comparisons by dividing the nominal significance level by this number. The following numbers of independent variance components were estimated for the individual experiments: experiment 1 = 11 (MEG) / 12 (EEG), experiment 2 = 12, experiment 3 = 12, experiment 4 = 13, experiment 5 = 14. For the comparison of different colors in experiment 1 (MEG), numbers of independent variance components were estimated separately for the colors, yielding 15 for red, 14 for magenta and 12 for blue.

3.4.2. Current source analysis

Since the MEG data provide the better resolution (cf. section 2.1) only the MEG data were used for the CSD estimates. Note, the field distributions of EEG and MEG were consistent, with the EEG giving no reason to expect different or additional sources (see analysis of experiment 1, section 4.1.3).

Grand average analysis

Source analysis was done with Curry 7 Neuroimaging Suite (Compumedics Neuroscan, Compumedics USA, Ltd., Charlotte, NC, USA) using a distributed source model based on the minimum norm least squares (MNLS) approach (M. S. Hämäläinen & Ilmoniemi, 1984; Fuchs et al., 1999). The inverse modeling was constrained by realistic anatomical data of the MNI (Montreal Neurological Institute) brain (ICBM-152 template, average of 152 T1-weighted stereotaxic volumes of the ICBM project). The volume conductor and current source compartment of the MNI brain were derived by 3D-surface segmentations (boundary element

method) of the cerebrospinal fluid space and the grey matter layer, respectively (Fuchs et al., 1998). The minimum norm approach is known to show a stronger bias towards superficial sources than LORETA-based estimates (Fuchs et al., 1999). Where the localization of deeper cortical activity was required (i.e., anterior cingulate cortex, experiment 1, see Supplementary section S.2.2), the sLORETA estimates were computed (standardized low resolution brain electromagnetic tomography) as implemented in Curry 7 Neuroimaging Suite (Pascual-Marqui, 2002). The sLORETA was calculated on a 3D grid (3mm spacing) covering the whole MNI brain with segmentations of the cerebrospinal fluid serving as volume conductor.

Alignment of individual head positions (repositioning)

The subjects were seated below a rigid dewar containing the MEG sensors. Because the subjects' head positions varied with respect to the MEG sensor array, the individual MEG datasets had to be aligned before computing the grand average across subjects. Specifically, the data measured with the subject's individual sensor positions were repositioned to reference sensor locations representing the most canonical position of the sensors relative to the anatomical landmarks. The reference sensor set was selected from 1500 MEG recording sessions and was the one that best matched the mean distance between five selected sensors (A214, A226, A121, A1, A220) and the spatially corresponding anatomical landmarks (left pre-auricular point, right pre-auricular point, nasion, caesion, inion), and that best resembled the mean head size (as derived from the landmarks). Repositioning was performed in the following way. For each subject, the individual leadfield (a matrix containing the projection weights of all dipoles in the source space on the different MEG sensors) was computed with Curry 7 Neuroimaging Suite using the MNI brain as source space and volume conductor model. By (pseudo-)inverting the individual leadfield matrix (MNLS approach) the subject's dataset was transformed from the sensor- into the source-space of the MNI brain and afterwards backprojected into the sensor-space of the reference sensor set by a forward projection using the leadfield of the reference sensor set. This way, the individual data of the subjects were aligned as if they would have been recorded with the reference sensor positions (i.e., the same reference head position), as schematically illustrated in Figure 3.4.
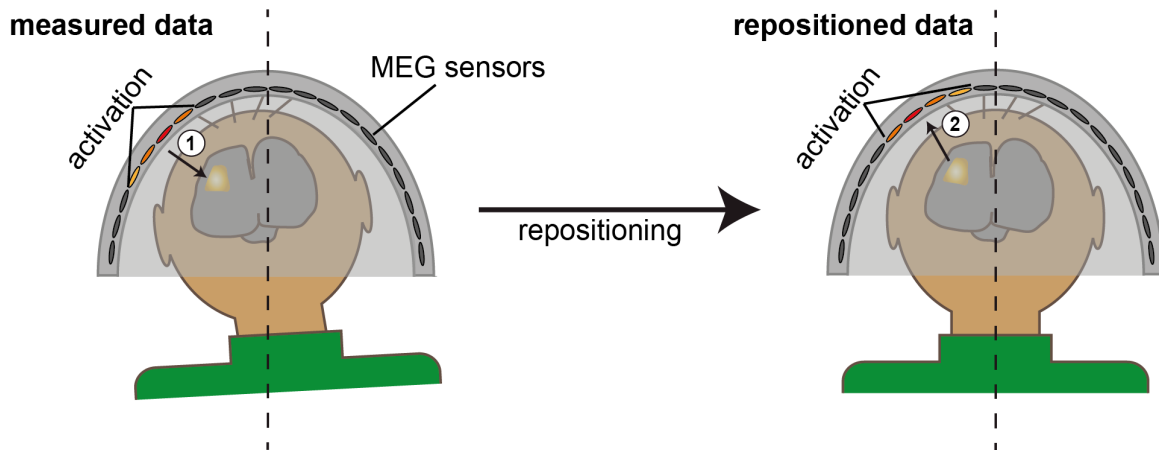
Figure 3.4. **Repositioning of individual datasets**. **(1)** With the individually obtained leadfield and a MNLS account the measured sensor data were converted into the source space localizing the current source (here shown as yellow activation). **(2)** The reference leadfield belonging to the reference head position (here: more vertical) was then used to calculate a forward solution resulting in those sensor data that would have been measured if the subject's head would have had the same spatial relationship than the reference head-sensor configuration. Thus, after repositioning, the source activations in the same brain region should for all subjects be represented by activations of similar MEG sensors facilitating a grand average across sensor datasets of different subjects.

Single subject analysis

Although the individual datasets were repositioned prior to the grand average analysis as described above, differences between individual brains (e.g., size, cortical folding) as well as subject specific variations in the time courses of the investigated effects limit the precision of the source localization when data are averaged across subjects. Furthermore, since sources found in a grand average are always the result of the averaging across subjects, they do not necessarily resemble the precise source location of any one subject. Thus, it would be desirable to gain information about the precise source location within single subjects. Unfortunately, with the present experimental design the statistical power gained in a single observer is comparably low and in most cases not sufficient for a reliable source localization. Fortunately, all of the reported experiments contained at least one condition that was comparable to the original experimental setup of experiment 1 (i.e., color/shape task of experiment 2, distractor-present condition of experiment 3, one-/two-color condition of experiment 4 and discrimination task of experiment 5) so that the data could be averaged across these conditions prior to source analysis to increase the signal-to-noise ratio. Therefore, current source analysis could be done in four selected subjects that took part in at least three of the reported experiments. Analogously to repositioning data for the grand average analysis, the datasets of each subject were aligned with respect to the most canonical dataset among them (the one coming closest to the mean head-to-sensors position of the specific subject) prior to averaging. Source analysis on each subject's average dataset was performed using the minimum norm least squares (MNLS) approach as

implemented in Curry 7 Neuroimaging Suite. The inverse modeling was constrained by subject-specific anatomical data of the volume conductor and current source compartment obtained from segmentations of high resolution MR scans (3T Siemens Trio Scanner: T1-weighted three-dimensional spoiled gradient echo sequence; field of view 25 x 25 cm; 256 x 256 matrix; 124 slices; slice thickness 1.5 mm; in plane resolution 0.97 mm x 0.97 mm; echo time 8 ms; repetition time 24 ms; flip angle 30°). The segmentation of the cerebrospinal fluid space – serving as volume conductor – was performed with Curry 7 boundary element method, Fuchs et al. (1998), for the surface segmentations of the subjects' individual grey matter layer – serving as current source compartment – routines of the free-available FreeSurfer software (V.5.1.0) were used.

3.4.3. Retinotopic mapping

To be able to localize the effects of global color-based attention as precisely as possible, retinotopic mapping was done in the four individual subjects selected for single source analysis (see 3.4.2). Specifically, the individual borders of the early visual areas (V1-V4) were determined with functional magnetic resonance imaging (fMRI) using standard phase-encoded retinotopic mapping (Sereno et al., 1995; Engel et al., 1997). Subjects were presented contrast-reversing rotating-wedge and expanding/contracting-ring checkerboards while the responses to these stimuli were recorded with the fMRI. The stimuli passed cyclically consecutive regions of the visual field, leading to a wave of neural activity traveling through the retinotopically organized early visual areas: topographic cortex locations responding to a specific polar angle (angle from the center-of-gaze, assessed by rotating wedges) or eccentricity (distance from the center-of-gaze, assessed by expanding/contracting rings), corresponded to a certain phase within the stimulus cycle (therefore 'phase-encoded' retinal stimulation). The stimuli for the retinotpic mapping were taken from a circular patch of 36 x 36 isopolar and eccentricity scaled checkerboard segments with each segment having a width-to-radian ratio of 1:2. The wegde stimulus corresponded to one quadrant (90°) of the circular patch rotating 20°/TR either clock- or counterclockwise. The ring stimulus was composed of 9 eccentricity segments (25% of the circular patch) and could expand or contract with 2 out of 18 eccentricity steps per TR. All subjects performed eight blocks, two of each possible stimulus type (wedge rotating clock- or counterclockwise, ring expanding or contracting), with each block containing ten full cycles (one cycle = 18 TRs) of stimulation. To control for fixation, the subjects were not only asked to maintain the fixation at the central cross, but also to report the onset of a small dot, randomly appearing every 166-8300ms in the middle of the fixation cross. The functional MRI data were acquired according to the following parameters: TE = 30ms, TR = 2sec, 90° flip angle, 2.0 x 2.0 x 2.0 mm voxel size and 28 coronal slices perpendicular to the calcerine fissure. The functional scans were realigned to reduce movement artifacts, resliced and smoothed with a kernel of 2mm. Anatomical data for the structural segmentation of the cortex were provided by a high-resolution anatomical scan (3T Siemens Trio Scanner: MPRAGE-volume, 1x1x1 mm resolution) performed for each subject prior to the functional scans. For the segmentation as well as the subsequent unfolding of the cortical surface ('inflating'), routines of the open source software

suite FreeSurfer (V.5.1.0) and the FMRIB Software Library (FSL, http://www.fmrib.ox.ac.uk/fsl/) were used.

LOC localizer

Parts of the activations of interest of the 'grand average' data seemed to be located in a more anterior-lateral ventral occipito-temporal cortex region located anteriorly beyond V4 (see 4.1.3). To investigate whether these activation parts originated from the lateral occipital complex (LOC), a region involved in perceiving object shape (Kourtzi & Kanwisher, 2000), the subjects performed an additional localizer scan to identify the LOC. The subjects were presented a rapid stream of pictures (9.2° x 6.9° visual angle) with twenty different objects taken from the Amsterdam Library of Object Images (ALOI, http://aloi.science.uva.nl). Objects were presented in four different versions either as a grey-scale object, as line drawing (only rudimentary object boundaries shown) or as scrambled versions of either the grey-scale or the line drawing. Pictures of the same version (e.g., line drawings) were presented blockwise with each being displayed for 250ms followed by a blank interval of 550ms. Subjects performed four blocks of each image version in a pseudo-randomized order resulting in a total of 16 blocks. To localize the LOC, the brain responses to scrambled pictures were contrasted to those of the respective intact versions (grey-scale objects or line-drawings).

3.4.4. Behavioral data

The temporal onsets and the identity of the stimuli and given responses were registered by the program that coordinated the stimulus presentation (Presentation, Neurobehavioral Systems Inc., Albany, CA). Performance and reaction times were computed using MATLAB (MathWorks Inc., Natick, MA, USA). Accordingly to the ERP/ERMF data only responses given in a realistic time range were considered (between 200ms and the shortest possible SOA, cf. section 3.3 Artifact rejection). For the RSVP task of experiment 2 responses given between the presentation of the last letter and 800ms were accepted. The reaction times were calculated based on correct responses only. For statistical validation the data were analyzed with analysis tools of the software package SPSS (SPSS Inc., Chicago,IL, USA) (repeated measures ANOVAs, Student's t-tests).

4. Experimental series

Overview of the conducted experiments

Experiment 1 served to establish the effects of global color-based attention (GCBA) in the EEG and MEG response. The stimulus configuration of experiment 1 was used as a control condition in the subsequent experiments so that experimental effects could always be directly compared with the original effects found in experiment 1. **Experiment 2** was designed to control whether color imbalances or other physical parameters of the general stimulus design accounted for the GCBA effects observed in experiment 1. Having ruled out such confounds, **experiment 3** addressed the question as to whether color competition in the focus of attention accounts for global color-based selection. To this end, the competing distractor color in the focus of attention was removed. This experimental manipulation did not eliminate the modulations of GCBA. Furthermore, experiment 3 suggested that effects of GCBA are elicited when the discrimination of a colored object does not explicitly require color discrimination itself (implying an object-based mediation of GCBA). **Experiment 4** went a step further by showing that initial parts of the global color-based modulation were even present for colors that were task-relevant but absent from the FOA. Since colors that were absent from the FOA were also not contained in the target object, object-based mediation could be ruled out for these early parts of GCBA. **Experiment 5** finally showed that all effects of GCBA were eliminated under conditions of a pure onset-detection task, suggesting that the active discrimination of the colored object is needed for effects of GCBA to arise.

Throughout all experiments EEG and MEG were simultaneously recorded. The data analysis of experiment 1 provides a characterization and comparison of the EEG and MEG field distributions and waveforms. For all subsequent experiments (2-5) only the MEG data are shown.

4.1. Experiment 1: GCBA under conditions of color competition

4.1.1. Motivation

GCBA refers to the prioritized selection of colors outside the focus of attention in case they match the currently-attended color. Effects of GCBA were proposed to depend on feature competition in the focus of attention (Sàenz et al., 2003; Zhang & Luck, 2009). The first experiment was performed to characterize the electromagnetic correlates of global color-based selection under conditions of color competition in the focus of attention. Note, the experimental setup of experiment 1 will serve as a control condition in all subsequent experiments, so that their effects can be compared directly to the 'reference' effect established in experiment 1.

4.1.2. Methods

Subjects

Twenty-one subjects (14 females, mean age 25.8 years, all right-handed) participated in Experiment 1.

Stimuli and Task

The stimulus design is illustrated in Figure 4.1A. The stimulus geometry (size and position of the items) and timing was equivalent to that described in the general stimulus design (see 3.1). The RGB and luminance values of the used colors are listed in Table 3.1 of section 3.1. The subjects' fixation remained on the central cross while they covertly attended to the bicolored circle in the left visual field. One half of the circle was drawn in the target color, which was assigned at the beginning of each experimental block (red, magenta or blue). Subjects were to report with a two-alternative button press whether the curved section of the half circle drawn in target color faced to the left or right (left: index finger, right: middle finger). The color of the other half circle (distractor half circle) varied from trial to trial (green, grey or yellow). The task-irrelevant unicolored probe was simultaneously presented in the right visual field. The probe color was randomly chosen from the three possible target colors (red, magenta or blue) on each trial. Thus, the probe's color matched the target color on one third of the trials (match trials, M) while it differed on the remaining trials (non-match trials, NM). Effects of GCBA were assessed by comparing the brain response contralateral to the unattended color probe (left hemisphere) by subtracting non-match trials from match trials (M-NM difference). The current experimental design allowed for two different match to non-match comparisons:

a) the compared match and non-match trials contained the same target color, but probe color differed (*target color constant* non-match)

b) the compared match and non-match trials contained the same probe color, but target color differed (*probe color constant* non-match)

Thus, depending on which non-match trials were chosen either the probe color or the target color was kept constant in the M-NM difference as illustrated in Figure 4.1B. Importantly, comparing the match to the *probe color constant* non-match allowed to compare the brain's response to physically identical probes when attending to different target colors. The observed effects for the individual colors as well as for the probe and target color constant conditions were quite similar (see Supplementary section S.1 for ERMF data and Supplementary section S.2.1 for behavioral data). The data were therefore averaged across all colors and types of non-match trials in all experiments to increase the overall statistical power.

Each subject performed 195 trials per block and a total of nine experimental blocks. The block order was randomly drawn from a set of six possible block orders each with three blocks of every

target color and no repetition of the same target color on subsequent blocks. This yielded a total of 585 match and 1170 non-match trials in each subject.
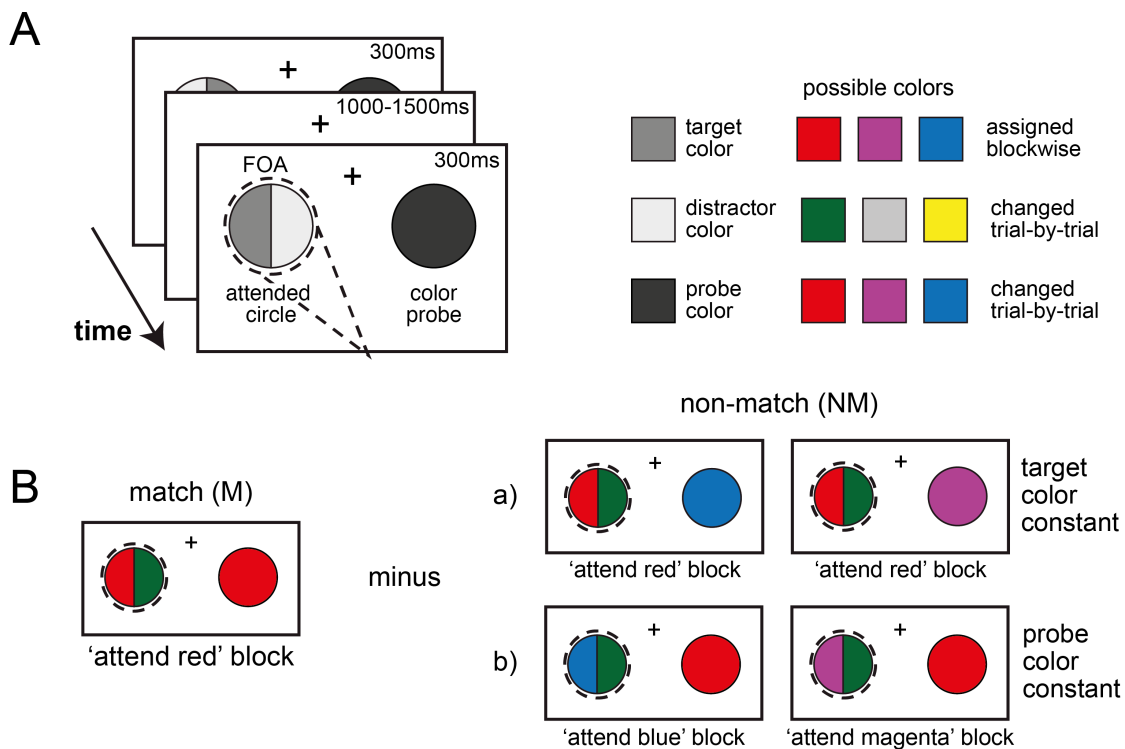
Figure 4.1. Stimulus setup for experiment 1. (A) The stimulus was composed of a centered fixation cross, a bicolored circle in the left visual field within the spatial focus of attention (FOA) and a uniformly colored probe in the right visual field. The target color was constantly either red, magenta or blue throughout an experimental block while the distractor color and probe color varied randomly from trial to trial between grey, yellow and green (distractor) or red, magenta and blue (probe). The subject was to report with a button press whether the curved section of the half circle drawn in the target color faced left or right. **(B)** The response to the probe was analyzed by subtracting conditions in which it differed from the target color (non-match, NM) from conditions where it matched the target color (match, M). The trials were exemplary chosen from trials of the match condition of 'attend red' and the corresponding non-match conditions. Depending on whether non-match trials were taken from same ('attend red') or different experimental blocks ('attend blue' and 'attend magenta') either the target color (a) or the probe color (b) was constant in the match vs. non-match comparison.

4.1.3. Results

Behavioral Performance

The behavioral performance is summarized in Figure 4.2. Response accuracy (percentage of correct responses) and response time are compared for match and non-match trials. While the response accuracy is equally high for both trial types, the responses are slightly slower on match trials. A repeated measures ANOVA with the factor MATCH (match/non-match) revealed no

significant effect of response accuracy (F[1,20] = 0.23, p = 0.63), but a significant effect of response slowing for match trials (F[1,20] = 29.32, p < 0.0005). A subsequent more detailed analysis showed that the slowing on match trials was due to a prolonged response time for the target half circles facing to the left, which was not fully compensated by a response speeding for the target half circles facing to the right. The Supplementary section S.2.1 provides a detailed analysis of this finding for all experiments as well as for individual colors and different non-match conditions (target vs. probe color constant) of experiment 1.
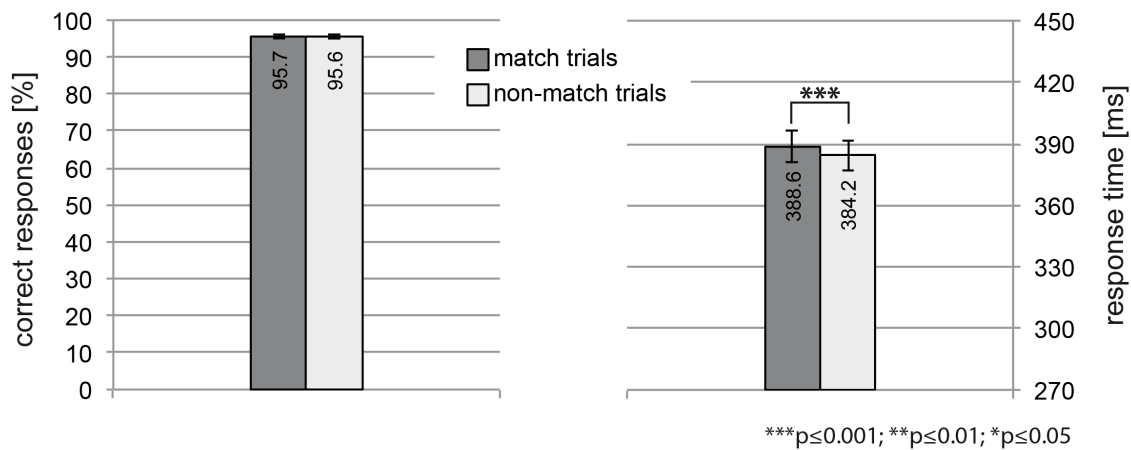
Figure 4.2. **Behavioral performance of experiment 1**. The percentage of correct responses and the response time for match (dark grey) and non-match (light grey) trials are displayed here. The error bars reflect the standard error of the mean (SEM). There was no difference in response accuracy, but a small significant increase in response time for match compared to non-match trials.

Event-related potentials and event-related magnetic field responses

The ERPs and ERMFs elicited by the unattended probe presented in the RVF were analyzed as a function of whether the probe's color matched the currently-attended target color in the LVF (match trials, M) or not (non-match trials, NM). As described above, non-match trials were subtracted from match trials with the modulation difference serving as an index of global color-based attention (see illustration in Figure 4.3).

ERP

ERMF
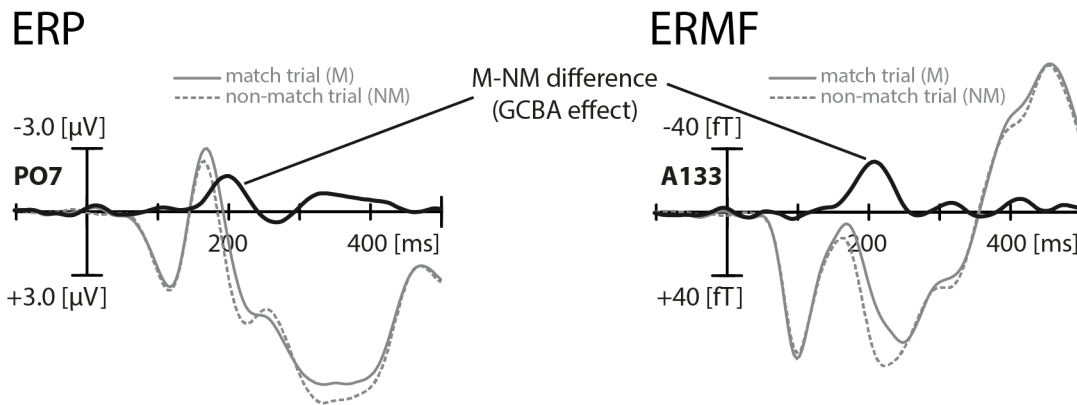
Figure 4.3. Derivation of GCBA effects. Effects of GCBA were assessed by analyzing the response to the unattended color probe in the RVF. Trials on which the probe did not match the color currently attended in the LVF (non-match trials, NM) were subtracted from trials where it did match (match trials, M). Here schematically shown for the grand average data of experiment 1 (averaged across subjects) and the measured signals of an electrode (PO7) and a MEG sensor (A133) located contralateral to the probe close to the left visual cortex. The M-NM response difference served as an index of GCBA.

Grand average data

Figure 4.4 shows the M-NM difference of the grand average across all subjects. The displayed sensor/electrode sites were chosen close to the maximum field responses at time-points of modulation maxima. The shown ERMF waveforms were collapsed by averaging across one sensor at the efflux maximum and one at the influx maximum. The ERP waveforms represent the response at an electrode close to the negative field maximum (200ms, black trace), or the response collapsed over electrodes at corresponding positive and negative voltage maxima (280ms, grey trace). To account for the opposite polarity of the ERMF efflux and influx waveforms, the efflux response was reversed in polarity prior to averaging. To account for the opposite polarity of the ERP waveforms at the positive and negative voltage maxima, the waveform at the positive voltage maxima was reversed before averaging.

Both the ERPs and ERMFs reveal that global color-based selection is indexed by an early modulation around 200ms (black waveform) and a late modulation around 280ms (grey waveform). There is a third effect showing a maximum at 346ms. As detailed in the Supplementary section S.2.2, this effect turns out to reflect a form of response-conflict.

When comparing the field distributions of the early and late ERP and ERMF modulation, the field effects are orthogonal to each other as would be expected for EEG and MEG data (cf. 2.1, Figure 2.3). The late ERMF modulation appears as a simple posterior propagation of the early modulation effect (black/grey ellipses). For the ERP field, the situation is more complicated. For the early modulation only the negative, but no corresponding positive voltage maximum can be seen. Hence, only one electrode was chosen to display the respective early modulation over time. For the late modulation, instead, positive and negative field components are visible and the signal

could be collapsed across electrodes near the positive and negative voltage maximum. Statistical validation of the modulation effects was done by sliding window t-tests on the selected single or collapsed sensors comparing the waveforms of match and non-match trials between 0 and 500ms after stimulus onset (30ms window width, $p < 0.05$, corrected for multiple comparisons as described in 3.4.1). As indicated by the black and grey horizontal bars in Figure 4.4 (time ranges of significant waveform differences), the early modulation onsets at about 160ms while the late modulation starts 90ms later at about 250ms.
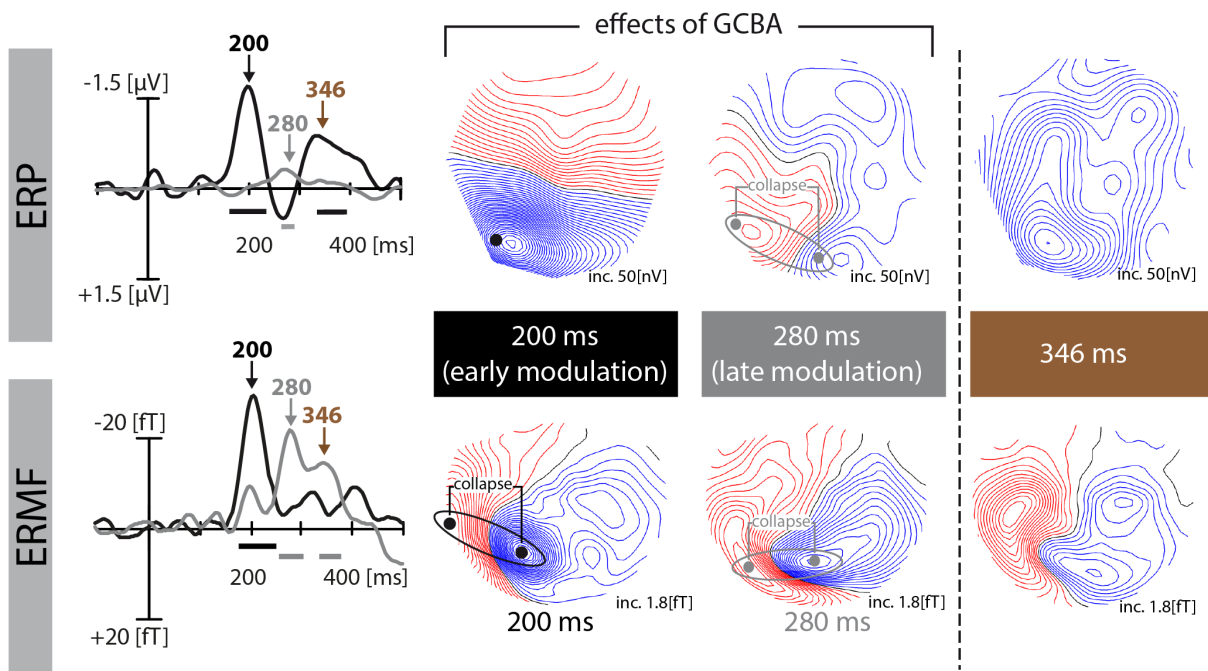
Figure 4.4. **ERP and ERMF responses of experiment 1 (grand average data)**. The field distributions of the match minus non-match (M-NM) differences are shown at time points of modulation maxima. The corresponding ERMF waveforms of the early (black trace) and late (grey trace) GCBA modulation reflect the averaged signal of selected sensor sites close to the efflux maximum (polarity inverted before averaging) and influx maximum (black/grey dots). The corresponding ERP waveform of the late (grey trace) GCBA modulation reflects the averaged signal of selected electrode sites close to the positive voltage maximum (polarity inverted before averaging) and negative voltage maximum (black/grey dots). For the early ERP modulation only one electrode near the negative field maximum was chosen to display the effect (no corresponding positive voltage maximum visible). Time ranges of significant response differences (M vs. NM comparison, sliding window t-test, $p < 0.05$, corrected for multiple comparisons as described in 3.4.1) are highlighted with black/grey horizontal bars. Both ERPs and ERMFs show an early and a late modulation. The third effect around 346ms presumably reflects a form of response conflict, discussed in the Supplementary section S.2.2.

As mentioned above, the field distributions of EEG and MEG are orthogonal to each other, as expected for electric and magnetic fields generated by a common underlying cortical source (cf. 2.1, Figure 2.3). To confirm that the observed EEG and MEG field distributions reflected the same underlying source activity, the early and late effect were modeled with single equivalent dipoles using Curry 7 Neuroimaging Suite (Compumedics Neuroscan, Compumedics USA, Ltd., Charlotte, NC, USA) and the Montreal Neurological Institute brain, ICBM-152 template with a three-layer

conductivity model (cerebrospinal fluid, bone, skin). The dipoles were manually adjusted until the field distributions calculated by a forward solution closely matched those actually recorded in the experiment. As shown in Figure 4.5, the MEG and EEG fields of the simulated early and late dipoles fit very well the recorded fields, affirming that the observed EEG and MEG data refer to the same underlying cortical current sources.
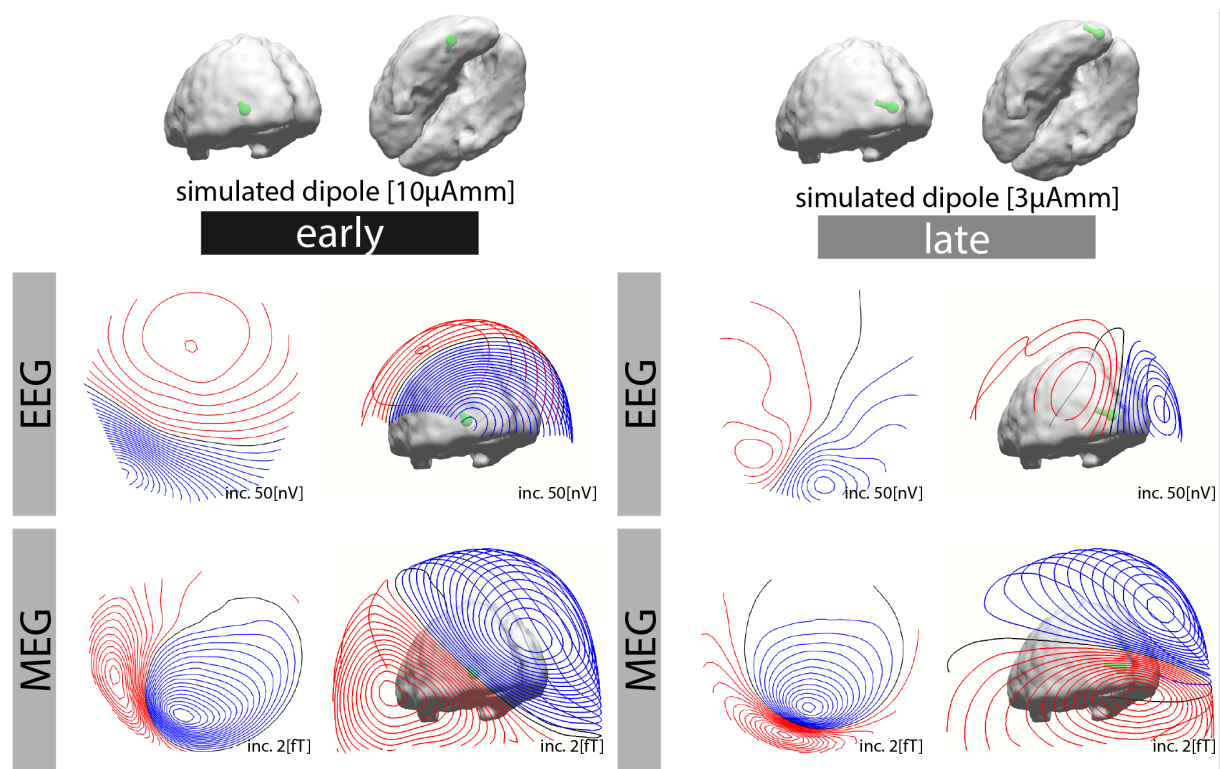
Figure 4.5. Dipole simulation of the early and late effects of GCBA. To confirm the consistency of the measured EEG and MEG field distributions, Curry 7 Neuroimaging Suite was used to model the early and late GCBA modulation each with a single dipole, whose strength, location and orientation was adjusted to come as close as possible to the originally measured field distributions. Displayed are the flat and 3D maps of the EEG and MEG field distributions as calculated by a forward solution using the source compartment and three-layer conductivity model (cerebrospinal fluid, skull, skin) of the MNI brain. The similarity of the simulated with the actually measured data (cf. Figure 4.4) underlines the consistency of the observed EEG and MEG field distributions that indeed seem to display acitivity of the same cortical sources.

Figure 4.6 replots the ERMF responses of experiment 1 (grand average data across all subjects) together with results of an independent component analysis of the respective ERMF responses, as well as corresponding current source density estimates (CSD). An independent component analysis (ICA) was computed to affirm that the field distributions of the early and late GCBA effect reflect statistically independent modulations that belong to different cortical sources. The ICA decomposes the EMRF data into maximally independent activity patterns (component processes), each reflecting a different underlying source configuration (Makeig et al., 1996; Onton & Makeig, 2006). Apparently, the two ICA components explaining the largest amount of variance in the data (IC-1 [20.3%] and IC-2 [18.4%]) perfectly match the time course and spatial field

distribution of the early and late GCBA modulations (see Figure 4.6). Hence, it can be assumed that the early and late phase of GCBA indeed arise from spatio-temporally independent cortical processes. Concerning the effect localization, the field distribution maps indicate, that the early modulation maximum arises over the left lateral occipito-temporal cortex (black ellipse), while a more posterior source in the occipital left hemisphere underlies the late modulation maximum (grey ellipse). Current source density (CSD) estimates (using a distributed source model with the minimum norm least squares account, see 3.4.2) confirmed an early maximum in the more anterior-lateral ventral occipito-temporal cortex and a late maximum in a more posterior-medial ventral visual cortex region.
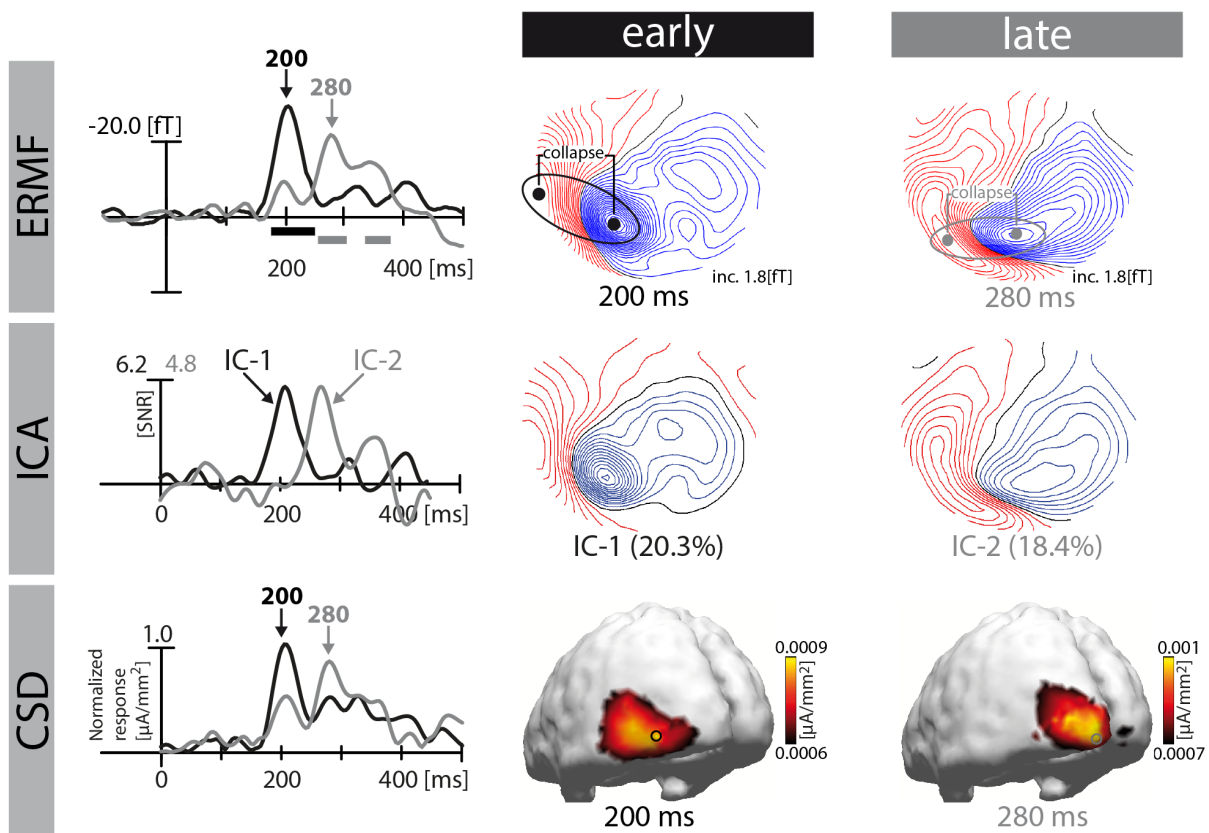
Figure 4.6. ERMF responses, ICA pattern and source localizations of experiment 1. Upper row: Displayed are again the field distributions of the early and late modulation of GCBA at time points of maximum effect size together with the corresponding ERMF waveforms of the early (black trace) and late (grey trace) modulations reflecting the averaged signal of selected sensor sites close to the efflux (polarity inverted before averaging) and influx maxima (black/grey dots). Black and grey horizontal bars indicate time ranges of significant amplitude differences (M vs. NM comparison, $p < 0.05$, corrected for multiple comparisons as described in 3.4.1). **Middle row**: Time course and field distribution pattern of the two independent components explaining the largest portion of variance in the data (IC-1, 20.3% and IC-2, 18.4%; expressed as signal-to-noise ratio in the timegraph) that resulted from an independent component analysis (ICA) of the data displayed in the upper row. **Lower row**: Results of the current source density analysis (CSD), shown are the 3D models at time points of the early and late GCBA modulation together with the time course of the normalized source activity at cortical locations picked at the modulation maxima (black/ grey circle).

Single subject data

Due to the variability of individual brains, the grand average data can only reveal average effect localizations, but not determine anatomical sources as precise as it is possible in a single observer. Thus, to gain more specific insight into where the sources of the early and late modulation were located, four individual subjects (so70, ox81, tq62, xp38) were selected that took part in at least three of the experiments reported in the current work. As all experiments contained at least one condition comparable to experiment 1, the data could be averaged across these conditions. This increased the number of trials and hence improved the signal-to-noise ratio. The current source density estimates were computed individually for all of the selected observers (see 3.4.2) and coregistered with the individual retinotopic field sign map as well as with a localizer of the lateral occipital complex (LOC) (see 3.4.3). Figure 4.7 displays the current source density (CSD) localizations of the early and late effect as well as the time course of the CSD at locations of the early and late modulation for the individual observers. All subjects consistently showed an early modulation peaking around 200ms and a later phase around 280ms. Source maxima of the early modulation were located in the lateral occipital complex LOC (so70, ox81) or close to it (tq62, xp38) as well as in a more posterior-medial area anterior to V4 (so70, tq62, xp38). The late modulation maximum was more variable in time across subjects (250-310ms), but showed consistent activations in the more posterior early retinotopic areas V3/V4 (for ox81 additionally in V1).
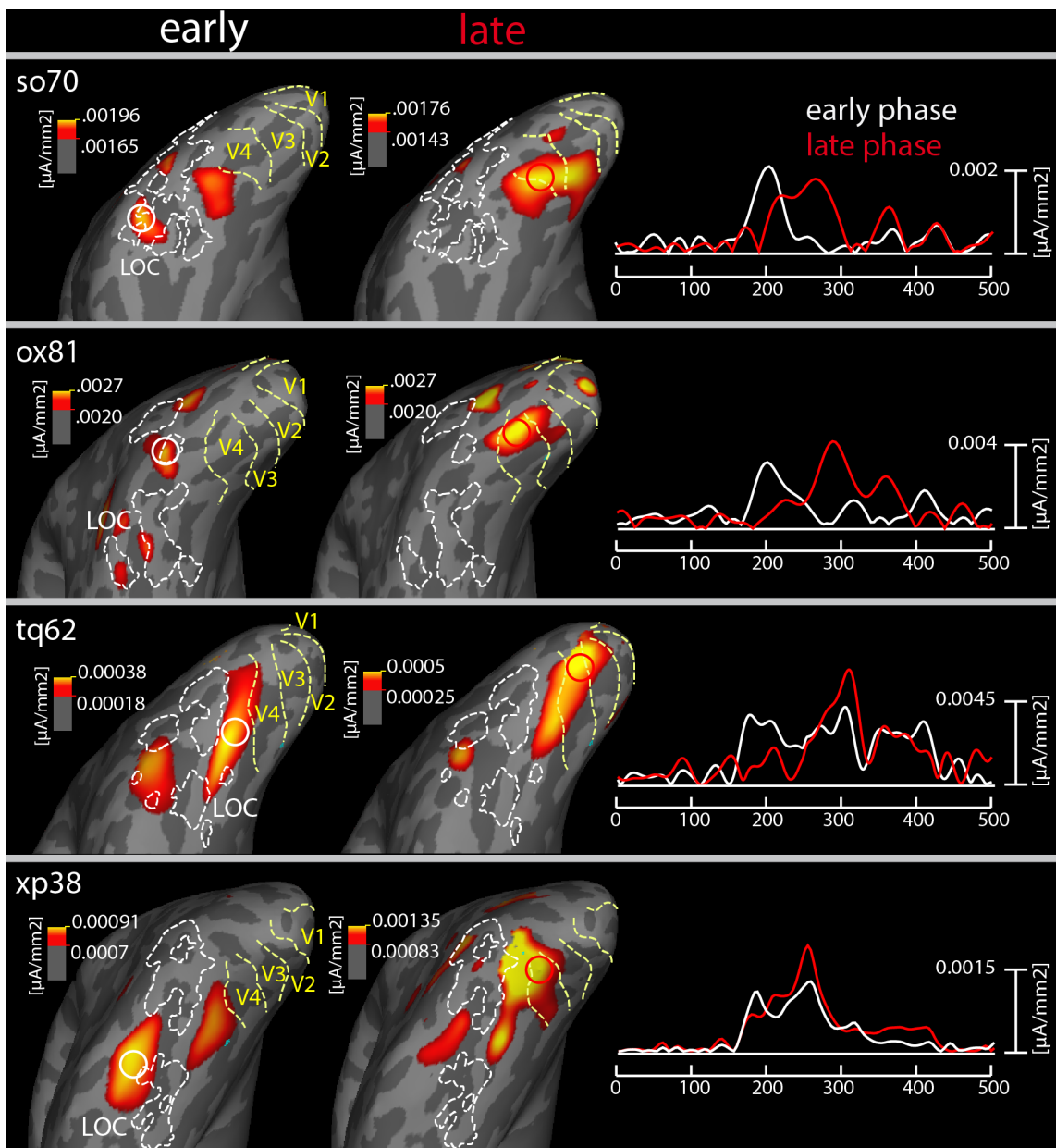
Figure 4.7. CSD localizations of single observers (data averaged across experiments). Each row represents data of a single subject with the 3D maps of the current source distributions (left ventral exrastriate cortex, inflated) presented in the left and middle column and the corresponding time course of the current source activity at the encircled locations (white/red circle) in the right column. While the early phase of GCBA colocalized with parts of the lateral occipital complex (LOC, white dashed outline) (so70, ox81) and more posterior-medial areas anterior to V4 (so70, tq62, xp38), the late phase emerged at early visual retinotopic regions (V3/4, V1, yellow dashed outline).

4.1.4. Discussion

Establishing effects of GCBA

In line with previous observations (Sàenz et al., 2003; Zhang & Luck, 2009), global effects of color-based attention were observed under conditions of feature competition in the focus of attention. That is, unattended probes in the right visual field elicited an enhanced brain response (ERMF, ERP) when their color matched the currently-attended target color in the left visual field as compared to when the color of the probe did not match. Moreover, the GCBA effect is composed of a sequence of independent modulations propagating from more anterior-lateral parts of ventral extrastriate visual cortex to more posterior-medial regions.

Early modulation

The current source analyis in single observers revealed that the early modulation (around 200ms) arose in or near the lateral occipital complex (LOC), an area known to be selective for object shape (Kourtzi & Kanwisher, 2000) as well as in more posterior-medial regions anterior to V4. Since the retinotopic mapping as performed here (see 3.4.3) is limited to V1-V4, it cannot be determined with certainty, which cortical region gave rise to this more posterior-medial activation. However, it would be congruent with underlying sources in VO-1/2, that is, in color- and object-selective regions of the ventral occipital cortex (Brewer et al., 2005; Wandell et al., 2007).

Late modulation

The late GCBA modulation (around 280ms, individually varying from 250-310ms) showed activations in posterior early retinotopic areas V3/V4 (for ox81 additionally in V1) that are known to be color selective, particularly in the case of V4 (Zeki et al., 1991; Motter, 1994; McKeefry & Zeki, 1997; Chawla et al., 1999; Gegenfurtner, 2003; Sàenz et al., 2003; Brewer et al., 2005; A. Wade et al., 2008; Brouwer & Heeger, 2009).

Reverse hierarchy selection

Importantly, the cortical regions activated during the early GCBA modulation (LOC, VO-1/2) represent a higher hierarchical level of visual representation than the cortical regions that gave rise to the late modulation (V3/4, V1). That is, the present data suggest that the modulations of GCBA propagated down the cortical hierarchy from higher to lower tier areas. This interpretation will be discussed in detail in section 6.3.

Separating brain responses to probes from those to targets

The current experimental design (with the target and the unattended color probe being presented in opposite visual hemifields) allowed the separation of the brain responses to the unattended probes from those responses to the attended targets. Due to the contralateral retinotopic organization of the visual cortex (e.g., Sereno et al., 1995), the target in the LVF should primarily

elicit responses in the right hemisphere, while responses to the unattended probes in the RVF were expected to arise in the left hemisphere. Indeed, the observed early and late modulations of GCBA were located in the left visual cortex, thereby asserting that they arose due to global selection of the probe's color in the unattended hemifield. The absence of prominent target-specific right-hemisphere modulations in the field distributions as well as in the CSD maps (cf. 4.1.3, Figure 4.6) is expected since the match vs. non-match comparison never involved attentional differences on the target side (the target was always attended).

Different number of trials for match and non-match conditions

As the number of trials was not balanced across match and non-match conditions (2/3 non-match trials, 1/3 match trials), the amplitude differences between respective conditions may reflect different signal-to-noise levels as described by Luck (2005, pp. 69-71,133). Specifically, the signal-to-noise ratio increases as a function of the square root of the number of trials, leading to a $\sqrt{2}$ ($\approx$ 1.4) times better signal-to-noise ratio for the non-match condition since it has twice as many trials as the match condition. The signal-to-noise ratio, in turn, influences the amplitude size with peak amplitudes being larger when the signal-to-noise ratio is lower. Thus, the higher peak amplitudes of match trials might not reflect an attentional enhancement, but just a poorer signal-to-noise ratio. To exclude the possibility that our effects were simply caused by differences in the trial numbers of the match and non-match condition, non-match conditions with half the amount of trials were compared to the match condition. Specifically, the non-match trials were split up into the two possible non-matching colors. For example, the red match trials (target and probe red) were compared to non-match trials containing magenta targets (target magenta, probe red) and to non-match trials containing blue targets (target blue, probe red). Figure 4.8 displays the respective match and non-match trials for red, magenta and blue probes focusing on sensors showing the early modulation of GCBA. It can be seen that the amplitudes of the non-match waveforms are still smaller than those of the match waveforms, even when both are calculated from the same amount of trials. Hence, an explanation of our findings in terms of an unbalanced number of trials for the match and non-match condition is highly unlikely.
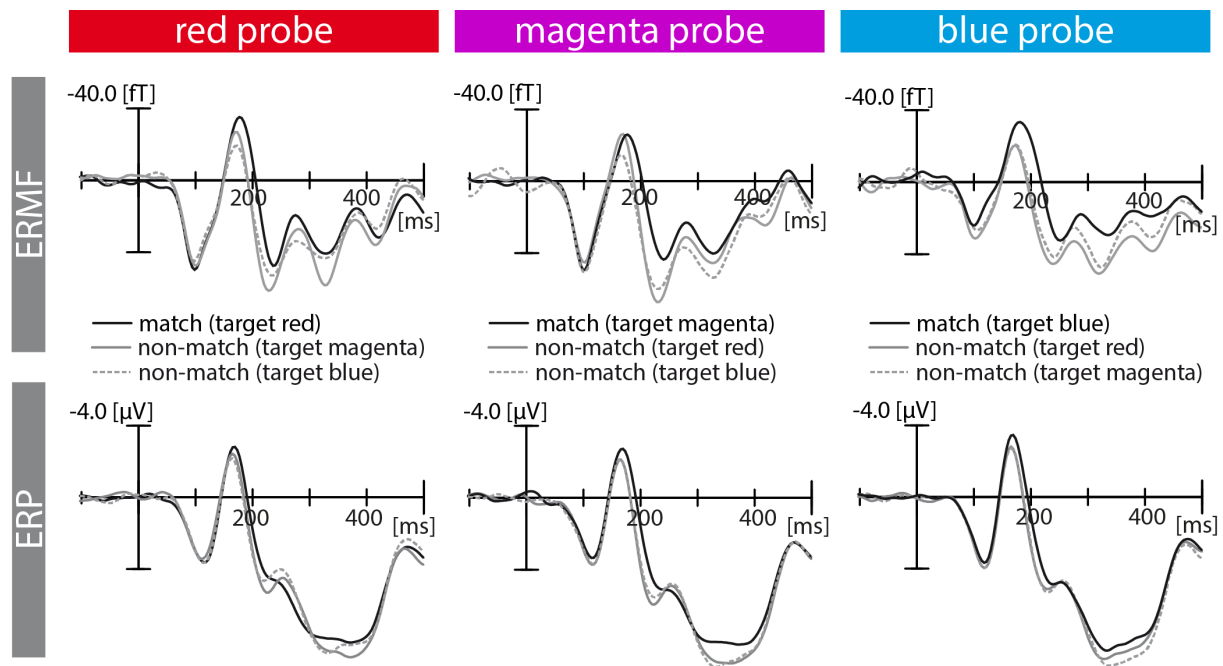
Figure 4.8. Match and non-match waveforms of comparable trial numbers. The ERMF and ERP waveforms of the match trials (black solid) for red, magenta and blue probes are compared to the two possible non-match trials (grey solid/dashed) of each probe color constant condition (target color varying). The sensors of the ERMF waveforms were chosen according to the early effect of the probe color constant condition (see Supplementary section S.1, Figure S.1.). For the ERP waveforms, the electrode PO7 was chosen according to the modulation maximum of the early effect (see section 4.1.3, Figure 4.4). All match waveforms still show an enhanced amplitude compared to the corresponding non-match waveforms.

4.2. Experiment 2: control for physical stimulus differences

4.2.1. Motivation

The purpose of experiment 2 was to address a potential stimulus confound that could have arisen from an imbalance of the color distribution for match and non-match trials: On match trials the target color appeared bilaterally, whereas on non-match trials every color in the visual display was presented unilaterally. In other words, the match versus non-match comparison (M-NM difference), performed to derive the effects of global color-based selection, always involved a comparison of bilateral versus unilateral target color presentations. To rule out that such color imbalance accounts for the observed modulation sequence, a modified version of experiment 1 was run, in which a rapid serial visual presentation (RSVP) stream was added immediately above the fixation dot. Subjects attended blockwise either to the colored circles as in experiment 1 (attend to color) or performed the RSVP task (attend to characters). Because the RSVP task puts high demands on focusing attention upon the letters, the subjects' attention should be completely removed from the colored circles and hence all modulations arising due to the attentional selection of color should be eliminated. Observing the modulations reported in experiment 1 (see

4.1.3) during the RSVP task would speak against global color-based attention as an underlying mechanism and rather favor an interpretation in terms of physical color imbalances.

4.2.2. Methods

Subjects

Nineteen subjects (15 females, mean age 26.6 years, all right-handed) participated in Experiment 2.

Stimuli and Task

The stimulus design is illustrated in Figure 4.9. The stimuli were identical to those used in experiment 1 with the exception of the following modifications: 1) the SOA was shortened to 1330-1530ms (rectangular distribution) to account for an increased number of conditions while maintaining a reasonable number of trials per condition, 2) the fixation cross was replaced by a fixation dot, 3) an achromatic RSVP stream was added directly above fixation (same color as the fixation cross). The RSVP stream consisted of a sequence of eleven items randomly taken from a list of ten uppercase characters (A, E, I, K, L, N, O, T, V, Y; height: 0.5° visual angle) presented in a rapid sequence (SOA = 80 ms, character duration = 32 ms). On each trial, the RSVP sequence started 290ms before the onset of the colored circles and ended 290ms after the stimulus offset with the presentation of a question mark that lasted for 450-650ms. On half of the blocks the subjects were to ignore the colored circles, attend to the RSVP stream, and report the occurrence or absence of the target character 'O' by a button press immediately after the onset of the question mark ('O' present: index finger; 'O' absent: middle finger). The target character was present on 40% of the trials. On the other trial blocks, the subjects were asked to ignore the RSVP stream at fixation and perform the color/shape task as described in experiment 1 (i.e., decide whether the curved section of the half circle drawn in the target color faced to the left or to the right, 'left': index finger, 'right': middle finger). As in experiment 1, effects of GCBA were assessed by comparing the brain response to the probe as function of whether it matched or did not match the target color. Since the presentation of the colored circles was identical for color/shape and RSVP blocks (except a different trial randomization), the same match minus non-match comparisons could be performed for RSVP trials.

Each subject performed 162 trials per block and a total of 12 blocks (six RSVP and six color/shape blocks with the task alternating between subsequent blocks), yielding 324 match and 648 non-match trials per task-type. The block order was randomly drawn from a set of six possible block orders each starting with either the RSVP or the color/shape task. The three colors of the circle in the LVF alternated blockwise between red, magenta and blue with no repetition of the same color on subsequent blocks.
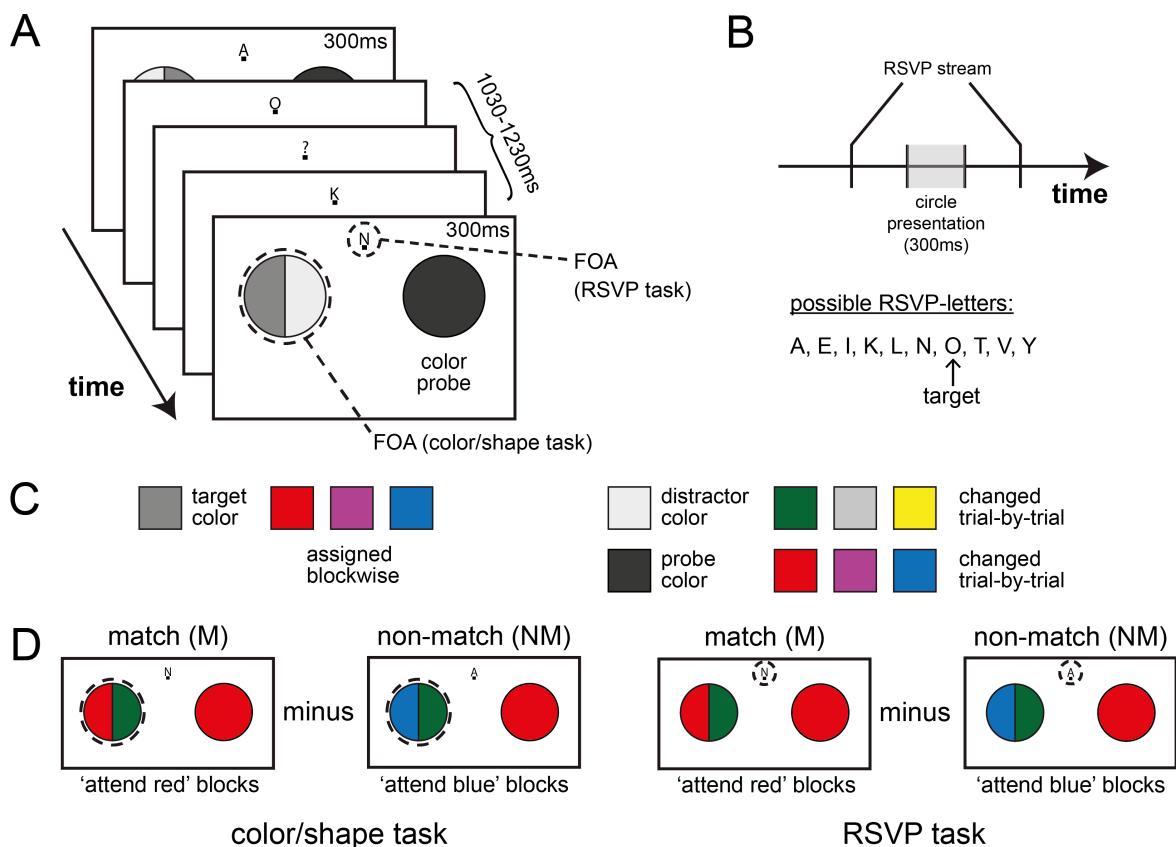
Figure 4.9. Stimulus setup for experiment 2. (A) The stimuli of experiment 1 were modified by adding an RSVP stream at fixation and by slightly shortening the SOA between the circle onsets. Subjects attended in alternating experimental blocks either to the left circle (color/shape discrimination task) or to the RSVP stream (RSVP task). **(B)** The RSVP stream started 290ms before circle onset, ended 290ms after circle offset and contained a sequence of eleven items (SOA: 80ms, letter duration: 32ms) randomly taken from a list of ten uppercase characters with the detection target 'O' being being present on 40% of the trials. **(C)** The same colors as in experiment 1 were assigned as target, distractor and probe colors. **(D)** An example of a match (M) and non-match (NM) trial for the color/shape and the RSVP task (here: probe color red), which were used to calculate the M-NM difference to retrieve effects of GCBA. Match and non-match trials were physically identical for color/shape and RSVP trials, while the task and spatial focus of attention (FOA) differed.

4.2.3. Results

Behavioral Performance

The behavioral performance is summarized in Figure 4.10. Response accuracy and response time were compared for the match and non-match trials of the different tasks (color/shape discrimination task, RSVP task). The response accuracy on match and non-match trials was equally high on both tasks with subjects being overall faster on the RSVP task (responses could be prepared before the question mark appeared). As in experiment 1, responses were slightly slower on match compared to non-match trials under conditions of the color/shape discrimination task. As expected, a two-way rANOVA with the factors TASK (color/shape or RSVP) and MATCH

(match/non-match) on response accuracy yielded no significant main effect of TASK ($F_{[1,18]} = 0.20$, $p = 0.66$), no significant effect of MATCH ($F_{[1,18]} = 0.02$, $p = 0.90$) and also no significant MATCH x TASK interaction ($F_{[1,18]} = 0.42$, $p = 0.52$). For response time, there was a significant effect of TASK ($F_{[1,18]} = 16.68$, $p = 0.001$), but no significant effects of MATCH ($F_{[1,18]} = 3.16$, $p = 0.09$) or a TASK x MATCH interaction ($F_{[1,18]} = 0.53$, $p = 0.48$). Although the factor MATCH and the TASK x MATCH interaction failed to reach significance, a subsequent analysis revealed that the slightly slower responses on match trials of the color/shape discrimination task emerged due to the same pattern underlying the slowing observed on match trials of experiment 1 (for details see Supplementary section S.2.1).
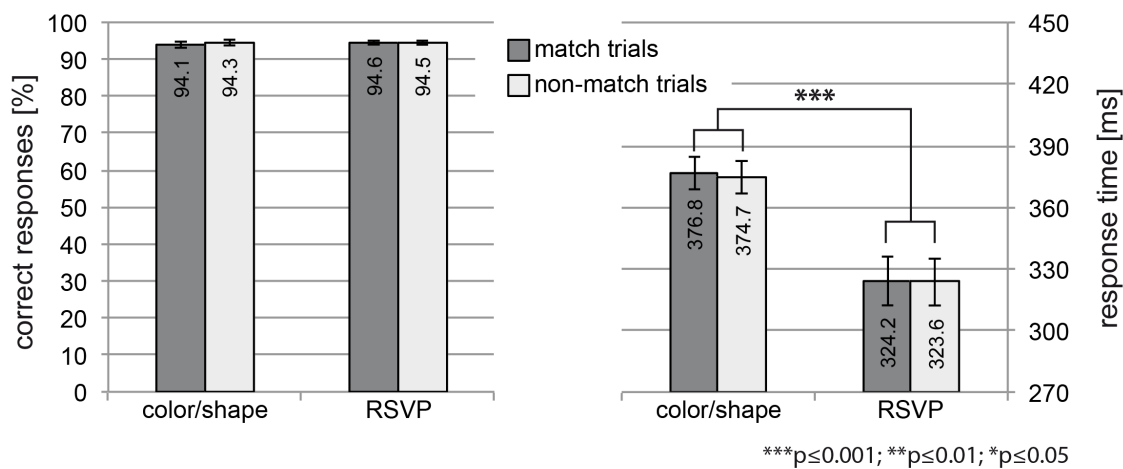
Figure 4.10. Behavioral performance of experiment 2. The response accuracy (percentage of correct responses) and the response time for the match (dark grey) and non-match (light grey) trials for both the color/shape discrimination task and the RSVP task are displayed here. The error bars reflect the standard error of the mean (SEM). While the response accuracy was equally high throughout all trials types, responses were faster under conditions of the RSVP task. For the color/shape discrimination task match trials seemed to be slightly slower than non-match trials though the effect failed to reach significance.

Event-related magnetic field responses

As described in detail for experiment 1 (see 4.1.3), the ERMF response elicited by the unattended probe presented in the RVF was analyzed as a function of whether the probe's color matched the target color currently attended in the LVF (match trials, M) or not (non-match trials, NM). Figure 4.11 shows the M-NM difference for conditions of the color/shape discrimination task (A) and the RSVP task (B). The field distribution maps and current source density (CSD) localizations are displayed for time points of maximum effect size of the early and late modulation of GCBA. Since no such modulation could be found for the RSVP task, the time points to display field distribution maps as well as the sensors sites to show ERMF waveforms corresponded to those selected for the color/shape trials. Likewise, the source waveforms corresponding to the current source density distribution show the normalized activity over time at locations of the CSD maxima of the color/shape discrimination task. As visible in Figure 4.11A, the color/shape discrimination task nicely replicates the modulation sequence seen in experiment 1. Again, GCBA is characterized by

an early more anterior modulation in lateral ventral occipito-temporal cortex peaking around 200ms, and a later modulation in more posterior-medial ventral visual cortex peaking around 280ms. In contrast, when subjects focused their attention on the RVSP letter stream, no effects of GCBA arose (Figure 4.11B).
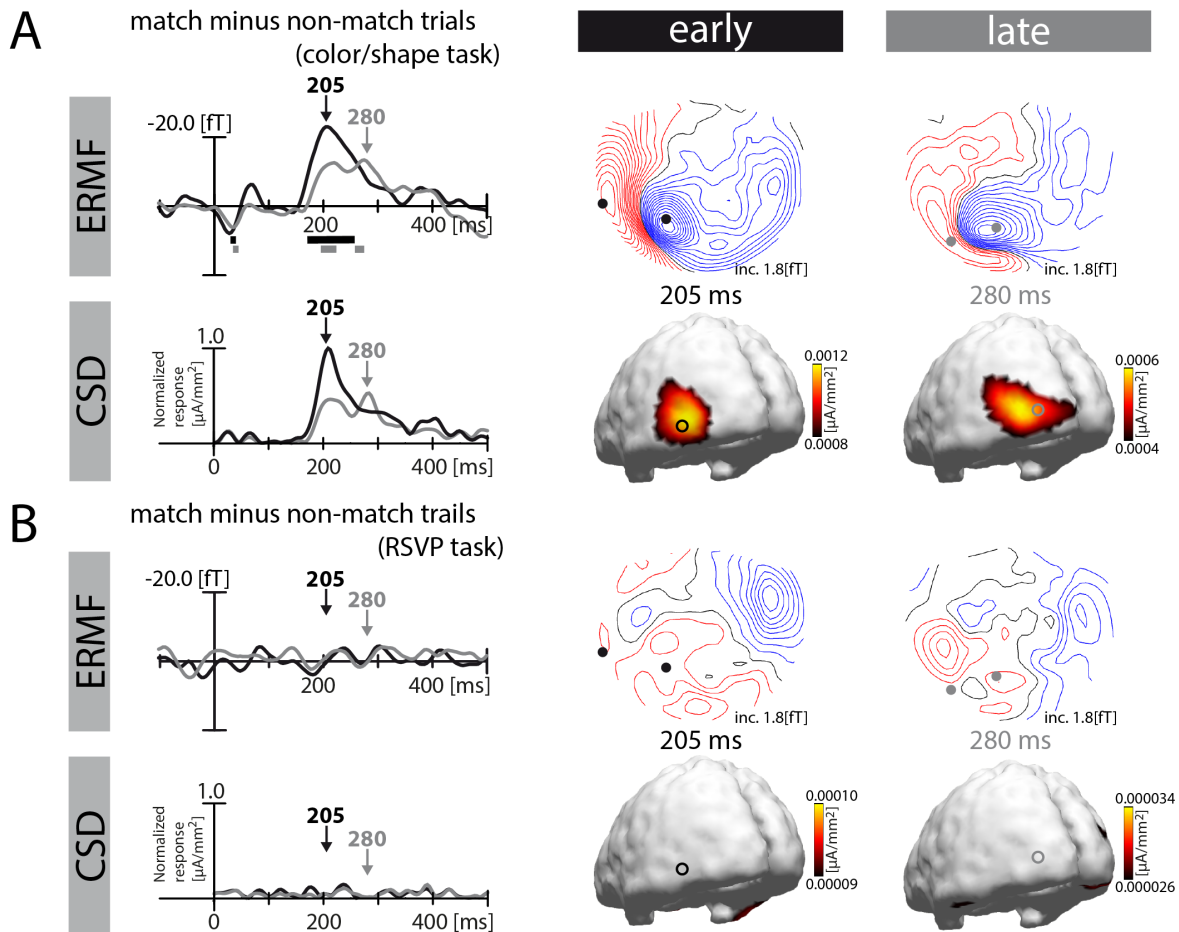
Figure 4.11. **ERMF responses of experiment** 2. The results for the color/shape discrimination task **(A)** as well as the RSVP task **(B)** are displayed here. The respective **upper rows** display the field distribution maps of the early and late modulation of GCBA – at time points of maximum effect size of the color/shape task – together with the corresponding ERMF waveforms (early modulation: black trace, late modulation: grey trace). The waveforms were collapsed over two sensor sites with one sensor position chosen close to the influx and and one chosen close to the efflux (polarity inverted before averaging) maximum of the field distributions of the color/shape task (black/ grey dots). The grey and black horizontal bars indicate time ranges of significance (match vs. non-match comparison, p < 0.05, corrected for multiple comparisons as described in 3.4.1). The **lower rows** show the corresponding current source density (CSD) distributions together with the source waveforms reflecting source activity obtained from cortical locations of the CSD maxima of the color/shape task (black/ grey circles), normalized by the activity of the early modulation of the color/shape discrimination task.

4.2.4. Discussion

Adding an achromatic RSVP stream directly above fixation rendered it possible to direct the subject's attention either towards the colored circle in the LVF or away from it towards the RSVP stream without changing the physical stimulus. All of the previously reported effects were replicated when subjects attended to the colored target, but were abolished when they attended to the characters of the RSVP stream. Experiment 2 therefore confirms that the modulation sequence documented in experiment 1 reflects attentional modulations and not low-level sensory color imbalances.

4.3. Experiment 3: GCBA with and without color competition

4.3.1. Motivation

Experiment 3 addressed the question as to whether effects of GCBA depend on the presence of a competing distractor color in the FOA as would be suggested by previous studies (Sàenz et al., 2003; Zhang & Luck, 2009). To this end, on half of the experimental blocks, only one color (the target color) was displayed in the FOA while the other half of the experimental blocks resembled experiment 1 with two colors (target and distractor color) being present in the FOA. Hence, conditions with and without color competition in the FOA could be compared directly within the same experimental session.

4.3.2. Methods

Subjects

Twenty-two subjects (16 females, mean age 25.9 years, all right-handed) participated in experiment 3.

Stimuli and Task

The stimulus design illustrated in Figure 4.12 was similar to experiment 1 with the following modifications: 1) The distractor color was only present on half of the experimental blocks (distractor-present trials), while it was removed on the remaining blocks with only the half circle drawn in the target color being presented in the LVF (distractor-absent trials), 2) the SOA was reduced to 1300-1500ms (rectangular distribution) to account for the increased number of conditions while maintaining a reasonable number of trials per condition. Independent of the trial type (distractor present or absent), the subjects had to perform the same task as in experiment 1 (i.e., to report whether the curved section of the half circle drawn in the target color faced to the left or right). Again, effects of GCBA were assessed by comparing the brain response to the unattended probe as function of wether it matched or not matched the target color.

Subjects performed a total of twelve experimental blocks with six distractor-present and six distractor-absent blocks in alternation. Each subject was assigned one out of six possible block orders with the three possible target colors (red, magenta, blue) alternating and never being repeated on subsequent blocks. With 162 trials per block, 324 match and 648 non-match trials per trial type (distractor present or absent), were collected for every subject.
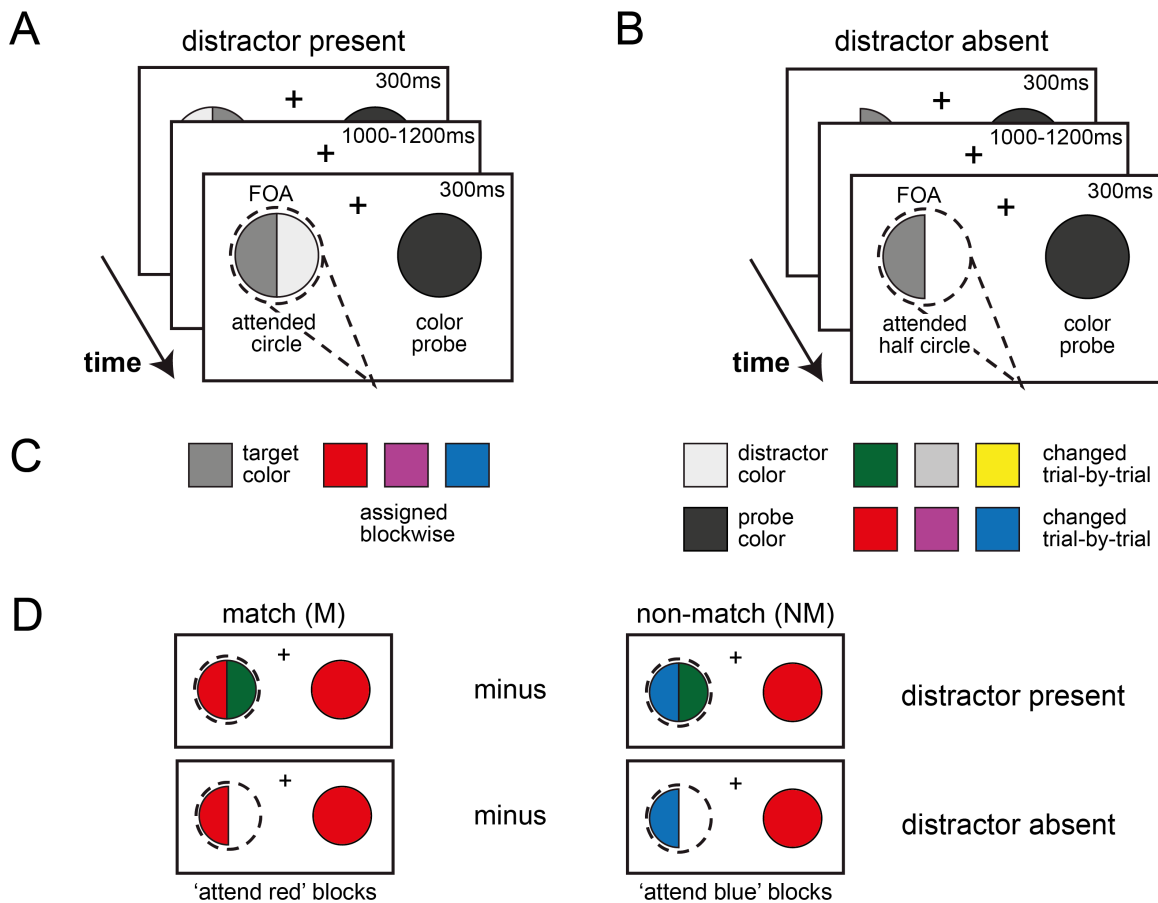
Figure 4.12. **Stimulus setup for experiment 3.** **(A)** On half of the experimental blocks, the stimuli were identical to experiment 1 with the exception of a slightly shortened SOA (distractor-present trials), **(B)** on the other half of the experimental blocks, the half circle drawn in the distractor color was removed from the focus of attention (distractor-absent trials). **(C)** Target, distractor and probe color assignment was identical to experiment 1. **(D)** For both trial types effects of global color-based attention were assessed by subtracting trials with probe and target color being different (non-match trials, NM) from trials with probe and target color being identical (match trials, M). The example shown here is for possible match/non-match combinations of red probes.

4.3.3. Results

Behavioral Performance

The behavioral performance is summarized in Figure 4.13. Response accuracy and response time are compared for the match and non-match trials performed on distractor-present or distractor-

absent trials. The response accuracy is slightly higher for distractor-present trials as compared to distractor-absent trials, with a marginal performance decrement on match compared to non-match trials for the distractor-present condition only. For both trial types, responses were slower on match compared to non-match trials. These observations are confirmed by two-way rANOVAs with the factors MATCH (match/non-match) and PRESENCE (distractor present/absent) yielding a significant main effect of MATCH ($F[1,21] = 5.45$, $p = 0.03$) and PRESENCE ($F[1,21] = 37.71$, $p < 0.0005$) as well as a significant interaction of MATCH x PRESENCE ($F[1,21] = 4.82$, $p = 0.04$) for response accuracy. As expected for response time, the factor MATCH was significant ($F[1,21] = 18.65$, $p < 0.0005$), while both PRESENCE ($F[1,21] = 3.87$, $p = 0.06$) and the MATCH x PRESENCE interaction ($F[1,21] = 3.33$, $p = 0.08$) failed to reach significance. Post-hoc pairwise comparisons (Student's t-test) affirmed a higher accuracy on non-match compared to match trials for the distractor-present ($p = 0.003$), but not the distractor-absent condition ($p = 0.65$). The response slowing on match trials was significant for both the distractor-present ($p = 0.001$) and the distractor-absent condition ($p = 0.004$). As previously mentioned for experiment 1 and 2, the response slowing on match trials presumably referred to an issue of response mapping. A detailed analysis is provided in the Supplementary section S.2.1.
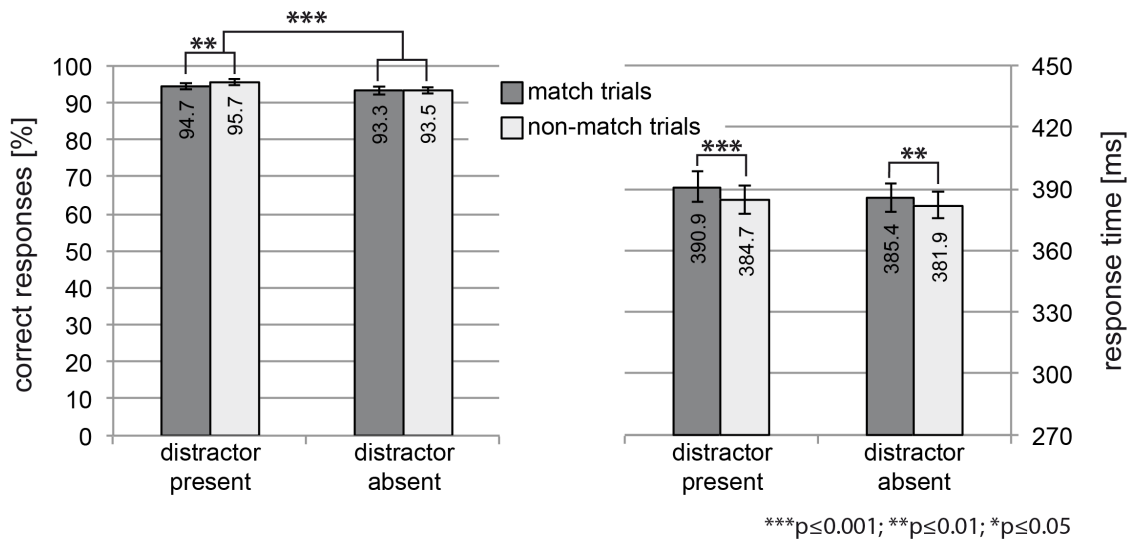
Figure 4.13. Behavioral performance of experiment 3. The percentage of correct responses and the response time for match (dark grey) and non-match (light grey) trials for both the distractor-present and the distractor-absent condition are shown. The error bars represent the standard error of the mean (SEM). Response accuracy is lower on distractor-absent trials as well as for match compared to non-match trials of the distractor-present condition. Responses are slowed on match compared to non-match trials irrespective of the distractor presence.

Event-related magnetic field responses

As in the previous experiments, the ERMF responses elicited contralateral to the unattended color probes were analyzed by subtracting brain responses to probes not matching the target color from those matching the target color. Figure 4.14 shows respective (M-NM) difference for the

distractor-present (A) and the distractor-absent condition (B). Both conditions resembled the modulation sequence in left ventral extrastriate visual cortex that was seen in experiment 1 with an early more anterior-lateral modulation maximum around 200ms (here: 205ms and 210ms) followed by a later more posterior-medial modulation maximum around 280ms. Although the late modulation seemed to be marginally weaker for the distractor-absent trials, the overall spatio-temporal pattern of the ERMF response was equivalent for both the distractor-absent and the distractor-present condition.
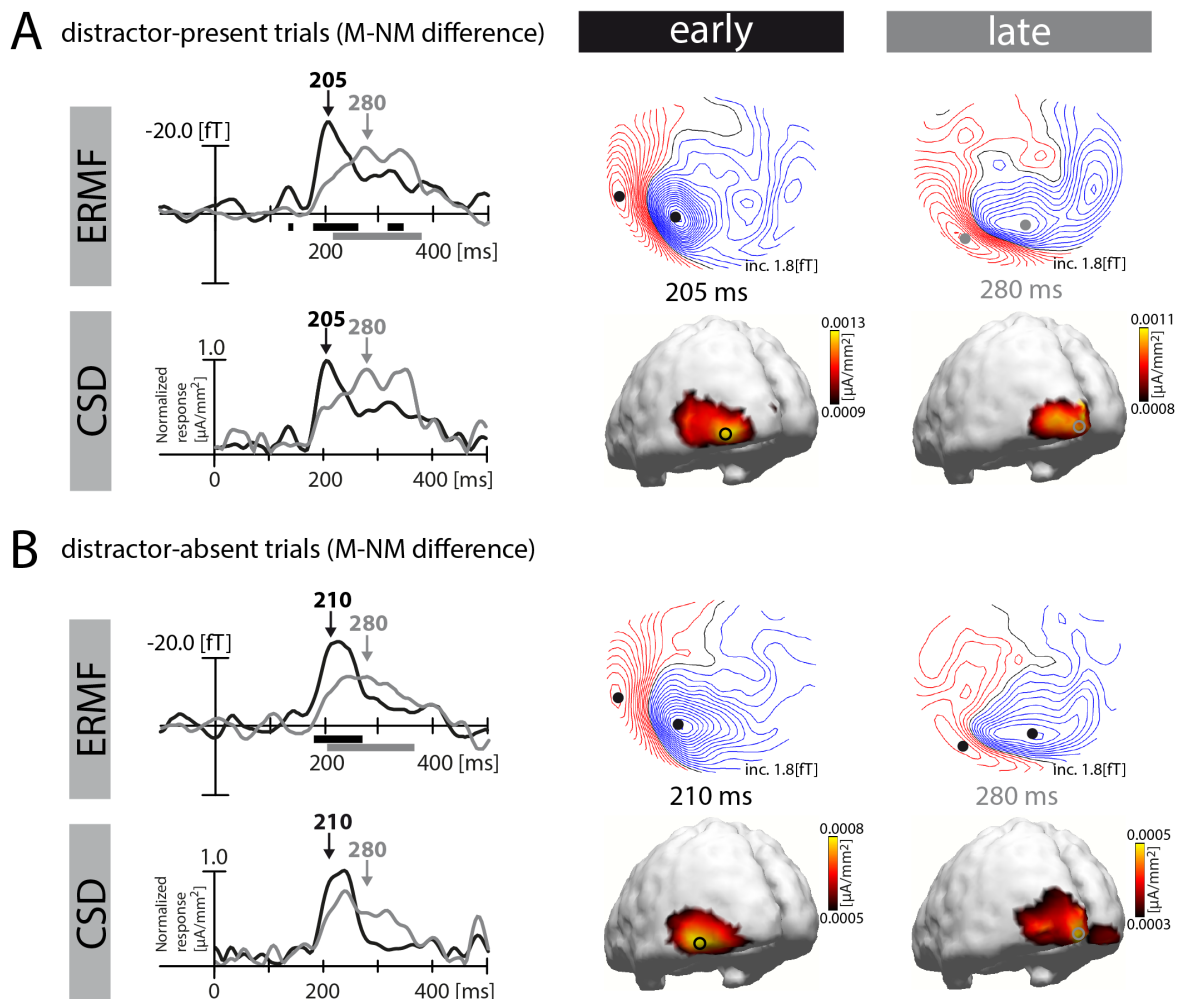
Figure 4.14. ERMF responses of experiment 3. (A/B) upper rows: The field distribution maps at time points of early and late modulation maxima of GCBA are displayed for the distractor-present condition **(A)** and the distractor-absent condition **(B)**. The corresponding ERMF waveforms of the early (black trace) and late (grey trace) modulation reflect the averaged signal of selected sensor sites close to the efflux (polarity inverted before averaging) and influx maxima (black/grey dots). The grey and black horizontal bars indicate time ranges of significance (match vs. non-match comparison, $p < 0.05$, corrected for multiple comparisons as described in 3.4.1). **(A/B) lower rows:** The 3D maps of the current source density (CSD) distributions of the selected early and late time points are shown together with the normalized source activity over time at locations of source density maxima (black/grey circles). Both early and late effects of GCBA were preserved without color competition in the focus of attention (distractor-absent condition).

4.3.4. Discussion

The prediction that GCBA depends on color competition in the spatial focus of attention could not be confirmed by the results of experiment 3. The same spatio-temporal pattern of GCBA modulations arose irrespective of whether a competing distractor color was present in the FOA or not. Although the late modulation seemed to be marginally smaller without a competing color (see discussion in section 6.4.4), whether or not the GCBA modulation sequence was elicited did not depend on color competition.

Effects of GCBA mediated by object-based attention?

Note, the removal of the distractor color from the circle in the LVF also eliminated the explicit need to select the target based on its color. That is, the decision to which side the convexity of the isolated half circle faced could in principle be solved solely by discriminating the shape of the half circle without registering its color. On the other hand, the subjects were instructed and hence encouraged to attend to the target's color (the task was to report whether the curved section of the half circle *drawn in the target color* faced to the left or right). Furthermore, the target's color was constant within experimental blocks, presumably prompting subjects to attend to the color to some extent.

Nonetheless, in case the subjects did not explicitly attend to the target's color, what would be the mechanism that caused GCBA effects to arise? One possibility would be that GCBA effects arose due to selection processes akin to object-based attention. As reviewed under section 1.2.2 ('object-based attention'), attending to an object mediates the concomitant selection of all of its features. The observed modulation sequence may therefore not reflect attention to color directly, but rather object-based color selection as a consequence of shape discrimination of the target object. Experiment 4 will provide further information on this issue. Specifically, the results will shed light on whether effects of GCBA appear for a task-relevant color that is absent from the FOA, and for which a bias of color selection can not arise from object-based attention.

4.4. Experiment 4: GCBA for colors absent from the FOA

4.4.1. Motivation

Ruling out color competition in the FOA as a critical determinant of GCBA (experiment 3), leaves the question as to what actually engenders global color selection processes. Previous studies failed to find effects of GFBA when the attended feature was absent from the attended hemifield (Hillyard & Münte, 1984; Wijers et al., 1989; Anllo-Vento & Hillyard, 1996). To address whether GCBA requires the attended color to be present in the spatial FOA, the color/shape discrimination experiment (experiment 1) was modified, such that on half of the trial blocks the target was defined by two possible colors with only one of them being randomly presented in the FOA on a

given trial. This allowed to analyze the brain's response to a task-relevant color as a function of whether the color was present or absent in the FOA. If effects of GCBA depend on the presence of the relevant color in the FOA, all previously reported modulations should disappear in the latter case.

Experiment 4 also helps to shed some light on the question as to whether the observed modulations reflect object-based color selection effects (see discussion of experiment 3, section 4.3.4). Specifically, if the previously observed effects of GCBA were also elicited by task-relevant colors absent from the FOA (and thus not contained in the target object), one would conclude that GCBA does not depend on the mediation by object-based attention.

4.4.2. Methods

Subjects

Twenty-five subjects (15 females, mean age 25.3 years, all right-handed) participated in experiment 4.

Stimuli and Task

The experimental setup is illustrated in Figure 4.15. The stimuli and task were similar to those used in experiment 1, with the exception of the following modifications: 1) The range of colors was changed with red, green, blue and yellow serving as target and probe colors and magenta serving as probe color only. 2) On half of the experimental blocks the subjects attended to one target color at a time (one-color blocks), while on the remaining blocks the target half circle was randomly assigned one out of two possible target colors on a given trial (either red or green on 'attend red/green blocks' or blue or yellow on 'attend blue/yellow' blocks). Thus, the subjects attended to two colors simultaneously with only one of them being presented in the LVF on a given trial (two-color blocks). 3) The SOA range was shortened to 1300-1500ms (rectangular distribution) to account for the increased number of conditions while maintaining a reasonable number of trials per condition.

One-color blocks: match and non-match trials

As in the previous experiments, the effects of GCBA were assessed by comparing the brain response to the unattended probe in the RVF as a function of whether it matched the target color presented in the LVF (match trial) or not (non-match trial).

Two-color blocks: match, cross-match and non-match trials

For the two-color blocks, the effects of GCBA could be assessed in two different ways: The brain response to the unattended probes not matching the target colors (non-match trial) could be either compared to probes matching the currently-presented target color (match trial) or to probes

matching the other target color that was currently not present in the LVF (cross-match trial), as illustrated in Figure 4.15C.

Subjects performed eight blocks of the one-color and eight blocks of the two-color condition with each block containing 120 trials. Each subject was assigned one out of sixteen possible block orders with one- and two-color blocks mixed such that target colors were never repeated on subsequent trials (i.e., a 'red/green' block was never followed by a 'green', a 'red' or another 'red/green' block). This yielded a total of 192 match, 192 cross-match and 576 non-match trials (192 of them with the probe color being the reference magenta) for the different trial types (one-/two-color blocks).
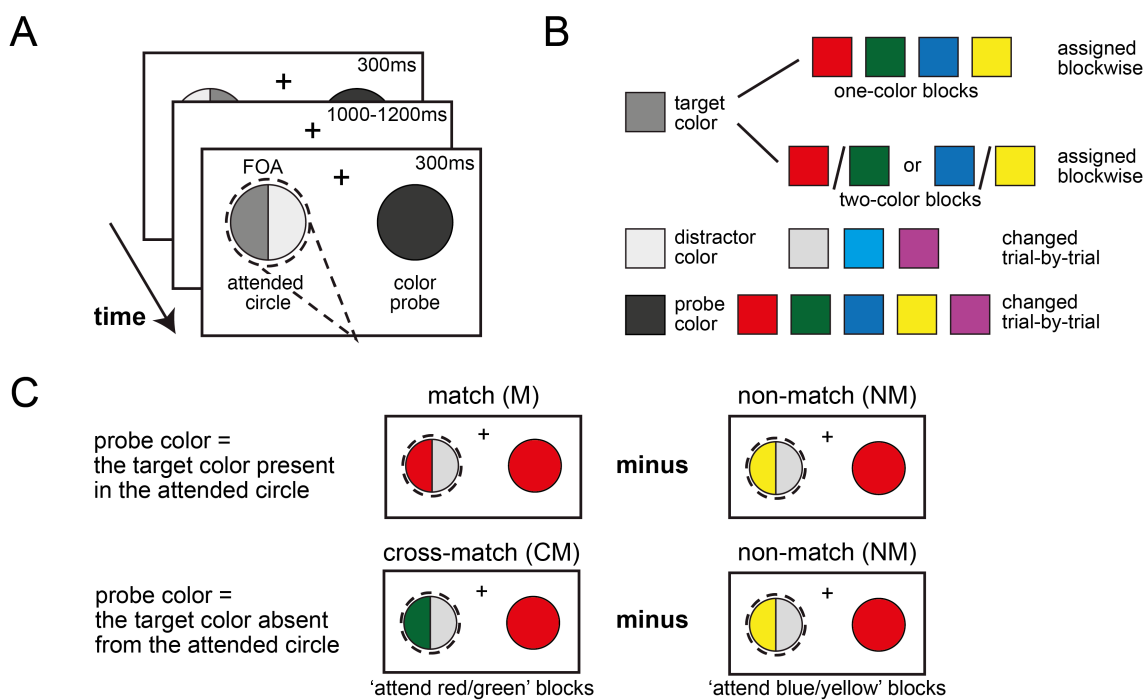
Figure 4.15. Experimental design of experiment 4. (A) The stimulus geometry was identical to experiment 1, however, the SOA was shortened to 1300-1500ms. **(B)** On half of the experimental blocks the subjects attended to one target color at a time – attend red, green, blue or yellow– (one-color blocks), while on the other half of the experimental blocks they attended to two possible target colors simultaneously with only one of them being assigned to the target object on a given trial – attend red/green or blue/yellow– (two-color blocks). Grey, cyan and magenta were used as distractor colors. The probe color varied trial-by-trial between the possible target colors and magenta (magenta was never simultaneously displayed as distractor and probe color). **(C)** Trial types of two-color blocks: trials with probe and target color being identical (match trials) as well as trials with the probe color matching the other target color not present in the FOA (cross-match trials) could be compared to trials with the probe color not being target-defining (non-match trials). The example shown here is for possible match, cross-match and non-match conditions of red probes.

4.4.3. Results

For the one-color blocks, behavioral performance and ERMF responses will be compared for match (M) and non-match (NM) trials. For the two-color blocks match (M) and non-match (NM) trials will be additionally compared to cross-match (CM) trials.

Behavioral Performance

The behavioral performance is illustrated in Figure 4.16. Because of the different number of match conditions, rANOVAs were conducted separately for the data of the one- and those of the two-color blocks. For the one-color blocks, the response accuracy was generally high with no difference between match and non-match trials. Regarding the reaction time, responses were slower on match compared to non-match trials. These observations were confirmed by rANOVAs with the factor MATCH (match/non-match) that yielded no significant effect ($F[1,24] = 0.45$, $p = 0.508$) for response accuracy, but a significant effect for response time ($F[1,24] = 16.48$, $p < 0.0005$). For the two-color blocks, the response accuracy was also generally high besides a slight performance decrement on cross-match trials. As in the one-color blocks, the responses were slower on match compared to non-match trials. However, the cross-match trials of the two-color blocks showed by far the slowest responses. The respective rANOVAs for the two-color blocks with the factor MATCH (match/non-match/cross-match) yielded significant effects of MATCH for both response accuracy ($F[2,23] = 10.87$, $p < 0.0005$) and response time ($F[2,23] = 42.44$, $p < 0.0005$). Post-hoc pairwise comparisons (Student's t-test) confirmed a significant decrease in response accuracy on cross-match compared to match and non-match trials (both p's < 0.0005), with no difference between match compared to non-match trials ($p = 0.31$). Concerning the response time on the two-color blocks, post-hoc comparisons affirmed the response slowing on match compared to non-match trials ($p < 0.0005$) with responses given on cross-match trials being slower than both those given on match and those given on non-match trials (both p's < 0.0005). A possible explanation for the prolonged response times on match and cross-match trials will be discussed in the Supplementary section S.2.1.

Of note, while both the one- and the two-color blocks showed the same pattern of prolonged response times for match compared to non-match trials, the responses seemed to be generally slowed on two-color blocks. To confirm this observation and to better compare the one- and two-color blocks, a rANOVA was conducted that contained the match and non-match conditions of both tasks (excluding the cross-match trials of the two-color condition). In fact, the respective two-way rANOVA with the factors TASK (one-color/two-color) and MATCH (match/non-match) yielded a significant main effect of TASK ($F[1,24] = 60.18$, $p < 0.0005$) and MATCH ($F[1,24] = 33.66$, $p < 0.0005$), but no significant TASK x MATCH interaction ($F[1,24] = 0.06$, $p < 0.812$). The absence of a significant TASK x MATCH interaction affirmed that the response time pattern for match and non-match trials was consistent for one- and two-color blocks, while the presence of a significant main effect of TASK confirmed the slower responses on the two-color blocks. The corresponding two-way rANOVA for response accuracy yielded only a

significant main effect of TASK (F[1,24] = 5.00, p < 0.035), but no effect of MATCH (F[1,24] < 0.0005, p = 0.991) and no significant TASK x MATCH interaction (F[1,24] = 1.63, p = 0.215). The significant effect of TASK reflected marginally more accurate responses for the match and non-match trials of the two-color task.
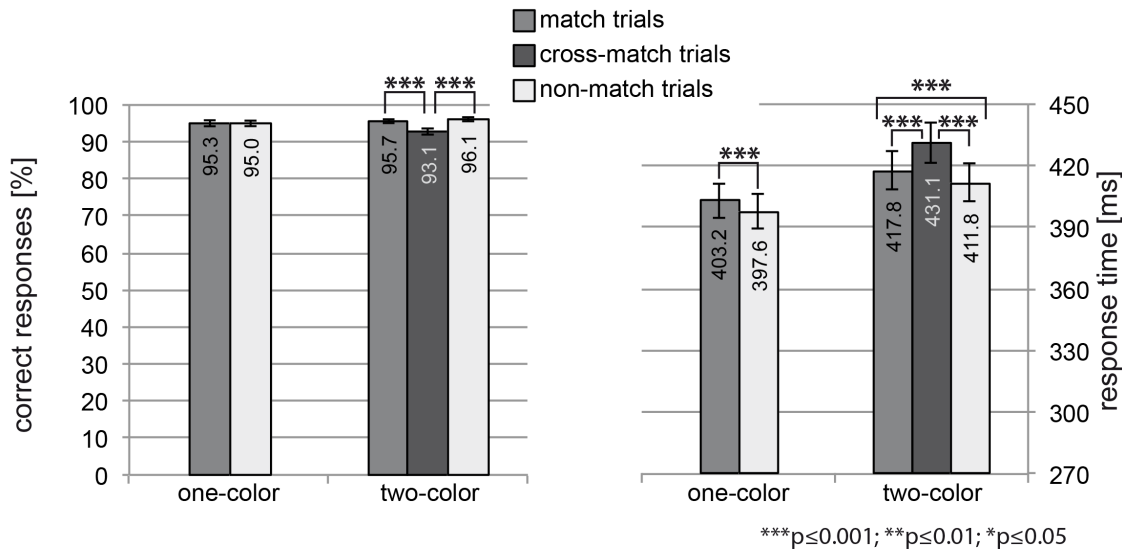
Figure 4.16. Behavioral performance of experiment 4. The percentage of correct responses and the response time are displayed for both the one- and the two-color task for match (grey), non-match (light grey) and cross-match trials (dark grey, only for two-color blocks). The error bars reflect the standard error of the mean (SEM). Response accuracy was high throughout all conditions with a small performance decrement on the cross-match trials of the two-color condition. The response time was prolonged for match compared to non-match trials. Responses to cross-match trials of the two-color blocks were slower than both responses to match and non-match trials.

Event-related magnetic field responses

As in the previous experiments, the ERMF responses to the unattended probes in the RVF were analyzed as a function of wether they matched (match, M) or did not match (non-match, NM) the currently-attended target color in the LVF (for a detailed description see experiment 1, 4.1.3). For two-color blocks, the non-match trials could additionally be compared to cross-match trials (CM) on which the probe color matched the second attended color that was absent from the target object. Figure 4.17 displays the respective M-NM difference for the one-color blocks (A) as well as the M-NM and CM-NM differences for the two-color blocks (B1/2).
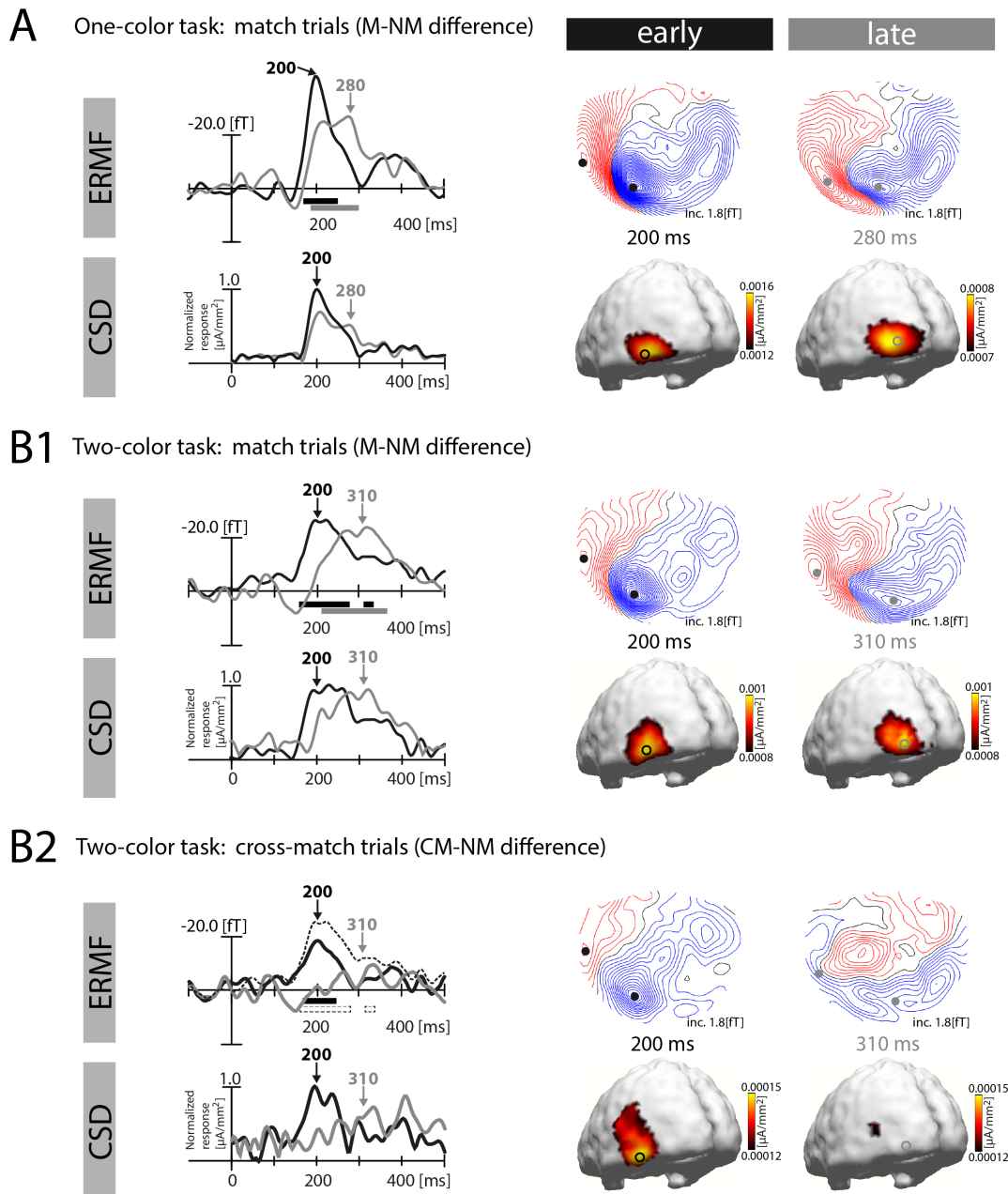
Figure 4.17. ERMF responses of Experiment 4. Field distribution maps at time points of early and late modulation maxima as well as ERMF waveforms are shown for match (M) trials of the one- (**A**) and two- (**B1**) color blocks and for cross-match (CM) trials of the two-color blocks (**B2)** (upper rows). The corresponding 3D current source density (CSD) distribution maps and source waveforms displaying the normalized source activity at locations of the CSD maxima (black/grey circles) are displayed in the respective lower rows. ERMF waveforms of the early (black trace) and late (grey trace) modulation reflect the averaged signal of sensors close to efflux (polarity inverted prior averaging) and influx maxima (black/grey dots). For a better comparison, the CM-NM waveform is shown together with the respective M-NM waveform of the two-color condition (dashed trace). Grey and black horizontal bars indicate significant time ranges (M vs. NM / CM vs. NM, p < 0.05, corrected for multiple comparisons, see 3.4.1). For the cross-match trials, time points, sensor sites and locations for CSD waveforms of the late effect were determined by the two-color match condition. Parts of the early, but not the late modulation were preserved on cross-match trials.

Match trials

Both the match trials of the one-color task and those of the two-color task nicely resemble the modulation sequence in ventral extrastriate visual cortex that was observed in the previous experiments. They show an early anterior-lateral maximum (peaking at 200ms) followed by a later more posterior-medial maximum (here: peak at 280ms for the one-color task and at 310ms for the two-color task). When comparing the ERMF waveforms of the match trials of the one- and two-color blocks, the peak of the early modulation is of smaller amplitude and appears to be broader for the two-color blocks. Furthermore, the late modulation seems to show a greater temporal delay on the two-color blocks.

Cross-match trials

Interestingly, the cross-match condition of the two-color task, indexing the response to an attended color absent from the FOA, reflected only parts of the initial modulation with no effect of GCBA seen in the later time range. Field distribution and current source density localization were comparable to those of the early effect of GCBA on the match trials, but with the effect size being reduced.

4.4.4. Discussion

Match trials

The early and late modulations of GCBA arose for both the one- and the two-color blocks, i.e., irrespective of the number of task-relevant colors. However, the early modulation was smaller in amplitude and appeared to be broader for the two- compared to the one-color blocks. Additionally, the late modulation seemed to show a greater temporal delay on the two color-blocks (for a further discussion of these observations see section 6.4.2).

Cross-match trials

Colors that were task-relevant, but not contained in the target object (cross-match (CM) trials of the two-color blocks), elicited early but not late parts of the previously-described modulation sequence of GCBA. This suggests that at least initial portions of the GCBA effect do not depend on the presence of the color in the FOA, and are not mediated by object-based attention. Hence, the early phase of GCBA apparently reflects whether the probe color matches the observer's internal set of task-relevant color descriptions. In the following, this effect will therefore be referred to as *'color template matching'* effect. Although early modulations underlying GCBA could be elicited by task-relevant colors absent from the FOA (cross-match trials), these modulations were smaller than those observed for colors present in the FOA (match trials). A more detailed discussion on this issue is provided in section 6.4.3.

Taken together, ...

... task-relevant colors absent from the FOA were able to elicit early effects of GCBA (color template matching), while late modulation parts seemed to depend on the presence of the task-relevant color at the attended location. Since the task required the subjects to discriminate the colored target object, the current experiment could not disentangle whether the late modulation depends on the mere presence of the color in the FOA or whether the color has to be involved in a discrimination process. To address this issue, experiment 5 compared the color/shape discrimination task with a simple onset-detection task that eliminates the need to discriminate the object in the FOA.

4.5. Experiment 5: GCBA effects eliminated by onset-detection

4.5.1. Motivation

The results of experiment 4 suggested that early parts of the global color-based modulations reflect a matching process against an internal color template ('color template matching') irrespective of whether the color is actually present in the FOA. Later parts, in contrast, seem to arise only for colors contained in the object under discrimination. If a discrimination process is a necessary condition for the appearance of the late phase of GCBA, abolishing the need to discriminate the target should eliminate the late phase modulation. Thus, a simple onset-detection of the target object – not requiring color selection – should eliminate the late phase modulation. In addition, a simple onset-detection task should also preempt the construction of an internal color template and thus eliminate the early phase modulation. Experiment 5 addressed these predictions by comparing the color/shape discrimination task of experiment 1 with a simple onset-detection task performed on the same stimuli.

4.5.2. Methods

Subjects

Twenty subjects (13 females, mean age 25.8 years, all right-handed except one left-handed subject) participated in experiment 5.

Stimuli and Task

The experimental setup of experiment 5 is illustrated in Figure 4.18. The stimuli were similar to that of experiment 1 with the exception of the following modifications: 1) On half of the experimental blocks subjects performed the color/shape discrimination task as in experiment 1, i.e., they reported whether the curved section of the target color half circle faced left or right (discrimination task). On the other half of the experimental blocks, color and shape were

irrelevant and the subjects were just to report the onset of the bicolored circle in the LVF as fast as possible by pressing a button with the index finger of the right hand (onset-detection task). 2) To increase temporal uncertainty of the target onset for the detection task, the SOA was set to a wider range of 1000-1800ms (rectangular distribution). 3) To control for correct performance of the detection task, the target was missing on 20% of the trials with only the probe being presented in isolation. On those catch trials, the subjects were asked to withhold their response. Catch trials were only present in the onset-detection blocks. Effects of GCBA were assessed by comparing brain responses elicited by probes matching the target's color (match trials, M) with those elicited by probes that did not match (non-match trials, NM). Catch trials were not subjected to data analysis.
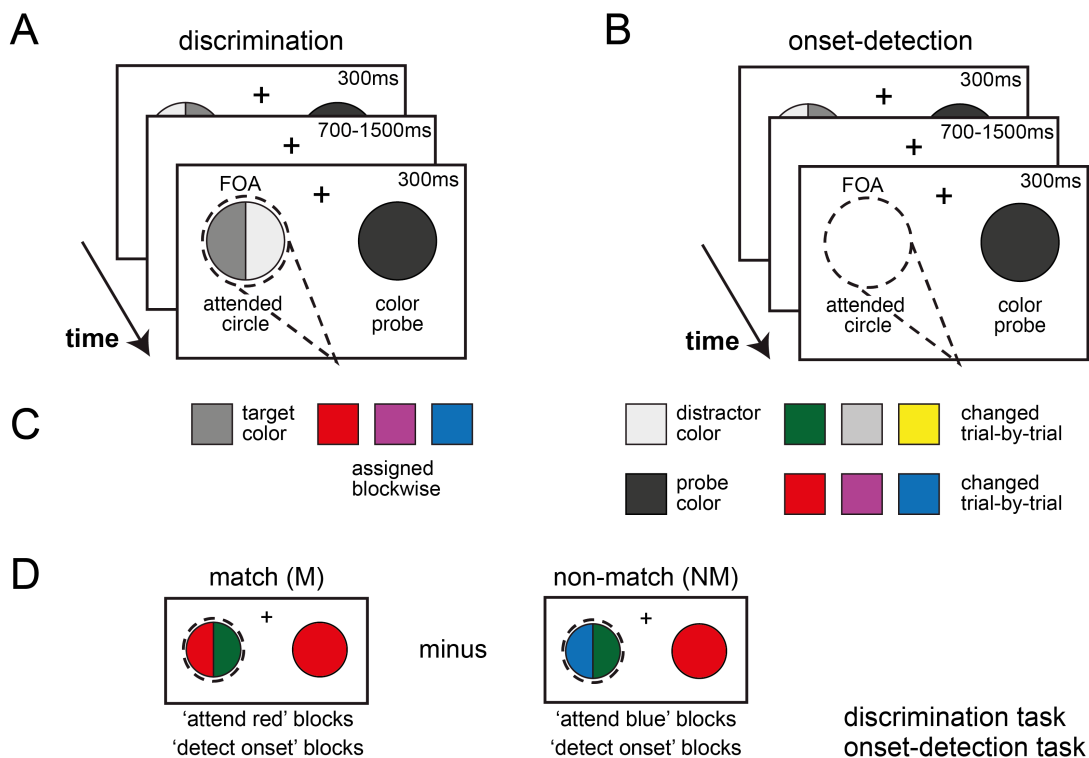
Figure 4.18. Experimental design of experiment 5. **(A)** On half of the experimental blocks, task and stimuli were identical to experiment 1 with the exception of a wider SOA range (discrimination task), **(B)** on the other half of the experimental blocks, the subjects were to report the onset of the circle in the LVF, which was present in 80% of the trials (onset-detection task). **(C)** Target, distractor and probe colors were identical to experiment 1. **(D)** For both trial types effects of GCBA were assessed by subtracting trials with the color of the probe and the color of the target being different (non-match trials, NM) from those trials where the colors matched (match trials, M). The example shown here is for trials with red probes. The match and non-match trials used for the discrimination and the onset-detection task were physically identical.

The subjects performed a total of twelve blocks with six discrimination and six onset-detection blocks in alternation. Each subject was assigned one out of six possible block orders with the target's color (red, magenta or blue) alternating and never being repeated on subsequent blocks. Subjects performed 162 trials on each experimental block (+ 20% catch trials for the onset-detection blocks), yielding a total of 324 match and 648 non-match trials per trial type (discrimination/onset-detection).

4.5.3. Results

Behavioral Performance

The behavioral performance is summarized in Figure 4.19. Response accuracy and response time are compared for the match and non-match trials under conditions of the discrimination and the onset-detection task. The response accuracy was generally high, but still better when subjects were performing the onset-detection task. Further, there was no apparent difference between match and non-match trials for either task. While the responses were overall faster for the onset-detection task, a slowing of match compared to non-match trials was only observed for the discrimination task. These findings were confirmed by a two-way rANOVA with the factors MATCH (match/non-match) and TASK (discrimination/onset-detection) yielding a significant main effect of TASK ($F[1,19] = 46.97$, $p < 0.0005$) but no significant effect of MATCH ($F[1,19] = 0.036$, $p = 0.85$) or the TASK x MATCH interaction ($F[1,19] = 0.45$, $p = 0.51$) for response accuracy. The respective rANOVA for response time revealed significant effects of TASK ($F[1,19] = 233.23$, $p < 0.0005$), MATCH ($F[1,19] = 6.01$, $p = 0.024$) and the TASK x MATCH interaction ($F[1,19] = 10.4$, $p = 0.004$). Post-hoc pairwise comparisons confirmed the presence of a response slowing of match compared to non-match trials for the discrimination ($p = 0.001$) but not the onset-detection task ($p = 0.423$). A possible explanation of the observed response slowing on match trials of the discrimination task is provided in section S.2.1.
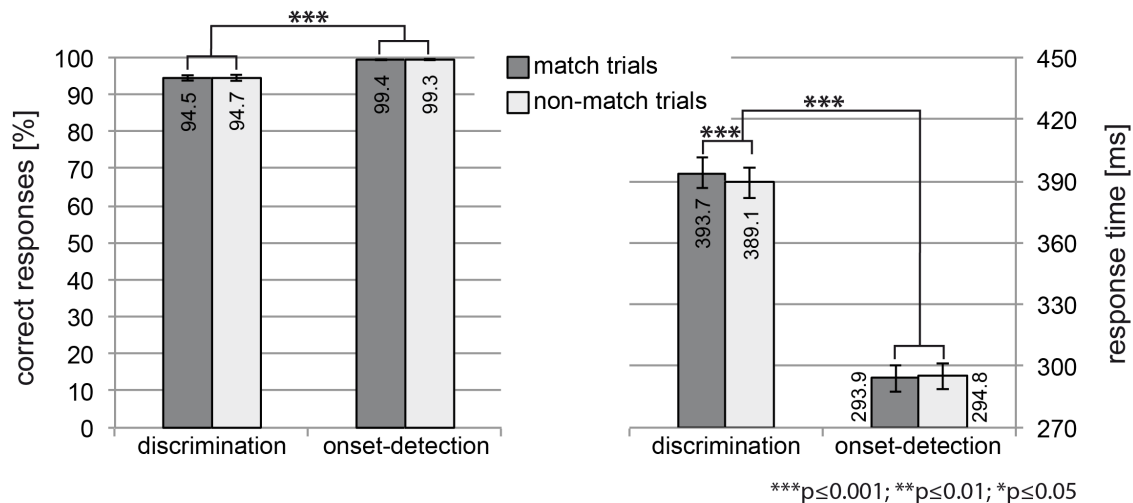
Figure 4.19. **Behavioural performance of experiment 5**. The percentage of correct responses and the response time are displayed for match (dark grey) and non-match (light grey) trials for both the discrimination and the onset-detection task. The error bars reflect the standard error of the mean (SEM). The response accuracy was comparable on match and non-match trials with higher accuracy for the onset-detection compared to the discrimination task. The responses were overall faster for the onset-detection task. A response slowing on match compared to non-match trials was only observed under conditions of the discrimination task.

Event-related magnetic field (ERMF) responses

To assess effects of GCBA, the responses elicited by the unattended color probes were analyzed as a function of wether they matched (match trial, M) or did not match (non-match trial, NM) the target's color in the FOA. The results for the respective M-NM differences are displayed in Figure 4.20. The discrimination task nicely replicated the GCBA modulation sequence in ventral extrastriate visual cortex seen in experiment 1: An early more anterior-lateral effect around 205ms was followed by a later more posterior-medial modulation around 290ms. For the onset-detection task, however, both the early and the late modulation were eliminated. Although the field distribution seemed to contain a minimal effect resembling the early GCBA modulation, the ERMF waveforms showed no significant modulation (sensor sites for ERMF waveforms and locations for the source waveforms were taken from the maxima of the discrimination task). Moreover, the CSD estimates yielded current maxima in a more parietal area.
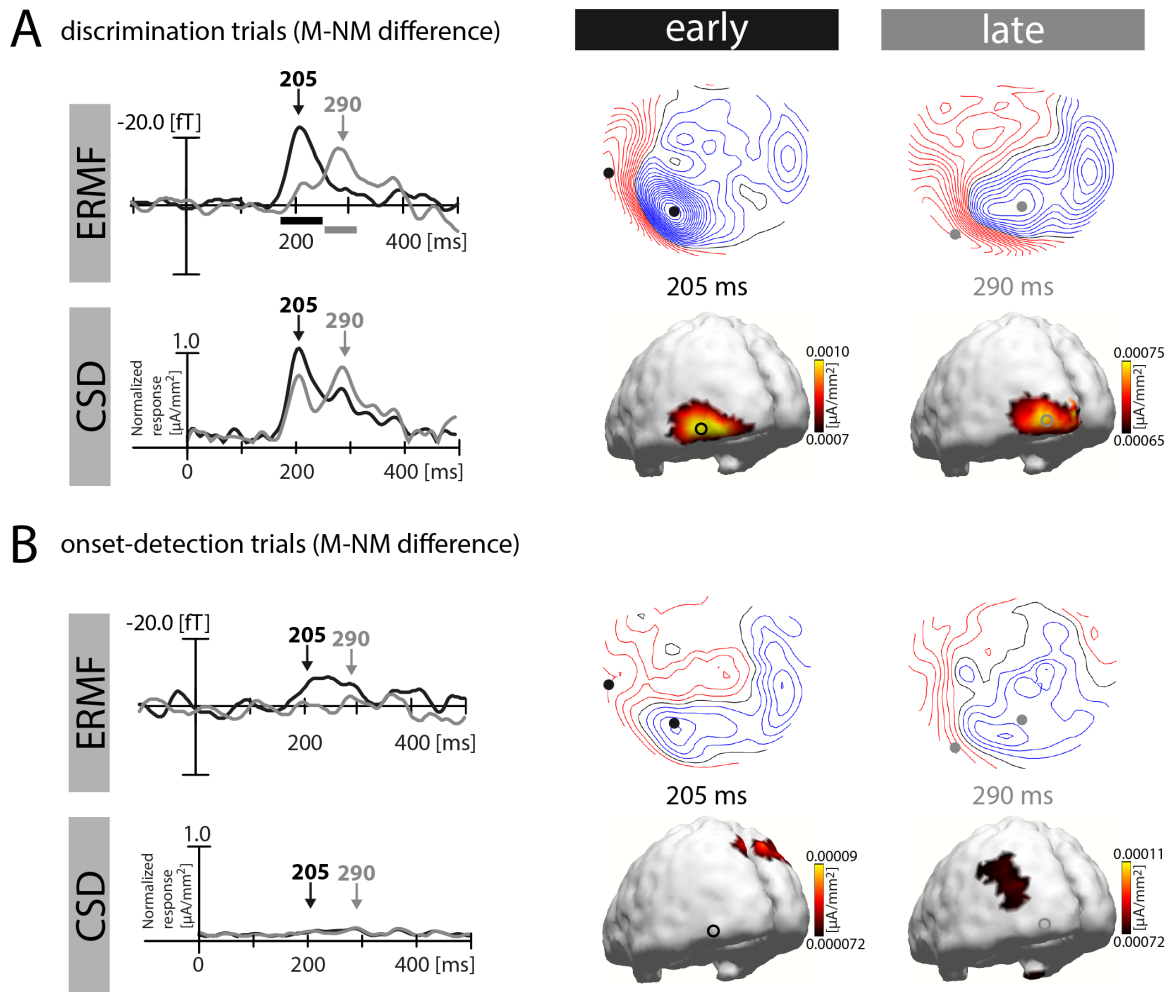
Figure 4.20. ERMF responses of experiment 5. (A/B) upper rows: The field distribution maps of the early and late modulation of GCBA are shown for the discrimination task **(A)** as well as the onset-detection task **(B)** at time points of modulation maxima of the discrimination task. The corresponding ERMF waveforms of the early (black trace) and late (grey trace) modulation reflect the averaged signal of selected sensor sites chosen close to the efflux (polarity inverted before averaging) and influx maxima of the discrimination task (black/grey dots). The grey and black horizontal bars indicate time ranges of significance (match vs. non-match comparison, $p < 0.05$, corrected for multiple comparisons as described in 3.4.1). **(A/B) lower rows**: The current source density (CSD) distribution 3D maps of the selected early and late time points are displayed together with the normalized source activity over time at locations of source density maxima of the discrimination task (black/grey circles). Under conditions of the onset-detection task, no significant early or late effects of GCBA could be observed.

4.5.4. Discussion

While the discrimination task nicely replicated the GCBA modulation sequence observed in experiment 1, both the early and the late phase of GCBA were abolished when performing the onset-detection task.

Early modulation

The absence of the early modulation perfectly fits the interpretation that early parts of GCBA reflect an internal 'color template' that was abolished when the target's color did no longer matter to the subjects. Nonetheless, the onset-detection trials seemed to contain traces of the early modulation of GCBA. It is possible that these small modulation parts arose due to color priming effects as further discussed in section 6.4.1.

Late modulation

The absence of the late modulation under conditions of the onset-detection task supports the idea that the late effect was elicited by a discrimination process performed on the colored object. That is, the mere presence of the color in the FOA was not sufficient to elicit effects of GCBA, unless this color information was part of a discrimination process. Whether this discrimination process reflects object-based selection of color or color discrimination per se cannot be disentangled with the current experimental setup (for a detailed discussion of this issue see section 6.5.1).

Taken together,...

... the results of experiment 5 are in line with the conclusion that early parts of GCBA need the color to be part of the attentional set ('color template matching'). Furthermore, it revealed that the late GCBA modulation requires the color to be part of a discrimination process. Thus, the late phase of GCBA will be referred to as *'discrimination matching'* effect.

5. Summary of the main findings

The reported experimental series was designed to characterize electromagnetic correlates of global color-based attention (GCBA), and to investigate which experimental conditions have to be met for color-based attention to work in a global manner (i.e., throughout the whole visual field). The following lists the questions and predictions that were initially put forward, together with the answers suggested by the experimental results.

Question 1) What are the electromagnetic correlates (ERP/ERMF) of GCBA when performing a color/shape discrimination task?

Prediction: According to previous findings for attention to orientation and motion (Hopf et al., 2004; Bondarenko et al., 2012; Stoppel et al., 2012), GCBA should be indexed by modulations of the ERPs/ERMFs in the N1/N2 time range. (experiment 1, 2)

Answer: Modulations underlying GCBA arise as early and late effect (in the N1/N2 time range) in ventral extrastriate visual cortex. The early modulation (~200ms) arises in more anterior-lateral ventral occipito-temporal cortex (presumably LOC, VO-1/2), while the late modulation (~280ms) originates more posterior-medial in early visual regions (V3/4, V1).

Question 2) Does GCBA depend on the competition of color values in the FOA?

Prediction: If GCBA depends on color competition in the FOA, GCBA modulations should be absent or at least substantially reduced without a competing distractor color in the FOA. (experiment 3)

Answer: Although the late modulation seems to be marginally weaker without a competing color in the FOA, both phases of the GCBA modulation do not depend on color competition in the FOA.

Question 3) Does GCBA depend on the physical presence of the attended color in the FOA?

Prediction: If GCBA is bound to the presence of the attended color in the FOA, it should be absent for a task-relevant color that is not contained in the FOA. (experiment 4)

Answer: At least early parts of the modulation sequence (~200ms) can arise for a task-relevant color that is absent from the FOA ('color template matching').

Question 4) Does GCBA depend on the discrimination of the target in the FOA?

Prediction: If GCBA requires the discrimination of the target in the FOA, it should be eliminated when performing a simple onset-detection task where the need to discriminate the colored target is abolished. (experiment 5)

Answer: Without the need to discriminate the colored target object in a simple onset-detection task, all modulations of GCBA are eliminated.

6.   General discussion

A stunning property of feature-based attention is its ability to operate outside the spatial focus of attention throughout the whole visual field. While a growing number of electromagnetic studies documented correlates (ERP, ERMF, SSVEP) of GFBA (Hopf et al., 2004; Zhang & Luck, 2009; Andersen et al., 2011; Boehler et al., 2011; Bondarenko et al., 2012; Stoppel et al., 2012; Andersen et al., 2013), earlier ERP studies reported feature-based attention to be bound to the spatially attended location (Hillyard & Münte, 1984; Wijers et al., 1989; Anllo-Vento & Hillyard, 1996). Hence, there seem to be certain experimental preconditions that have to be met in order for feature-based attention to operate in a global manner. The current work was designed to investigate possible determinants of GFBA. It was particularly motivated by recent ERP findings that suggested color competition to be crucial for a global operation mode of color-based attention (Zhang & Luck, 2009). To this end, a series of ERP/ERMF experiments was conducted. The first experiment served to characterize electromagnetic correlates of GCBA, while the subsequent experiments (2-5) investigated the influence of color competition and other possible determinants on GCBA. A detailed discussion of the experimental results will be provided in the following.

6.1.   Electromagnetic indices of GCBA

GCBA – a sequence of modulations in ventral extrastriate visual cortex

Experiment 1 served to characterize the electromagnetic correlates of GCBA under conditions of a simple color/shape discrimination task. The grand average data (signal averaged across subjects) revealed that attended colors elicited a sequence of independent modulations in ventral extrastriate visual cortex, with an early more anterior-lateral maximum around 200ms followed by a late more posterior-medial maximum around 280ms. The observation of a modulation sequence in the ventral visual pathway is consistent with the fact that ventral stream areas are known to respond to chromatic stimuli (Hadjikhani et al., 1998; A. R. Wade et al., 2002; Brewer et al., 2005). To gain more specific insight into the spatio-temporal pattern of GCBA modulations within individual observers, single subject data were used for a detailed localization analysis based on individual anatomical data. Specifically, four subjects were selected that took part in at least three experiments. Since all experiments contained a condition comparable to experiment 1, the data could be averaged across these conditions to increase the signal-to-noise ratio (see section 3.4.2). Furthermore, the borders of early visual areas (V1-V4) as well as the location of the lateral occipital complex (LOC) were individually determined for these subjects using fMRI-based retinotopic mapping and a LOC localizer scan (see section 3.4.3). According to the single subject analysis, the early modulation of the color/shape discrimination task arose in or around the lateral occipital complex (LOC), an array of areas known to mediate the perception of object shape (Kourtzi & Kanwisher, 2000; Larsson &

Heeger, 2006). Furthermore, the early modulation presumably involved the ventral occipital areas VO-1/2 that were reported to respond to color and objects (Brewer et al., 2005; Brouwer & Heeger, 2009). The late modulation was located in more posterior retinotopic regions (V3/4, V1) which are known to be color selective (Zeki et al., 1991; Chawla et al., 1999; Gegenfurtner, 2003; Sàenz et al., 2003; Brewer et al., 2005; A. Wade et al., 2008; Brouwer & Heeger, 2009). Notably, in line with previous findings in the orientation domain (Bondarenko et al., 2012), the early and late modulations propagated through ventral stream areas in reverse hierarchical order (from higher to lower tier areas).

6.2. Determinants of GCBA

Experiment 2-5 contained at least one condition identical or comparable to experiment 1, which always replicated the GCBA modulation sequence seen in experiment 1. Specifically, both the early and the late phase were elicited under experimental conditions requiring the discrimination of an object that contained the attended color (i.e., the color/shape task of experiment 1 and 2, the distractor present/absent tasks of experiment 3, the one/two-color color tasks of experiment 4 and the discrimination task of experiment 5). Notably, this robust replication is in apparent contrast to a number of earlier ERP studies that found no evidence for GCBA, but instead reported effects of color-based attention to be bound to the attended hemifield (Hillyard & Münte, 1984; Wijers et al., 1989; Anllo-Vento & Hillyard, 1996). Thus, the question arises of what experimental conditions make color-based attention to work in a spatially global manner. There were two major differences between the stimulus design of those earlier ERP studies and the current experimental setup used here: The earlier ERP studies 1) tested effects of GCBA when the attended color was absent from the FOA, 2) displayed colors always in isolation with no other competing color being simultaneously present (see 1.2.3, Figure 1.2 for the stimulus design), while more recent studies suggest GCBA to depend on color competition (Sàenz et al., 2003; Zhang & Luck, 2009). The current experimental series investigated the influence of those experimental design differences to reveal which factors are crucial for GCBA to arise. The factors tested and their impact on the early and late phase of GCBA, as suggested by the experimental results, are reported in the following.

6.2.1. The role of color competition in the FOA

One key question of the current work was as to whether GCBA depends on the presence of competing color values in the FOA. That is, the effects of GCBA characterized in experiment 1 might arise from the competition between the target and distractor color in the FOA. Indeed, competition is a well-known determinant of attentional selection: Sensory responses of e.g., MT/MST, inferotemporal (IT), V2 or V4 neurons are predominantly modulated by attention when stimuli compete for access to representation in the neuron's receptive field (Moran & Desimone, 1985; Chelazzi et al., 1993; Luck et al., 1997; Reynolds et al., 1999; Treue & Maunsell,

1999; Reynolds & Chelazzi, 2004; J. Lee & Maunsell, 2010). For example, Luck et al. (1997) found, that when a red and a green item were simultaneously presented in the receptive field of a V4 neuron preferring red, attention to the green item decreased the response to the red one. The size of this modulation was substantially reduced by a sequential presentation of the two items (only one at a time) and nearly abolished – weak and inconsistent – when the green item was displayed outside the receptive field with the preferred red stimulus left alone inside. Hence, it would seem reasonable that effects of GCBA reflect the operation of resolving the competition between different colors inside the FOA. In fact, there is behavioral and neurophysiological evidence suggesting that GCBA depends on color competition in the FOA (Sàenz et al., 2003; Zhang & Luck, 2009).

Sudies that suggest GCBA to depend on color competition in the FOA

Sàenz et al. (2003) had the subjects perform a luminance discrimination task on two spatially separated but simultaneously presented stimuli (one in the left and one in the right visual field). Each stimulus consisted of superimposed fields of red and green dots (see Figure 6.1A). The performance was significantly better when the subjects attended dots of the same color (either red or green) on both sides of the visual field compared to when they had to attend green in the one and red in the other visual hemifield. This processing increment throughout the visual field for stimuli sharing the attended color served as index of GCBA. However, the effect was clearly reduced when the stimuli on both sides were composed of dots of only one color (either red or green, no superimposition of red and green dots). Hence, the size of the GCBA effect observed by Sàenz et al. (2003) depended in fact on the presence of competing color values (red and green) within the stimulus in each visual hemifield. Further evidence that color competition plays a role for GCBA was provided by the ERP experiments of Zhang and Luck (2009). The authors required the subjects to attend to a continuous stream of randomly moving mixed red and green dots in one visual field in search of a luminance decrement of dots drawn in a particular color (e.g., red). In the meantime, either all-red or all-green dots were probed in the other, unattended visual field. Those unattended probes led to an enhanced ERP response (P1 amplitude) when they matched the attended color compared to when they matched the other, unattended color. Importantly, these effects of GCBA were abolished when the red and green dots on the target side were shown sequentially alternating, i.e., when no second competing color was present in the FOA (see Figure 6.1B).

Current experiments: GCBA modulations appeared independent of color competition in the FOA

In direct contrast to the just outlined studies, the results of the present experiments suggest that global-color based selection does not depend on the presence of a competing color in the FOA (see Figure 6.1C). In fact, removing the competing disctractor color in the FOA (distractor-absent trials of experiment 3, see 4.3.3) did neither eliminate nor substantially reduce the modulation sequence observed for GCBA. At a first glance these results seem to contradict those of Sàenz et al. (2003) and Zhang and Luck (2009), but there are substantial differences in the

experimental design that have to be considered. First, there were significant differences in the stimulus timing. In the current experiments the target and probe were simultaneously onset stimuli displayed for 300ms, and followed by at least a 1000ms interstimulus interval. Thus, the allocation of attention to color had a transient dynamic. On the contrary, Zhang and Luck (2009) presented a continuous stream of colored dots where the dots drawn in the target color were attended continuously. Similarly, in the design of Sàenz et al. (2003) the colored dots were attended for two subsequent 500ms intervals separated only by 100ms. That is, in both studies the subjects viewed the attended color (in search for a luminance change) for longer time periods, which probably led to a more sustained allocation of attention to color. Most importantly, while the target and probe shared a common off- and onset in the current experiments, Zhang and Luck (2009) flashed color probes to test effects of GCBA when subjects had already focused their attention onto the colored dot stream and presumably build up a strong color bias. In line with that interpretation Zhang and Luck (2009) found a modulation of the early P1 component suggesting a modulation bias of the feed-forward sweep of sensory processing in the visual cortex. In contrast, the earliest modulation of GCBA found in the present experiments occurred in the N1 time range, rather compatible with a modulation of the feed-back information flow. Second, the luminance detection paradigms were by far more challenging (performance: ~ 65-83% correct (Sàenz et al.) ~ 80% hits (Zhang & Luck)) than the current color/shape discrimination task (performance: 93-96% correct).

Taken together, it is possible that under experimental conditions that require a more sustained feature bias or a more continuous allocation of attentional resources to perform a challenging task, the resolving of color competition in the FOA becomes indeed a determinant of GCBA. Under conditions of a more transient allocation of attention paired with an easy color/shape discrimination task, effects of GCBA may not depend on the presence of a second competing color in the FOA.

Color competition between the left and right visual hemifield?

The modulation sequence for GCBA observed here turns out to be independent of color competition *within* the FOA. However, the possibility remains that color competition across visual fields might have played a role. Specifically, in all experimental conditions where GCBA appeared there were always two color items with one displayed in the left and one displayed in the right visual field (target and probe) that shared the color on match, and differed in color on non-match trials. If both the target and the probe were encompassed by a large receptive field of a single neuron, the color competition between the target and the probe would also have to be considered as a possible source of the GCBA modulation. However, since all the cortical structures that might be involved in the modulation sequence (LOC, VO-1/2, V3/4, V1) show a contralateral retinotopic organization (Sereno et al., 1995; Brewer et al., 2005; Larsson & Heeger, 2006; Wandell et al., 2007), it seems unlikely that their receptive fields simultaneously encompassed both the target and the probe presented in opposite visual hemifields.
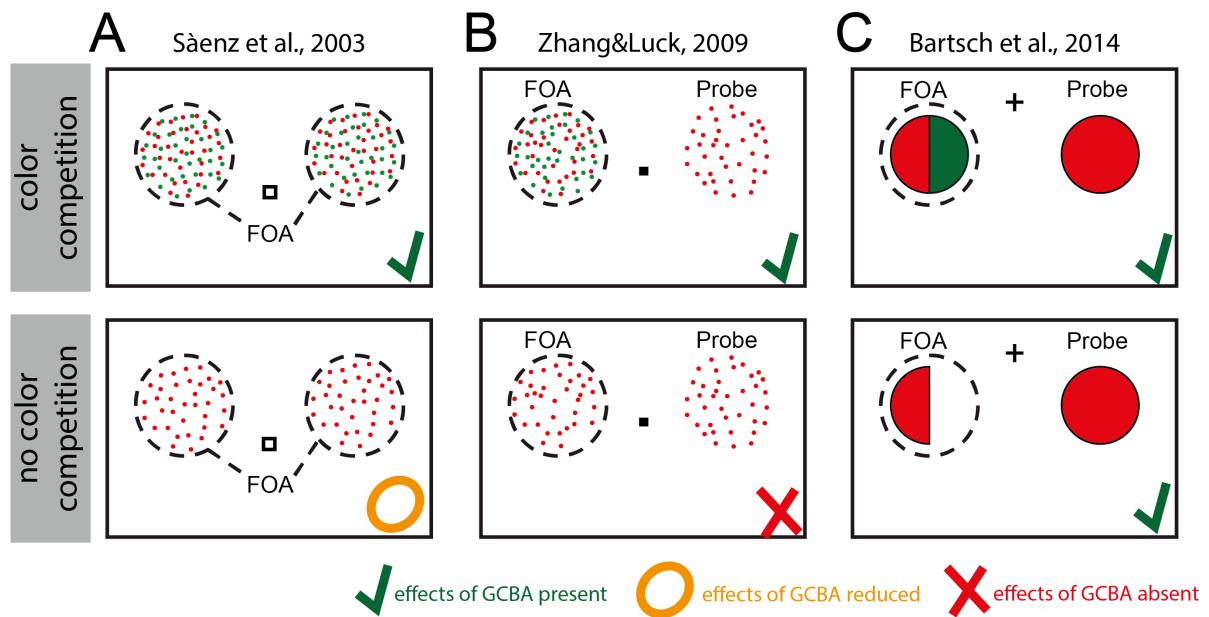
Figure 6.1. Stimulus designs of studies investigating the role of color competition for GCBA. The stimulus designs are schematically displayed for Sàenz et al. (2003) **(A)**, Zhang and Luck (2009) **(B)** and Bartsch et al. (2014) **(C)** under 'attend to red' conditions. **(A), (B)**: the subject's attention remained on the red dots in search for a luminance change. The dots in the FOA were presented continuously (B) or shown every 3.3 seconds for two subsequent 500ms time intervals separated by 100ms (A). **(C)** The subjects attended to the red half circles that were presented for 300ms (SOA: 1000-1200ms). (B),(C): Probes were flashed for 100ms during a continuous target presentation in the FOA (B) or shared a common on- and offset with the target (C). **Upper row**: All stimulus designs led to effects of GCBA when a second competing distractor color (here: green) was present in the FOA. **Lower row**: When only a single color value was shown in the FOA (no color competition), the effects of GCBA did not considerably change for Bartsch et al. (2014), but were clearly reduced or absent for Sàenz et al. (2003) and Zhang and Luck (2009).

6.2.2. The role of the presence of the color in the FOA

Given that GFBA is independent of feature competition, the question remains as to whether GCBA depends on the actual presence of the target color in the FOA. Experiment 4 addressed this question by introducing a second target color. That way, the target was defined by two possible target colors with only one of them being randomly present in the FOA on a given trial. Importantly, the task-relevant colors elicited early (but not late) parts of the GCBA modulation irrespective of their presence in the FOA. For example, when the subjects had to attend to a target that could be either red or green, a green probe, presented in the unattended visual hemifield, elicited early effects of GCBA even if the target in the FOA turned out to be red on the current trial (cross-match trials of experiment 4, section 4.4.3). This early modulation effect that depended only on the task-relevance, but not on the actual presence of the color in the FOA was thus referred to as *'color template matching'*. However, late parts of the GCBA modulation did not arise for colors absent from the FOA, but required the colors to be part of the target object presented there.

Early modulation: converging evidence for a template matching process

The interpretation of the early phase of GCBA as a matching process against the observer's internal set of task-relevant colors is supported by recent findings of an ERP/ERMF study for attention to orientation. Bondarenko et al. (2012) also reported the early phase of GFBA to depend on an internal set of task-relevant orientations (horizontal and vertical), but not on the actual presence of these orientation in the FOA. In an experimental design similar to the one reported here, the subjects were presented a task-relevant orientation grating (target) in the LVF together with a task-irrelevant orientation grating (probe) in the RVF. The subjects were to report the orientation of the target in the LVF that could be either horizontal or vertical (0° or 90°) on a given trial. Effects of GFBA were assessed by analyzing brain responses to the task-irrelevant orientation probes (vertical, horizontal or orientations in between) as a function of the orientation similarity between the target and the probe. The authors demonstrated that probes containing the task-relevant orientations (horizontal and vertical) elicited an early effect of GFBA irrespective of which of the two orientations was actually presented in the FOA ('template matching'). Importantly, the template matching for attention to orientation reported by Bondarenko et al. (2012) and the color template matching found here reflect both a modulation in the N1 time range originating from ventral extrastriate visual cortex regions located more anteriolateral than the respective late modulations of GFBA.

Explicit or implicit template?

Of note, neither the current experiments nor those of Bondarenko et al. (2012) could decide whether the template of task-relevant features reflected the explicit task-descriptions ("attend to red and green" / "attend to horizontal and vertical") or whether the repeated presentation (priming) of those target features led to an implicit template. The latter could potentially account for why subjects showed effects of template matching when the color was not explicitly needed to select the target (distractor-absent trials of experiment 3, see 4.3.3). It is possible that task-irrelevant colors or orientations can also elicit effects of template matching just by virtue of being repeatedly part of the discriminated object. Future experiments have to reveal whether the template matching effect refers to an explicit or an implicit one (see section 7.5).

6.2.3. The role of target discrimination

The results of experiment 4 showed that late parts of GCBA did not appear for colors when they were absent from the FOA (cross-match trials, section 4.4.3). In contrast, the late modulation always appeared for target colors that were involved in a discrimination process in the FOA (e.g., match trials of experiment 4, section 4.4.3). Thus, the question arose as to whether late effects of GCBA require active target discrimination or whether the mere presence of a color in the FOA would be sufficient to elicit the late GCBA modulation. Experiment 5 therefore compared effects of GCBA under conditions of target discrimination task (color/shape) to those of a simple onset-detection task that abolished the need to discriminate the colored target in the

FOA. All effects of GCBA were eliminated under conditions of a simple onset-detection. That is, when the subjects were only to report the onset of the colored targets irrespective of their color or shape, neither the early nor the late modulation of GCBA was observed. The absence of the early modulation fits the interpretation that the early phase of GCBA reflects a template of task-relevant colors. Since the target's color did not matter in the onset-detection task, the subjects were not required to build up an internal set of task-relevant colors. The late phase of GCBA was also absent when the task did not involve the discrimination of the colored target. Together with the fact that the late phase arose only for colors that were present in the FOA, this suggests, that the late phase was elicited by a discrimination process performed on the colored target. The late GCBA modulation that arose in early visual areas (V3/4, V1) was thus referred to as *'discrimination matching'*.

Late modulation: converging evidence for a discrimination matching process

The interpretation of the late phase of GCBA as 'discrimination matching' process fits with recent observations in the rhesus monkey (Ipata et al., 2012). That is, V4 neurons were reported to display feature selectivity (e.g., shape: upper vs. lower case 'T') only when the monkeys had to discriminate a saccade target (find the upper case 'T' among lower case 't's and tell whether its orientation is 'upright' or 'inverted'), but not when the monkeys were to saccade to the location of the same item without discriminating its feature pattern (only item displayed at a time, report its location). Hence, it seems perfectly reasonable, that the late modulation of GCBA – localized in early retinotopic areas (V3/4, V1) – requires the target object to be discriminated. In line with this reasoning, recent ERP/ERMF studies in humans that reported a modulation in the N2 time range for global attention to orientation or motion also involved orientation or motion discrimination tasks (Bondarenko et al., 2012; Stoppel et al., 2012). Like in the current experimental series, those late modulations of GFBA were consistently observed in visual extrastriate cortex areas (motion: lateral middle occipito-temporal cortex; orientation: posteromedial parts of the ventral extrastriate visual cortex). Importantly, the N2 modulations for orientation and motion were reported to scale with the similarity between the feature values at the attended and the unattended location.

Taken together, it appears that the late modulation of GCBA reflects a color discrimination process that indexes the physical similarity between colors inside and outside the FOA. Since the current experimental setup provides no systematic variation of color similarity, future experiments will have to reveal as to whether the late phase of GCBA scales with color similarity between target and probe (see section 7.3).

6.2.4. Determinants of GCBA: Summary

The experimental results suggest that GCBA consists of an early and a late phase. A color has to be contained in the set of task-relevant colors to elicit early parts of GCBA ('color template matching'). For this early parts, the actual presence of the color in the FOA is not required. To

give rise to later parts of GCBA, a color has to be present in the FOA and further to be involved in a discrimination process ('discrimination matching'). If a color is neither used to select the target nor part of a discrimination process (onset-detection task), the mere presence of this color in the FOA will not lead to its global selection. Importantly, neither the early not the late phase of GCBA required color competition in the FOA.

6.3. GCBA propagates through areas of the visual cortex in reverse hierarchical order

As discussed in detail in the previous sections (6.1 and 6.2) GCBA was found to involve a sequence of both functionally and anatomically separable early and late modulations in ventral extrastriate visual cortex. Specifically, the early modulation reflecting color template matching peaked around 200ms in LOC/VO1-2 ('template matching'), while the late modulation arose around 280ms in early visual ares (V3/4, V1) presumably due to the discrimination of the colored target ('discrimination matching'). Importantly, the hierarchical level of representation in ventral extrastriate visual cortex increases from posterior-medial retinotopic regions to the more anterior-lateral areas (Grill-Spector & Malach, 2004). The early and the late modulation therefore reflect a propagation of GCBA effects that runs in reverse hierarchical order through ventral stream areas (from higher to lower tier areas). This observation nicely replicates the spatio-temporal pattern of the GFBA modulation sequence reported by Bondarenko et al. (2012) for attention to orientation. The authors found modulations in ventral extrastriate cortex with an early 'template matching' effect in more anterior-lateral (anatomically "late") areas followed by a late 'discrimination matching' effect in more posterior-medial (anatomically "early") areas.

At a first glance it seems surprising that the temporal order of the GFBA modulations does not follow the hierarchical order of the visual cortex in a bottom-up direction. However, recurrent feedback activations from higher- to lower-order cortical areas are proposed to play a crucial role in attentive vision and conscious visual perception (Lamme et al., 1998; Di Lollo et al., 2000; Lamme & Roelfsema, 2000; Bullier, 2001). Mehta et al. (2000a, 2000b) were, for example, able to demonstrate an inverse relationship between visual and attentional modulation latencies in the macaque monkey. While visual onset latencies generally increase along the stages of cortical hierarchy, attention modulation latencies were found to decrease (ventral pathway: along V1, V2, V4 and inferotemporal cortex). The temporal pattern was taken to indicate that attentional modulations start at higher hierarchical levels and progress back down the visual hierarchy. The mediation of attention via cortical feedback connections is also a key feature of computational models of visual attention (e.g., the 'biased competition' model: Desimone & Duncan, 1995; the 'Reverse Hierarchy Theory': Hochstein & Ahissar, 2002; the 'feedback model': Spratling & Johnson, 2004; the 'Selective Tuning model': Tsotsos, 2011).

The Reverse Hierarchy Theory (RHT), e.g., proposes that explicit visual perception begins when the initial feedforward processing reaches high cortical levels. This first explicit percept at high-

level visual areas is based on widespread attention (large receptive fields) associated with a crude representation of the gist of the visual scene based on basic level categorizations (e.g., faces vs. houses). To retrieve more detailed information (the exact location of an item, fine-grained color distinctions, etc.,), attention is focused via feedback connnections to specific lower-level visual areas that code these informations (i.e., details available only in the small receptive fields of lower cortical areas). Applied to the present experiments, the early 'template matching' phase of GCBA observed in high-level areas (LOC, VO-1/2) would be expected to provide a coarse color categorization while the late 'discrimination matching' phase in more low-level visual areas (V3/4, V1) should reflect more fine-grained color distinctions. Unfortunately, the current experiments provide no fine color gradations to address this hypothesis. However, for attention to orientation Bondarenko et al. (2012) found the early phase of GFBA to reflect an abstract categorical template while the late phase indeed scaled with the physical similarity of the displayed orientations. Whether global attention to color shows a similar behaviour has to be addressed in future experiments (see section 7.3).

6.4. Secondary findings

6.4.1. Traces of the early modulation for onset-detection

Experiment 5 demonstrated that no significant effects of GCBA were left under conditions of a simple onset-detection task (see section 4.5.3). Still, the field distribution map and ERMF waveform seemed to contain traces of the early GCBA modulation. As discussed in section 6.2.2, experiment 4 suggested that the early GCBA effect reflects a template of task-relevant colors ('color template matching'). Since the target's color was not task-relevant when performing the onset-detection task, the indication of a small early GCBA modulation (although not significant) is puzzling. One possible cause of the small modulation may be color repetition. Note, in all experiments, the target's color was constantly repeated within experimental blocks. The mere repetition of target color may have led to some form of 'implicit' color priming irrespective of the color's current task-relevance. In fact, it has been shown that the repetition of feature values on subsequent trials leads to priming effects (Kristjánsson, 2006; Theeuwes, 2013). Importantly, those effects of priming are not under conscious control of the subjects, and can even last as a memory trace for 5-8 eight trials (Maljkovic & Nakayama, 1994). Thus, the small early modulation observed for the onset-detection task might reflect an issue of unconscious color priming. Unfortunatey, the setup of experiment 4 does not allow to separate the contribution of explicit task-descriptions (explicit template) from unconscious color priming (implicit template). On the other hand, while color priming may account for a small part of the early modulation, it does not account for the biggest part of the template matching effect.

6.4.2. GCBA effects influenced by the number of attended colors

In experiment 4, the subjects attended either to one target color on a given experimental block (one-color blocks) or they attended simultaneously to two possible target colors (two-color blocks). While early and late effects could be found for match trials of both experimental conditions, the early modulation was smaller in amplitude for the two- compared to the one-color blocks (see section 4.4.3, Figure 4.17). It is possible that this amplitude difference reflects stronger trial-by-trial color priming (see previous section) on one-color blocks: In one-color blocks, the target color was present on every trial (strong priming) while in two-color blocks each color was randomly presented on 50% of the trials (weaker priming). Still, there are other possibilities. The amplitude reduction in the two-color condition might reflect limits of visual working memory capacity. Previous studies showed that feature-based selection is limited in capacity, such that attending to two feature values simultaneously would either result in a parallel matching of both feature templates with reduced efficacy or in serially attending to only one feature value (template) at a time (Houtkamp & Roelfsema, 2009; T. Liu et al., 2013). For example, Houtkamp and Roelfsema (2009) had the subjects searching for either one or two colors within an RSVP stream of colored items. Importantly, the search performance decreased for the two-color condition in a manner that could be best explained by a search template containing only one color at a time. The authors concluded that although the working memory is able to store multiple colors (visual working memory can store the colors of approximately 3-4 items: (Luck & Vogel, 1997)), the visual input can be matched to only one color at a time. Applied to the present experiment, the amplitude reduction of the two-color condition might reflect the fact that on a part of the trials the "wrong" color template was initially matched against the input. Such serial matching of color templates might also explain the broader appearance of the early two-color peak: a greater temporal jitter caused by serial matching processes would ramify into the peak appearing more smeared-out (i.e., broader). Furthermore, the need to first select the 'correct' target color on each trial could also account for the delayed onset of the late discrimination phase in the two-color blocks. Nevertheless, to settle this issue, further experiments would be required that systematically investigate the influence of the number of attended colors on effecs of GCBA.

6.4.3. Early GCBA effect smaller for colors absent from the FOA

Experiment 4 showed that task-relevant colors are able to elicit early parts of GCBA irrespective of their presence in the FOA ('color template matching'). However, the template matching effect elicited by colors absent from the FOA (cross-match trials) was substantially smaller in amplitude compared to the template matching effect elicited by colors actually present in the FOA (match trials) (see experiment 4, section 4.4.3, Figure 4.17). Thus, the actual presence of a color in the FOA somehow boosts the template matching effect. Another explanation would be that the later GCBA modulation – only elicited by colors present in the FOA – contributed to the bigger amplitude by overlapping with the template matching effect.

Furthermore, it is possible that the early phase of GCBA contained an additional modulation only triggered by colors present in the FOA. Finally, as discussed in the previous section, it might be that the visual input can only be matched to one color at a time. Even if such single-color template could be switched within trials, it would naturally be switched to the target color currently present in the FOA and thus to the match and not to the cross-match color. That way, the reduced amplitude on cross-match trials compared to match trials could also be in line with a 'one color at a time' template matching mechanism.

6.4.4. Late GCBA phase slightly smaller without color competition

Experiment 3 demonstrated that early and late modulations of GCBA could be elicited irrespective of the presence of a competing distractor color in the FOA (see section 4.3.3, Figure 4.14). However, expecially the late modulations seems to be marginally weaker without color competition (distractor-absent trials). Thus, it color competition might indeed influence the strength of the late phase of GCBA. Since the late phase seems to reflect a process arising due to the discrimination of the colored target (cf. section 6.2.3), such target discrimination processes might be enhanced by the need to filter out competing color values. However, it has to be kept in mind that there are physical differences between the stimuli of the distractor-present and the distractor-absent condition, which could as well account for the observed slight amplitude differences.

6.5. Experimental limitations and possible confounds

6.5.1. Effects of GCBA mediated by object-based attention?

Removing the distractor color from the target in experiment 3 showed that GCBA effects were preserved when eliminating color competition in the FOA (see distractor-absent trials, section 4.3.3). However, removing the distractor half circle led to a stimulus configuration that – strictly taken – preempted the need to discriminate color in order to perform the task (i.e., to decide whether the curved section of the half circle faces to the left or right). It is somewhat puzzling then that effects of GCBA could be observed even though color discrimination was not explicitly required. However, although color discrimination was not necessary to select the target object (and discriminate its shape), the subjects likely developed an internal bias for the target color (color template) because 1) the target's color was constant throughout an experimental block and 2) the task instructions prompted the subjects to attend to the target's color (i.e., "To which side does the convexity of the *red* half circle face?").

Another explanation would be that the discrimination of the target's shape entailed a concomitant selection of its color mediated by object-based attention. According to object-based attention theories, the attention to a particular object feature – like a certain color – automatically entails the selection of all of the other object's features (Desimone & Duncan,

1995; Blaser et al., 2000). Indeed, effects of GFBA have not only been reported for attended features, but also for irrelevant features that were contained in the target object. For example, attending to the color or luminance of moving dots elicited global effects of their motion direction as well (Melcher et al., 2005; Sohn et al., 2005; Arman et al., 2006; Katzner et al., 2009). When attending a specific color of a target object, another irrelevant color that was part of the target could also give rise to global color selection (Boehler et al., 2011). Applied to the present experiments, the discrimination of the target's shape might have entailed color selection thereby causing the observed effects of GCBA. Hence, GCBA may arise from object-based selection and/or from target color selection proper. Notably, the electromagnetic correlates indexing the global selection of a task-irrelevant color – and hence reflecting purely object-mediated effects of GCBA – were qualitatively different from those observed in the current experiments: Boehler et al. (2011) reported not a negative, but a positive enhancement of the ERP waveforms contralateral to the probe around 270-500ms. The issue of whether GCBA refers to a direct or an object-based selection process, however, cannot be resolved based on the results of experiment 3.

Early phase of the GCBA modulation

Experiment 4 provides some further insights by documenting early GCBA effects for colors that are task-relevant, but absent from the target object (color template matching) (see section 4.4.3, cross-match trials). Respective results show that at least these initial portions of the GCBA effect do not depend on object-based selection. Note, the fact that an early modulation phase was observed for the distractor-absent trials of experiment 3 (see section 4.3.3), suggests that the subjects actually built a color template although the task did not explicitly require it.

Late phase of the GCBA modulation

In contrast to the early phase modulation, the late modulation appeared only for colors present in the object under discrimination, and it disappeared when subjects were required to just detect the onset of the target without further discrimination (onset-detection task, experiment 5, see section 4.5.3). This suggests that the late phase of the GCBA reflects the actual discrimination of the target. Unfortunately, the current color/shape discrimination task does not allow to decide whether the effect was mediated by the color or shape discrimination. Apparently, a more detailed investigation of this issue requires new experiments that aim at a separation of color from shape discrimination (see section 7.7 for possible accounts).

6.5.2. GCBA mediated by color suppression or enhancement?

Moher et al. (2014): evidence for distractor color suppression

When comparing the brain's responses to probes matching and not matching the attended color, the resulting difference in the ERP/ERMF waveforms is typically interpreted as reflecting a processing bias towards probes drawn in the attended color. However, an ERP study by Moher

et al. (2014) showed that the modulation indexing GCBA can sometimes represent the suppression of the responses to a distractor color relative to the attended color. The authors had subjects watch a continuous stream of two spatially interleaved sets of color dots in one visual hemifield, while a set of task-irrelevant unicolored dots was occasionally flashed in the other hemifield (probe). The subjects were instructed to attend to one color of the continuous dot stream (target color) and report whenever the dots drawn in the target color were dimmed, while ignoring such luminance decrements occurring for the dots drawn in the other color (distractor color). The unicolored sets of dots in the unattended visual hemifield could either be drawn in the target color, in the distractor color or a in neutral color that was never presented on the target's side. Importantly, the authors found that the mean P1 amplitude to distractor probes was reduced relative to target probes, while there was no difference between the target and the neutral probes. Additionally, in a subsequent search paradigm, the performance was impaired for distractor-colored items only. These observations were taken to suggest that the effects of color-based attention were mediated by the inhibition of distractor colors rather than by an activation of target colors.

Differences between the current experimental design and Moher et al. (2014)

However, the account of GCBA in terms of color suppression does not easily apply to the current experiments. There are at least three differences between the current experimental setup and that of Moher et al. (2014) that seem to suggest different modes of GCBA mediation:

1) The luminance change detection task of Moher et al. (2014) put more demands on attention than the current color/shape discrimination task (luminance change detection: 85% hits, color/shape discrimination: 93-96% correct responses).

2) Moher et al. (2014) presented the color probes while the subjects were already attending to the target color dot stream, presumably leading to a deeper preset color bias and hence a modulation of an earlier component (P1 component).

3) Moher et al. (2014) kept the color assignment (target, distractor, neutral) constant throughout the whole experimental session (changing only between subjects), while in the current experiments the distractor color alternated from trial to trial and the target color changed blockwise.

All these factors together presumably led to a stronger and more sustained color bias in the experiment of Moher et al. (2014), particularly resulting in the buildup of a stable antibias for the distractor color that was always to be ignored. In fact, psychophysical studies on global attention to motion direction and orientation that alternated the attended and ignored feature values between experimental blocks found no suppression of distractor features, but only an enhanced sensitivity for the currently-attended direction or orientation (White & Carrasco, 2011). Since there was no constant assignment of target and distractor color in the current experiments, it is unlikely that the subjects were able to develop a systematic antibias for the distractor color.

Nevertheless, the subjects could try to suppress the distractor colors. But note, this would not contribute to the GCBA modulations reported here, because the distractor colors in the FOA never served as a reference for the GCBA effect. Instead, the attended colors were compared to those unattended colors not simultaneously present in the FOA. Most importantly, the effects were present even in the absence of any distractor color with only a single target color displayed in the left and a single probe color displayed in the right visual hemifield (distractor-absent trials of experiment 3). That is, the only potentially distracting (and hence potentially suppressed) color was presented in the opposite visual hemifield. Taking into account that attentional ressources appear to be independent for the left and right visual hemifield (Alvarez & Cavanagh, 2005), it seems unlikely that suppressive mechanisms were recruited at all to solve the task in the left visual hemifield (see also the following section). In line with this reasoning, SSVEP experiments showed suppressive stimuli interactions only when stimuli occupied the same spatial location (Andersen & Müller, 2010), but not when they were presented in opposite visual hemifields (Müller et al., 1998).

Bondarenko et al. (2012): evidence for target feature enhancement

Another argument in favor of an enhanced processing of the target feature is provided by an electromagnetic study on attention to orientation that used a stimulus design comparable to the present experiments (Bondarenko et al., 2012). In that study, the subjects discriminated the orientation of a grating in the left visual field, while gratings of different orientations were simultaneously probed in the unattended right visual field. In one experiment the probe presentation was interrupted for 50ms (gap) 150ms after probe onset. This was done to elicit an additional response at the probe's position that would delve into the time range of the cortical response reflecting feature selection upon target presentation. Notably, the gap elicited an enhanced feedforward response (P1) for gratings matching the currently-attended orientation, but not for neutral reference gratings that never served as a target (45 degree orientation offset). This finding was taken in favor of an enhanced processing of the target feature.

Taken together,...

... in the context of the current experimental design, the observed modulations of GCBA, rather than reflecting the suppression of the unattended colors, are more likely due to enhanced processing of the attended colors. To further investigate this issue, additional control experiments are required. For example, a subsequent search task could compare performance for a color previously used as a target color to that of a neutral color. If search performance was improved for the target color compared to the neutral color, this would be indicative of enhanced processing of target color.

6.5.3. Attentional capture by the probe?

In the current experimental design, target and probe position were kept constant throughout the experiment. The target was always presented in the LVF quite distant from the probe

presented in the unattended RVF (see General stimulus design, section 3.1). Thus, the subjects should be able to focus their attention on the target side without being distracted by the probe. However, it is hard to know with certainty whether the subjects set themselves continuously for the target position or whether their spatial FOA remained rather diffuse prior to target onset encompassing both target and probe location. Moreover, the simultaneous onset transients of target and probe might have atttracted attention to both visual fields. That is, the probe might have captured attention immediately after stimulus onset. It is well-know that stimuli are able to involuntarily capture attention when they are contingent on the attentional set of the observer (Folk et al., 1992; Gibson & Kelsey, 1998). Specifically, when searching for a target defined by a color, a color cue at an invalid position will increase the reaction time relative to uncued trials even when subjects know that the color cue is 100% invalid (i.e., the target will never appear at the cued position) (Folk et al., 1992). Since the target of the current experimental setup was defined by color, the task-irrelevant color probe in the RVF might indeed have captured attention to some extent. Now, the probes matching the target color might have attracted more attention than those not matching the target color. The early phase of GCBA (color template matching) could then reflect the consequence of a stronger suppression of matching probes in order to facilitate (re-)focusing on the target location.

The suppression of a distractor is typically indexed by a distractor positivity (PD)

A recently discovered ERP component has been reported to reflect the active suppression of distractors to prevent attention from being captured by them. This so-called distractor positivity or P_D component can be observed as a voltage deflection at lateral occipital electrodes sides (PO7/PO8) that is more positive contralateral than ipsilateral to the suppressed item (Hickey et al., 2009; Sawaki & Luck, 2010, 2011). Sawaki and Luck (2011) showed such P_D for colored distractors matching the content of the visual working memory. Specifically, when subjects performed an orientation-matching task on two sequentially presented colored bars, a probe shown after the first but before the second bar elicited a P_D when it matched the color of the bar held in working memory. Hence, if the color probes in the current paradigm were more strongly suppressed when they matched the attended color as compared to when they did not match, the ERP waveforms (match minus non-match) should contain the remaining P_D modulation. To find out, whether a P_D actually underlies the early phase of GCBA, ERP waveforms ipsi- and contralateral to the probe were compared (so far there is no characterization of the neuromagnetic counterpart of the P_D component). For a better comparison, Figure 6.2 replots the early ERMF and ERP modulations of experiment 1 that were assessed contralateral to the probe together with the ipsilateral ERP response. It can be clearly seen that the contralateral response was not more positive, but in fact more negative compared to the ipsilateral response. Hence, there was no evidence for a P_D in the match minus non-match difference. It is therefore unlikely that the early modulation was caused by a stronger suppression of the probes drawn in the target color. Furthermore, a stronger suppression of the probe matching the target color would also predict a stronger refocusing onto the target that would be expected to be indexed by an increased target negativity (N_T) contralateral to the target (Hickey et al., 2009). As Figure

6.2 shows, there was no pronounced negative deflection on the side contralateral to the target (= ipsilateral to the probe). The observed pattern of ERP responses does neither fit with effects of distractor suppression nor with the refocusing onto the target.
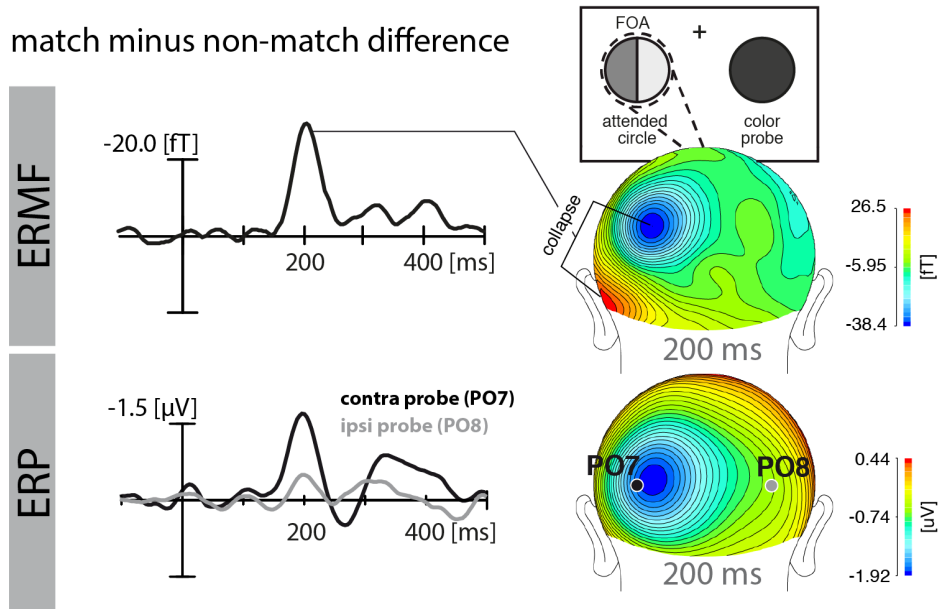

Figure 6.2. Early GCBA modulation – ERP responses ipsi and contralateral to the probe. The ERMF and ERP waveforms of the early phase of experiment 1 (match trials minus non-match trials) are replotted here together with the ERP response ipsilateral to the unattended color probe. The ERP waveforms contralateral to the probe (PO7) showed a negative voltage deflection relative to the ipsilateral ERP response (PO8) in the time range of the early effect of GCBA. Since a distractor suppression process reflected by a P_D would be expected to elicit a more positive modulation contralateral compared to ipsilateral to the probe, there was no evidence for a stronger suppression of the probes matching the target color that would result in a positive modulation of the difference waveform. Furthermore there was no prominent negative modulation contralateral to the target (= ipsilateral to the probe) that would have been expected for a stronger refocusing onto the target on match trials (target negativity, Hickey et al., 2009).

Taken together,...

... even if it cannot be completely ruled out that the spatial focus has transiently encompassed the probe, the observed early modulation of GCBA is unlikely to reflect processes of spatial refocusing and distractor suppression. This is in line with previous behavioral and fMRI studies that have shown effects of GFBA when attentional capture is not possible, i.e., at remote unstimulated locations (Arman et al., 2006; Serences & Boynton, 2007; T. Liu & Hou, 2011; T. Liu & Mance, 2011). Nevertheless, possible confounds of the early GCBA modulation in terms of a wide spatial focus immediately arising after stimulus onset cannot be ruled out. One way to address this issue would be to more effectively anchor the subject's spatial attention on the target's side prior to stimulus onset (e.g., by an exogenous location marker, see section 7.6).

7.   Outlook – open questions and future research

The current work contributes to the growing literature of global feature-based attention by establishing electromagnetic correlates of color-based attention under conditions of a color/shape discrimination task. For the first time a modulation sequence operation in reverse hierarchical direction could be documented for color, which confirms and extends recent observations in the orientation domain (Bondarenko et al., 2012). While some important issues could be solved (see section 5 for a short summary), the current work gives rise to a number of further questions worth being addressed in subsequent studies. Some of them will be sketched in the following.

7.1.   How do onset and continuous feature presentations effect GCBA?

When the attended color was probed during a continuous presentation of the target color in the FOA, GCBA led to modulations of the P1 component (Zhang & Luck, 2009). Importantly, the authors suggested that this very early effect depends on the presence of a competing color in the FOA. In contrast, with the current experimental setup (onset stimuli) modulations of later ERP components (N1 and subsequent time range) were observed which do not depend on color competition (see experiment 3, section 4.3.3). Hence, the correlates of GCBA apparently differ between sustained and onset presentations. To further investigate this issue, the current experimental design should be modified such that correlates of continuous and onset presentation can be compared more directly. For example, on half of the experimental blocks, the target could be constantly present, while unattended color probes would be flashed in the unattended hemifield. On the other half of the blocks, target and probe would both be presented with common onset. In both cases, the subjects would have to report a change of luminance or hue on the target side. Probes flashed during the sustained target presentation would be expected to give rise to early (P1) modulations and probes presented together with the target onset should elicit modulations starting in the N1 time range. Additionally, performing the experiment with and without color competition in the FOA will eventually reveal whether color competition is relevant for GCBA to appear under conditions of a continuous color represention.

7.2.   Does task difficulty influence GCBA?

Under conditions of the current experimental setup, GCBA did not depend on the presence of a competing distractor color (see experiment 3, section 4.3.3). However, whether or not GCBA is influenced by color competition might also depend on the difficulty of the discrimination task. Specifically, the color/shape discrimination task of the current experimental series was fairly easy (performance: 93-96% correct). In contrast, experiments that found effects of GCBA to be reduced or absent without color competition used challenging tasks requiring luminance-

change detection (performance: ~ 65-83% correct (Sàenz et al.) ~ 80% hits (Zhang & Luck)). Hence, the higher task difficulty in those experiments might have limited attentional ressources for the global spread of color-based attention leading to a stronger dependence of GCBA on being boosted by mechanisms of color competition. To clarify the influence of task difficulty on the described modulation sequence of GCBA, the current experimental design could be modified introducing different degrees of difficulty for the color/shape discrimination task that are tested with and without color competition in the FOA as illustrated in Figure 7.1. Color competition would not be expected to play a role under conditions of an easy discrimination task. However, a more difficult discrimination would be expected to lead to a faster and stronger focusing onto the target thereby decreasing the spread of color attention throughout the visual field. Color competition might then indeed play a crucial role in boosting effects of GCBA.

task   Is the gap in the target color half circle rectangular or round?
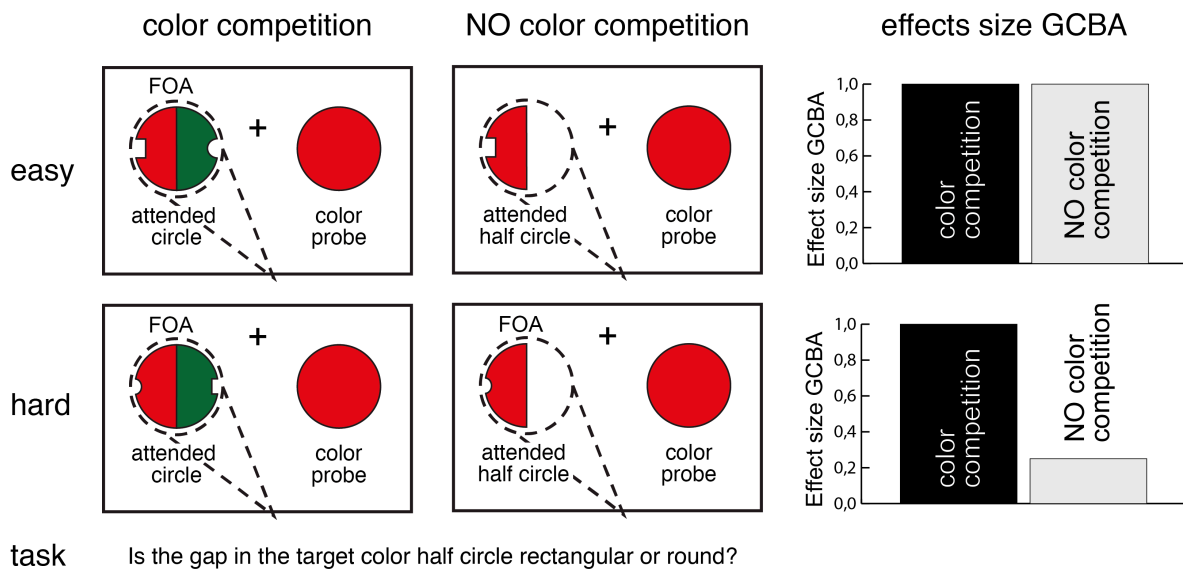
Figure 7.1. Influence of task difficulty on GCBA. The color/shape discrimination task could be modified by introducing a gap in the target color half circle that could be either rectangular or round on a given trial. The task difficulty could then be modified by varying the gap size (easy: big gap, hard: small gap). The effect size of GCBA could e.g., depend on color competition for the hard, but not for the easy task. To ensure the comparability of the easy and hard task, physical imbalances between the stimuli (gap size) would have to be controlled for by e.g., an RSVP task (see 4.2).

7.3. How does the color similarity profile of GCBA look like?

The target and probe colors used in the current experiments (red, magenta, blue, green, yellow) are all well-distinguishable and too distant in color space to investigate whether GCBA scales with color similarity. Effects of GCBA could, e.g., scale linearly with the color similarity between target and probe. According to the 'selective tuning' ST model (Tsotsos, 2011),

however, the profile of GCBA could also reflect a more complex 'center-surround' pattern as observed for the spatial focus of attention (Hopf et al., 2006). Specifically, colors very similar to the attended one would then be suppressed. Furthermore, effects of GCBA could follow an 'all or nothing' rule with modulations being only observed for colors matching the target color or colors that are within the same color category (e.g., all 'reds'). To address this isssue, future experiments should provide a finer sampling of color values. Of note, the color similarity profile of GCBA could substantially differ between the early and the late modulation. Specifically, in line with the Reverse Hierarchy Theory (Hochstein & Ahissar, 2002) the initial 'color template matching' process could be indexed by a coarse categorical color representation, while the later 'discrimination matching' might provide a more fine-graded separation of the color space.
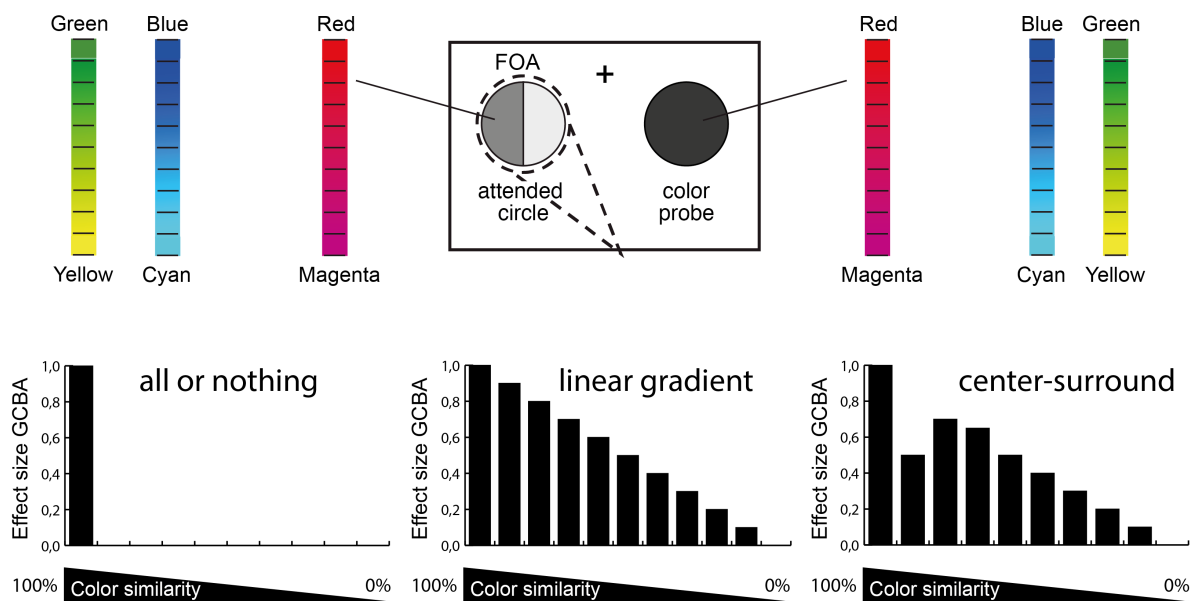

Figure 7.2. **The profile of GCBA**. A sytematic variation of the target and probe color along certain color axes (e.g., from red to magenta) would allow to investigate effects of GCBA as a function of color similarity. Effects of GCBA could e.g., only arise for colors matching the target color, gradually increase with color similarity or show a more complex pattern like the center-surround profile observed for spatial attention (Hopf et al., 2006) with a suppression of colors similar to the attended one.

7.4. Does GCBA depend on the stimulus duration?

Experiments that used very short stimulus durations with colored items being presented only for 32-60ms (Hillyard & Münte, 1984; Wijers et al., 1989) or consisting of two seqentially 33ms presentations with onsets separated by 50-150ms (Anllo-Vento & Hillyard, 1996) could not observe effects of GCBA. In contrast, those experiments reporting electromagnetic correlates of global feature-based attention usually used longer stimulus durations of at least 700ms (Hopf et al., 2004; Andersen et al., 2011; Boehler et al., 2011; Bondarenko et al., 2012; Andersen et al., 2013) or probed features briefly (100-200ms) during a continuous presention of the attended

feature (Zhang & Luck, 2009, experiment 1a/b; Stoppel et al., 2012). Hence, effects of GFBA were found when the subjects viewed the attended feature for a comparably long time period. The current experimental series shows that a transient color presentation of 300ms is sufficient to elicit effects of GCBA, but since the stimulus duration was not manipulated throughout the experimental series, it remains an open question as to whether effects of GCBA require a minimum stimulus presentation time. To fill this gap, the current experimental design could be modified such that the stimulus presentation is systematically shortened. If GCBA needs target and probe to be displayed for a critical time period, the modulation sequence should be abolished when the stimulus duration falls below that critical value.

Of note, if the critical stimulus duration turns out to be above 32-60ms, at least one of the ealier ERP paradigms (e.g., Hillyard & Münte, 1984) should be repeated with sufficiently long stimulus presentations.

7.5.   Early phase of GCBA modulated by effects of color frequency?

The results of experiment 4 suggested that parts of the early modulation reflect an internal template of task-relevant colors (see section 4.4.3). However, the early modulation of GCBA could also be observed when subjects did not explicitly need to discriminate the target's color but just its shape to perform the task (distractor-absent trials experiment 3, see section 4.3.3). Thus, the subjects were either explicitly or implicitly building a template for the color of the target although it was not explicitly required to solve the task. However, since the target's color was constant within trial blocks, a color may have led to a template matching effect just by virtue of being repeatedly contained in the discriminated target. To test this hypothesis, experiment 3 could be modified such that the target's color is either constant on a given experimental block or changes randomly from trial to trial. In the latter case, the subjects are not able to build up any internal color template and hence should show no early phase of GCBA as illustrated in Figure 7.3A. To better quantify possible influences of color frequency, the frequency of certain colors on the target side could be changed within experimental blocks. If the early phase of GCBA scales with color frequency, more frequent colors should elicit bigger GCBA effects than less frequent colors (see Figure 7.3B). Importantly, the template matching effect of GCBA may be elicited by colors whose frequency is increased without subjects becoming aware of the increase. This would reveal whether the color template can emerge automatically and unconsciously.
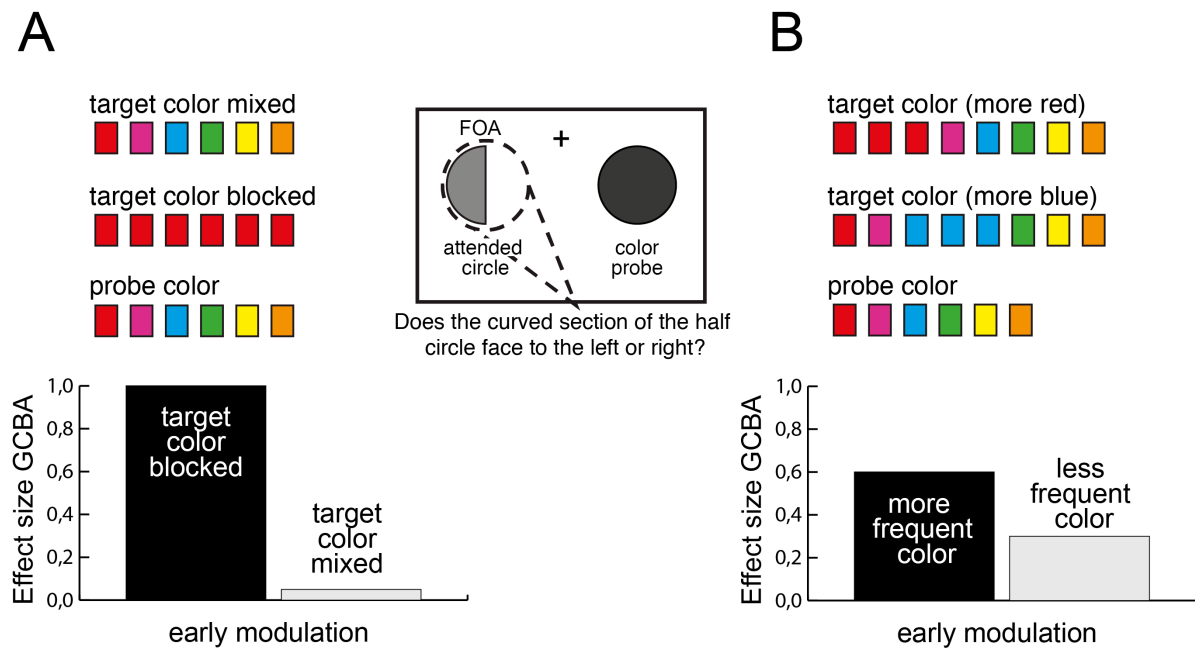
Figure 7.3. **Varying the target's color within experimental blocks**. When performing a shape discrimination task on a single half circle without a second color in the FOA (distractor-absent trials, experiment 3), the color of the target could be changed in a random trial-by-trial manner. **(A)** As in experiment 3, a blockwise constant target color should be able to elicit early color template matching effects of GCBA. The randomly changing target color on mixed blocks, however, should preempt the build-up of an internal color template and hence, eliminate the early GCBA modulation. **(B)** Varying the proportion of certain colors in the mixed condition should reveal whether the early phase of GCBA indexes the frequency of certain colors. **(A/B)** The probe's color always changes randomly in a trial-by-trial manner with all possible colors being presented equally often.

7.6.   Is the early phase of GCBA confounded by a wide spatial focus?

In the current experimental design, the target position in the LVF was kept constant throughout the whole experimental session and was quite distant from the site of probe presentation in the RVF. Hence, the subjects should be easily able to focus their attention on the upcoming target prior to stimulus onset. Nevertheless, it is hard to control whether the subjects set themselves continuously for the target position. It might be that their spatial attention remained rather diffuse prior to target onset, with the FOA encompassing the location of the probe as well. To address this issue, an exogenous location marker could be presented at the position of the upcoming target prior to the actual target onset. That way, the FOA could be anchored more effectively on the target's side before target and probe appear. According to cuing experiments, such peripheral location marker should be able to facilitate target selection when presented 150ms prior to target onset (Posner & Cohen, 1984). To test the influence of such location marker on the GCBA modulation sequence, the target's location should be marked on half of the experimental blocks and the results then compared to blocks without location marker (see Figure 7.4). If the early modulation would be present without location marker, but substantially

reduced or absent when a peripheral marker can be used to anchor the FOA prior to target onset, the early phase of GCBA would presumably be confounded by a wide spatial FOA. That is, the template matching effect might not reflect global color selection outside the FOA, but arise when target and probe are initially both encompassed by the spatial focus of attention.
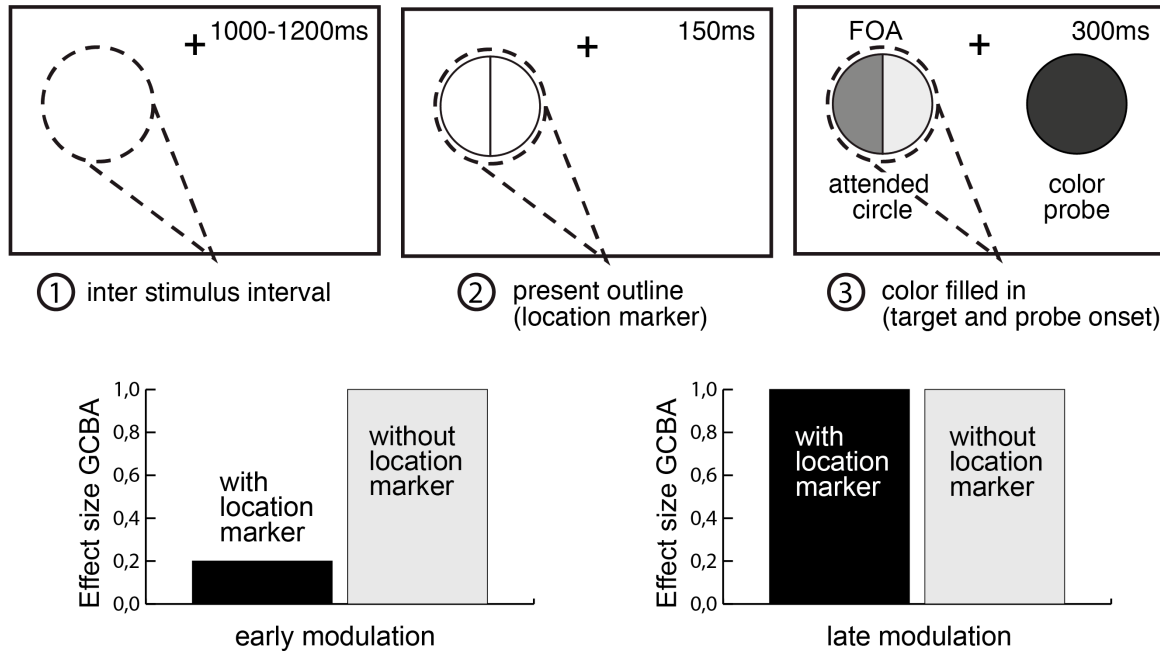

Figure 7.4. **Presentation of a location marker prior to target onset**. The presentation of a peripheral location marker (here: the outline of the target circle) indicating the position of the subsequently presented target should help to more effectively allocate spatial attention prior to target onset. If a more diffuse distribution of spatial attention across the visual field would account for the early modulation of GCBA, this modulation part should be greatly reduced when a spatial cue is used to guide spatial attention towards the location of the upcoming target. The later phase of GCBA is less likely to be affected by such cuing since spatial attention should already be focused onto the target when the late modulation of GCBA emerges (subjects should be able to focus there spatial attention within 200ms (Remington & Pierce, 1984)).

7.7.   Does the late phase of GCBA require shape discrimination?

The color/shape discrimination task, used throughout the experimental series, did not allow to disentangle whether color and/or shape discrimination underlies the late phase GCBA effect. Specifically, it is unclear whether the discrimination matching effect reflects color selection in 'service' of shape discrimination, or color discrimination more directly. There is no simple way to separate color from shape discrimination since the presentation of a color is typically bound to the presentation of an object that is colored and that has a shape. One possible way to preempt the shape's discrimination would be an onset-detection task comparable to that of experiment 5, but with colors being task-relevant. Specifically, the subjects should not respond to all objects in the FOA, but only press a button when they detect an object of a particular

color. This way, the subjects would be forced to discriminate the target's color, but there would be no need to derive its shape (see Figure 7.5A). However, the subjects could still discriminate the shape of the target object once they have detected it (effects of GCBA might require a comparably long stimulus duration, as discussed in section 7.4). An extension of this experimental approach would be to discourage subjects from discriminating the object's shape by making the shape discrimination unfavorable for the subject. That is, the stimuli could be designed such that attending to an object's color would be impaired by attending to its shape or vice versa. This impairment could e.g., take place at the level of response mapping (color and shape information of the same object could be mapped on incongruent response alternatives, see Figure 7.5B).
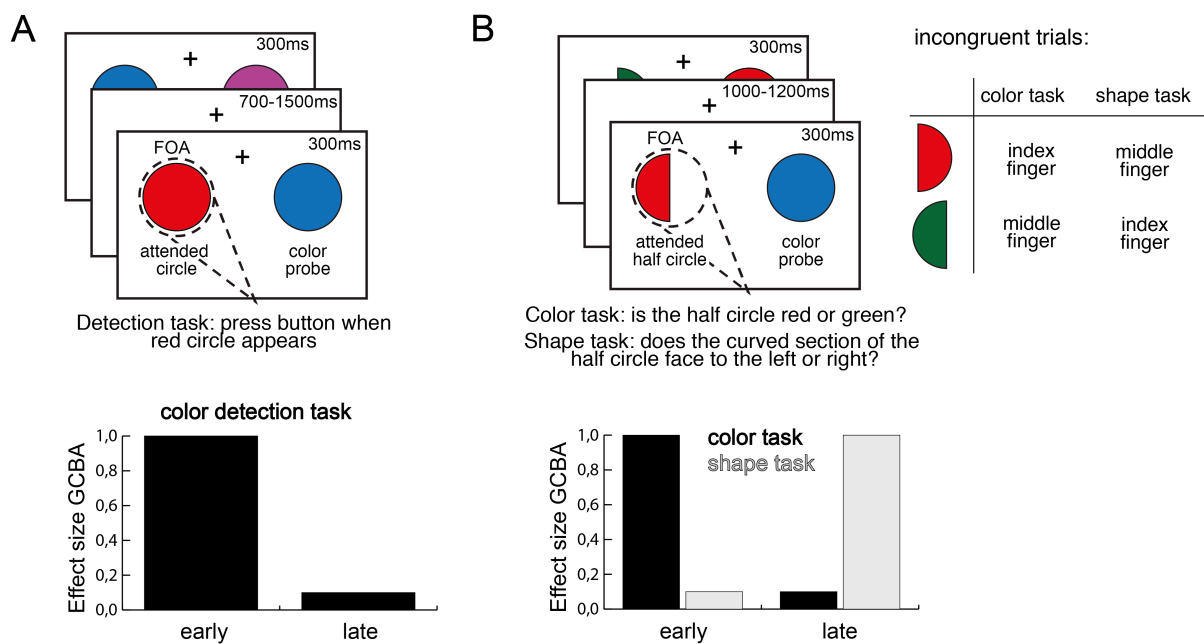
Figure 7.5. **Stimuli to better separate shape and color discrimination.** **(A)** A simple onset-detection task of circles of a certain color (here: red) could preempt shape discrimination. If the late GCBA modulation requires shape discrimination, it should be abolished. **(B)** The color and shape responses to the same stimuli could be incongruently mapped on the response buttons, such that attending to the color would impair performing the shape task and vice versa. The respective congruent trials (red half circle facing to the left and green half circle facing to the right are not shown here). When performing the color task, subjects should build up a color template (early modulation), but suppress shape discrimination. In contrast, when performing the shape task, subjects are not expected to built up a color template (early modulation), but to discriminate the target's shape. If the late phase of GCBA depends on shape discrimination, it should be abolished under conditions of the color task but not under conditions of the shape task.

S. Supplementary

S.1. GCBA for different colors / types of non-match trials (ERMFs)

To increase the number of trials and thus the signal-to-noise ratio, the data were collapsed across colors for the match and non-match conditions in all of the reported experiments. To control whether the effects of GCBA can be consistently observed for the individual colors, the data of experiment 1 were split up into red, magenta and blue. Furthermore, with the current experimental design, match trials were always compared to physically non-identical non-match trials. That is, either the probe's or the target's color differed between match and non-match trials. In the main analyses the different types of non-match trials (either target or probe color kept constant with respect to the match trial, see section 4.1.2, Figure 4.1) were averaged together. However, the dissociation of the different types of non-match trials allows to better control for the physical differences in the match minus non-match (M-NM) difference. That is, match and non-match trials can be compared in two possible ways: either the probe's color or the target's color could be kept constant. In the first case (probe color constant), the brain's response – measured contralateral to the probe – was not confounded by sensory differences of the probe (see 'Hillyard Principle' in cf. 2.2). However, the color variation on the target side may have influenced the observed effects of GCBA. In the second case (target color constant) any confounds due to alternating colors on the target side are excluded, but the GCBA effect could simply reflect a response variation due to the differences of the probe color. Hence, if the effects of GCBA were preserved under both conditions, it would speak against the possibility that they solely arose due to color differences on either the probes's or the target's side. Figure S.1. provides the global color-based attention ERMF responses of experiment 1 (waveforms, field distributions and current source density analyses) separated into the individual colors and non-match types. The GCBA modulations (early and late phase) could consistently be observed throughout all colors for both target and probe color constant conditions. Hence, the effects of GCBA did not depend on a specific color. Furthermore it is very unlikely that they were borne by color differences on either the probe's or the target's side. The corresponding behavioral data reported in the following section (S.2.1) were additionally split up into 'left' and 'right' responses, and overall, support this view.
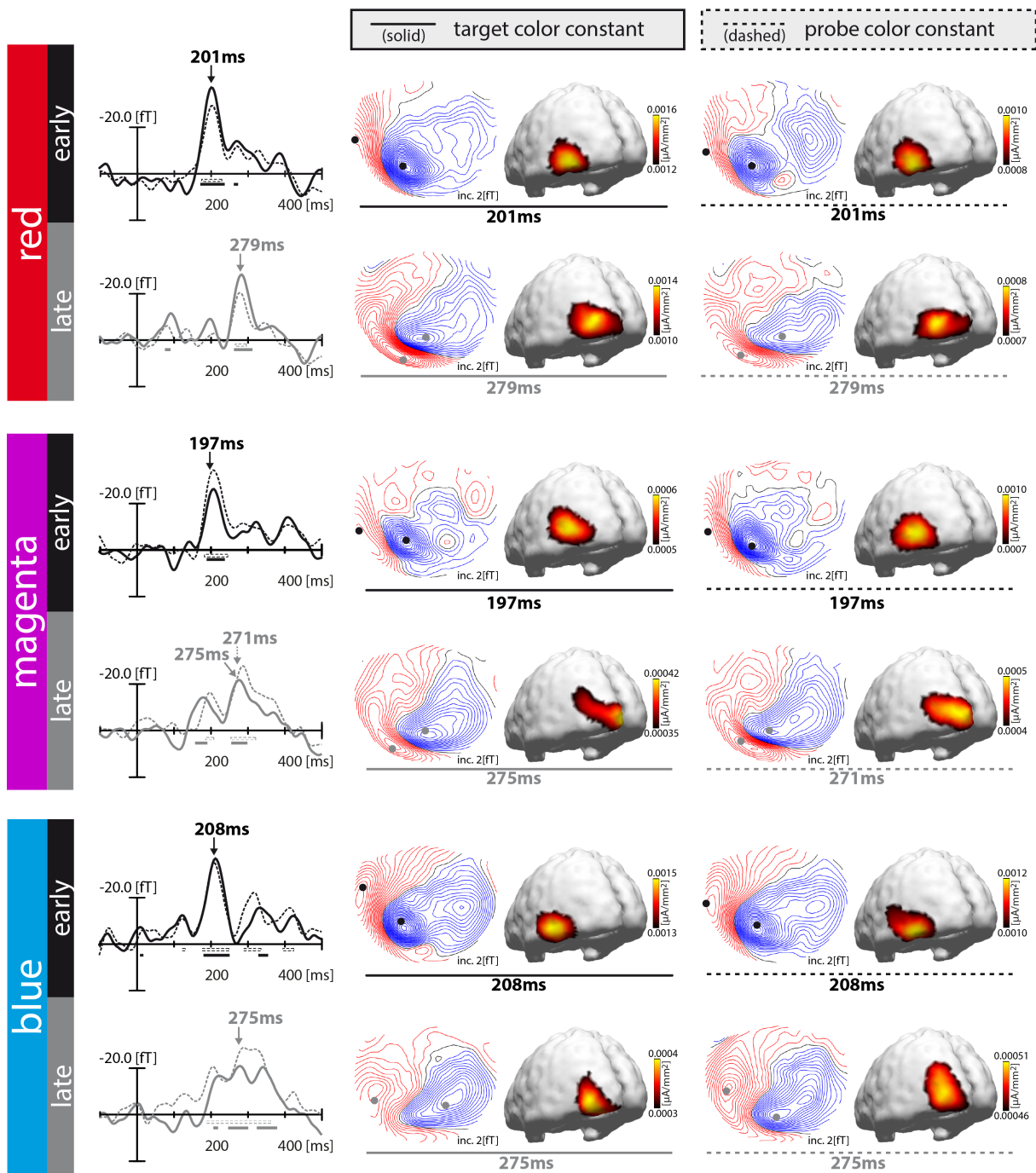
Figure S.1. GCBA effects of experiment 1 for individual colors under probe or target color constant conditions (ERMFs). For each of the three possible colors (red, magenta, blue) the match minus non-match difference indexing GCBA is shown for target (**middle column**) or probe color (**right column**) constant trials. For each color, the **upper row** represents field distribution maps and 3D maps of the current source density estimates at time points of maximum effect size of the early modulation of GCBA. The corresponding **lower row** displays the respective maps for the late modulation. The **left column** shows the ERMF waveforms of the early (black traces) and late (grey traces) effects with each waveform reflecting the averaged signal of two selected sensor sites chosen close to the efflux (polarity inverted before averaging) and influx maxima of the distribution maps (black/grey dots). Horizontal bars mark time ranges of significant match vs. non-match differences (p < 0.05, corrected for multiple comparisons as described in 3.4.1). A sequence of early and late GCBA modulations was consistently observed across all colors independent of whether that the target or the probe color was kept constant between match and non-match trials.

S.2. GCBA for 'left' vs. 'right' responses

Since the orientation of the half circles drawn in the target color would not be expected to influence the effects of global color-based selection, the data were averaged across half circles with the curved section facing to the left (left-facing targets; response: 'left', index finger) and those with the curved section facing to the right (right-facing targets; response: 'right', middle finger) in all of the reported experiments. However, as reported below, the increase in response time observed for match compared to non-match trials varied systematically with the orientation of the target. The ERMF data (experiment 1) were therefore analyzed again after splitting them up into 'left' and 'right' facing targets. The analysis below will reveal that the respective response asymmetry likely reflects a conflict of response mapping on match versus to non-match trials that always appears for targets requiring a 'left' response.

S.2.1. Behavioral performance

The response slowing observed for match compared to non-match trials was significant in all of the reported experiments with the exception of experiment 2. To further investigate this effect, responses to left-facing targets (response: 'left', index finger) were separated from responses to right-facing targets (response: 'right', middle finger) on both match and non-match trials. The behavioral data of experiment 1 – providing the highest resolution in terms of trial number – were additionally split up into the different colors and non-match conditions (target or probe color kept constant). The results of the respective rANOVAs and post-hoc pairwise comparisons (Student's t-tests) are summarized in Table S.1. and Table S.2., respectively.

Experiment 1 (average across colors and non-match types)

Figure S.2.A shows the behavioral performance data of experiment 1 split into 'left' and 'right' responses. As can be seen, both the response time and the response accuracy varied with the response alternatives.

Comparison of responses between match and non-match trials

While 'left' responses were slower and less accurate on match trials compared to non-match trials, 'right' responses were more accurate and faster in the match condition. These observations were confirmed by two-way rANOVAs with the factors MATCH (match/non-match) and SIDE (response left/right). They revealed a significant MATCH x SIDE interaction for both response accuracy and response time. Since the interaction pattern was perfectly mirror-symmetric for the response accuracy (overall accuracy stayed the same for match and non-match trials as well as for 'left' and 'right' responses) there were no significant main effects for accuracy, while the response time showed main effects of both MATCH and SIDE. Specifically, the prolonged response time in the match condition for 'left' was not fully compensated by the faster responses for 'right' leading to the overall response slowing on

match compared to non-match trials as reported in the results section of experiment 1 (see 4.1.3). Post-hoc pairwise comparisons (Student's t-test) confirmed, that in the match compared to the non-match condition, the speeded responses and higher accuracy for right-facing targets as well as the response slowing and decreased accuracy for left-facing targets were highly significant (all p's < 0.0005).

Comparison of responses within match and non-match trials

The second obvious pattern emerged by comparing 'left' and 'right' trials (SIDE) within the match and within the non-match condition. For match trials, 'left' responses were slower and less accurate than 'right' responses while the reverse pattern was observed for non-match trials. Post-hoc pairwise comparisons confirmed that these effects were significant for response accuracy (all p's < 0.0005). For response time only the SIDE effect of match trials reached significance (match trials: p < 0.0005, non-match trials: p = 0.17).

How to explain this variation of response time and accuracy with target orientation? An explanation in terms of stimulus-response mapping compatibility would seem plausible. The subjects were always to respond with the index finger (left button) to a left-facing target and with the middle finger (right button) to a right-facing target. Importantly, the target was always presented in the left visual field, i.e., in a left position relative to the egocentric space representation. It has been shown, that relative spatial relations between stimuli and responses influence reaction times even when the spatial cue provided by the stimulus is task-irrelevant (the 'Simon effect', Nicoletti et al., 1982; Nicoletti et al., 1984; Nicoletti & Umiltà, 1994). Applied to the present experiments, reaction times to stimuli in the LVF should be faster when requiring a response with the index finger that is positioned left (on the hand) relative to the response alternative (i.e., left to the middle finger). Conversely, slower reaction times should be seen when a response is required with the middle finger positioned on the right relative to the response alternative (i.e., right to the index finger). In fact, this response pattern was observed for the non-match trials, which showed slower and less accurate responses for right-facing targets (response: middle finger) as compared to left-facing targets (response: index finger). However, only the effect of response accuracy was significant (see Table S.2.).

On match trials the exactly opposite pattern was observed: the responses were prolonged and less accurate for 'left' and faster and more accurate for 'right' responses. Again, an explanation akin to the 'Simon effect' may account for the response pattern. On match trials the target color appeared in both VFs, i.e., also to the right of the target, which likely prompted an automatic 'right'-mapped response. This would then conflict with the response to a left-facing target which requires a 'left' finger response – hence the slower and less accurate responses to left-facing targets on match trials. Responses to right-facing targets, on the other hand, were consistent in terms of automatic response mapping with the target color being shown in the RVF. This would explain the faster and more accurate 'right' responses on match trials.

Notably,...

... the better performance for right-facing targets on match compared to non-match trials speaks against attention being simply more strongly attracted by the RVF probes matching the target color. If the slowing on match trials would result from shifting the focus of attention towards the probes, the performance for left- and right-facing targets should have been equally impaired. Hence, the observed performance pattern seems to be independent of the attentional selection of the target and rather reflects downstream issues of stimulus-response mapping and execution. In fact, as shown in the following section S.2.2, the ERMF responses of the match minus non-match condition show an additional late activation around 346ms for 'left' but not for 'right' responses that is consistent with an interpretation in terms of a response conflict.

Experiment 1 (separation of colors and non-match types)

As described in the methods section of experiment 1 (see 4.1.2), the effects were averaged across the different colors as well as across the different types of non-matches (target or probe color constant) to improve the signal-to-noise ratio. Since experiment 1 had the highest number of trials for the match and the non-match conditions (almost twice as many trials as in the other experiments), it provided the most robust way to analyze the different colors and non-match conditions separately. Figure S.2.B displays the behavioral performance data of experiment 1 split up into 'left' and 'right' responses for each of the different colors (red, magenta and blue) including a split-up into probe color and target color constant non-matches. It is important to acknowledge that non-matches with the target versus the probe color kept constant (with respect to the match trial) could only be compared when considering individual colors. This is beause non-matches with the target color constant of one color corresponded to non-matches with the probe color constant of another color. For example, a red target with a blue probe could serve as a target color constant non-match for red, or as a probe color constant non-match for blue. Hence, averaging across colors would make the different types of non-matches indistinguishable.

Comparison of responses between match and non-match trials

The previously described pattern (slower and less accurate responses for left-facing targets as well as faster and more accurate responses for right-facing targets on match relative to non-match trials) was preserved across all colors and independent of the non-match type. These results were confirmed both for the target and probe color constant conditions by two separate three-way rANOVAs with the factors COLOR (red/magenta/blue), MATCH (match/non-match) and SIDE (response left/right). Concerning the factors MATCH, SIDE and the MATCH x SIDE interaction, all effects resembled exactly those seen for the collapsed data reported in the previous section (all effects were significant for response time, while for response accuracy only the MATCH x SIDE interaction was significant). Post-hoc pairwise comparisons revealed that for all colors and both types of non-matches the left responses were slower and less accurate for

match compared to non-match trials, while the right responses were faster and more accurate (all p's ≤ 0.001).

Comparison of responses within match and within non-match trials

The performance difference between 'left' and 'right' responses within the match or within the non-match trials (match trials: slower and less accurate for 'left' compared to 'right' responses; non-match trials: inverse pattern) was significant for response accuracy (all p's < 0.0005). For response time this pattern could be confirmed for match trials (all p's < 0.0005), but failed to reach significance for non-match trials (p's > 0.121, significant only for blue probe color constant non-matches: p = 0.025). As summarized in Table S.1. , the three-way rANOVAs with the factors COLOR (red/magenta/blue), MATCH (match/non-match) and SIDE (response left/right) also revealed main effects of COLOR as well as several interaction effects of COLOR with SIDE and MATCH. While performance differences due to the specific colors will not receive a detailed consideration here, it is worth noting that responses were faster for the color red compared to the other colors on match and target color constant non-match trials (that is, on trials with red targets in the LVF). For probe color constant non-match trials of the color red (that is, trials with blue or magenta as target in the LVF and red probes in the RVF) responses seemed to be slowed compared to the probe color constant non-match trials with magenta or blue probes in the RVF. Post-hoc pairwise comparisons confirmed that responses to red targets were indeed faster than responses to blue targets (p = 0.016) or magenta targets (p = 0.009). The overall slowing of the responses to red probes in the RVF, however, failed to reach significance (compared to magenta probes: p = 0.166, compared to blue probes: p = 0.096).

In sum,…

… the response slowing on match trials is presumably a result of a response conflict akin to the Simon 'effect' leading to disproportionally prolonged response times for left-facing targets. The behavioral data provide no indication for differences between different colors and non-match types that would account for the GCBA effects.
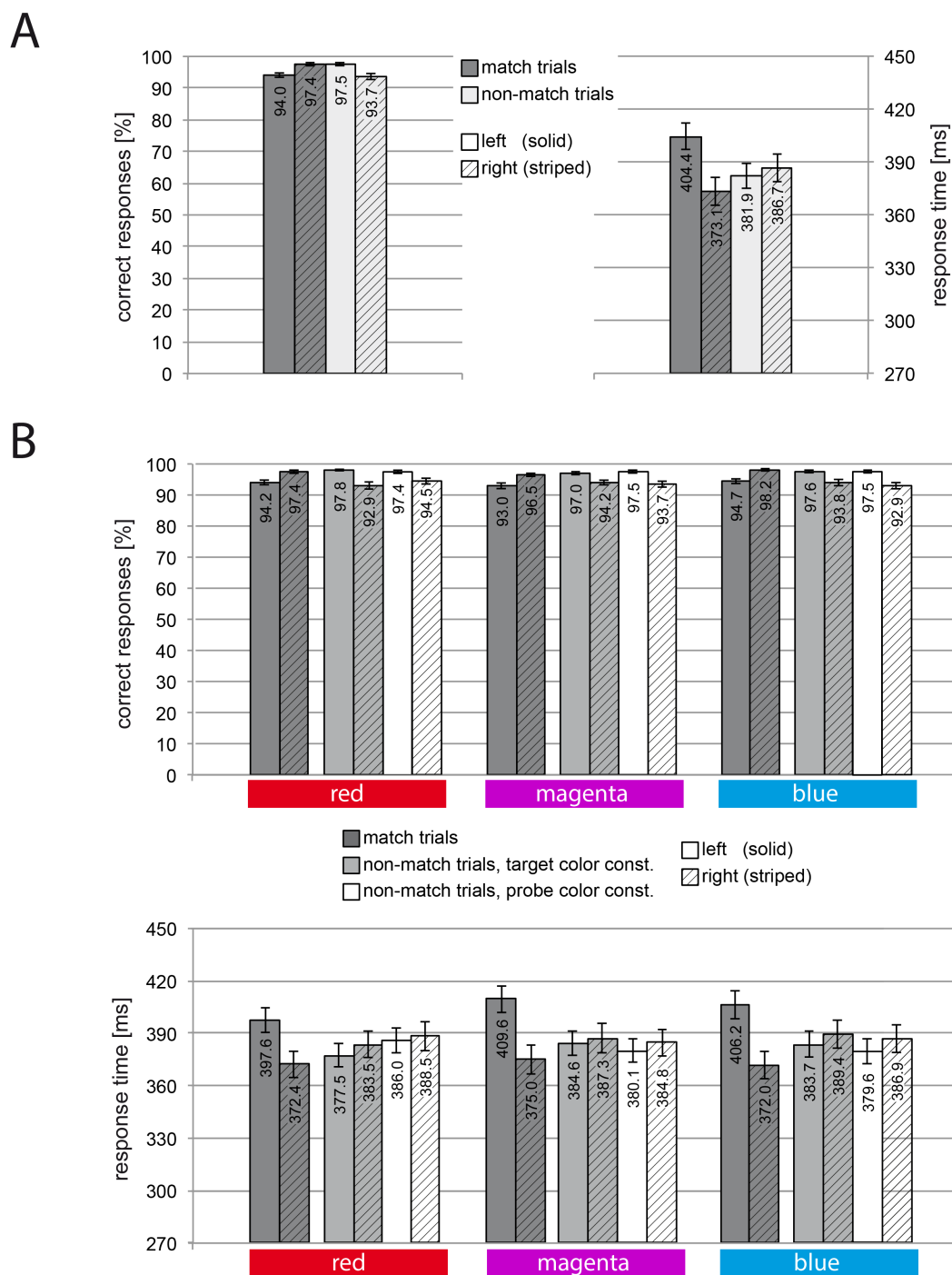
Figure S.2. Behavioral performance data of experiment 1 split into 'left' and 'right' responses. (A) Data averaged across different colors and non-matching conditions. For match trials relative to non-match trials responses were slower and less accurate on 'left', but faster and more accurate on 'right' trials. The slowing on 'left' trials was not fully compensated by the speedup on 'right' trials, leading to an overall prolonged reaction time on match trials. **(B)** Behavioral data separated for different colors (red, magenta, blue) and different types of non-match (target/probe constant). The error bars reflect the standard error of the mean (SEM). The response pattern is preserved across all colors as well as both types of non-matches (making it reasonable to average across these conditions).

Experiments 2 - 5

Figure S.3. displays the behavioral data of experiments 2, 3, 4 and 5 (corresponding to the behavioral data reported in 4.2.3, 4.3.3, 4.4.3 and 4.5.3) split into trials with left- and right-facing targets. All of the experiments contained at least one condition that required a 'left/right' discrimination of the target – i.e., the color/shape task of experiment 2, the distractor-present/absent tasks of experiment 3, the one-color and two-color tasks of experiment 4 and the discrimination task of experiment 5. All of these conditions showed the response pattern described above for experiment 1.

Comparison of responses between match, cross-match and non-match trials

For match relative to non-match trials, responses were slower and less accurate for left-facing targets (response 'left', index finger) as well as faster and more accurate for right-facing ones (response 'right', middle finger). Three-way rANOVAs were performed for experiment 2, 3 and 5 with the factors MATCH (match/non-match), SIDE (response left/right) and TASK (experiment 2: color/shape or RSVP, experiment 3: distractor absent or present, experiment 5: discrimination or onset-detection). For experiment 4, two-way rANOVAs with the factors MATCH (one-color: match/non-match, two-color: match/cross-match/non-match) and SIDE (response left/right) were conducted separately for the data of the one- and those of the two-color blocks because of the different number of match conditions (hence, no factor TASK in the rANOVAs of experiment 4).

All rANOVAs revealed significant main effects of SIDE and significant MATCH x SIDE interactions for response time as well as significant MATCH x SIDE interactions for response accuracy (statistical parameters for all rANOVAs are summarized in Table S.1.). The rANOVAs for experiment 2, 3 and 5 also showed significant effects of reaction time for the interactions of TASK x SIDE and TASK x SIDE x MATCH. These TASK interactions reflected the fact that the response pattern was absent in the RSVP task of experiment 2 and in the onset-detection task of experiment 5. Furthermore the response time effects were smaller on the disctractor-absent compared to the distractor-present blocks of experiment 3.

Post-hoc pairwise comparisons confirmed that the slower and less accurate 'left' and faster and more accurate 'right' responses on match compared to non-match trials were significant for all experimental conditions requiring a 'left/right' discrimination (all p's ≤ 0.003) with the following exceptions: the distractor-absent condition of experiment 3 lacked the significantly faster 'right' responses (p = 0.3) and the one-color and two-color conditions of experiment 4 showed no significant decrement of accuracy on the respective 'left' trials. The slowing for 'left' responses on match trials was again, not fully compensated by the speedup for 'right' responses, leading to an overall slowing for responses on match trials in all of the experiments (not significant for the color/shape task of experiment 2). For the two-color condition of experiment 4, match and non-match trials could additionally be compared to cross-match trials. That is, to trials where the probe in the RVF contained the second task-relevant color that was

not simultaneously present in the FOA. Responses on cross-match trials were both for 'left' and for 'right' responses slower and less accurate compared to match and non-match trials (all p's ≤ 0.006, no significant decrement of response accuracy on 'right' responses for cross-match compared to non-match trials: p = 0.067). Hence, when two colors were task-relevant (A and B), the presentation of a probe containing color A might have added an additional response conflict when subjects simultaneously tried to respond to color B in the spatial FOA.

Comparison of responses within match, within cross-match and within non-match trials

The second response pattern described for experiment 1, above, referred to comparisons of 'left' and 'right' responses within match and within non-match trials. Again, all experimental conditions requiring a 'left/right' discrimination showed significantly slower and less accurate 'left' as compared to 'right' responses on match trials (all p's ≤ 0.024, no significant effect of accuracy for the distractor-absent condition of experiment 3: p = 0.476, and the two-color condition of experiment 4: p = 0.454). On non-match trials of those experimental conditions, 'left' responses were more accurate than 'right' responses (all p's ≤ 0.011, except the one-color condition of experiment 4: p = 0.324) with no significant effect of response time (all p's ≥ 0.056). The cross-match trials of the two-color task of experiment 4 mimicked the response time pattern of match trials (i.e., 'left' responses slower than 'right' responses, p = 0.003), with the responses accuracy being equal on both 'left' and 'right' trials (p = 0.560).

Taken together,...

... for all experiments, the longer reaction times on match trials could be traced back to slowed 'left' responses, arising from a conflict of response mapping on those trials. For a detailed discussion see Experiment 1 above (behavioral data) and section S.2.2 below (EMRF data).
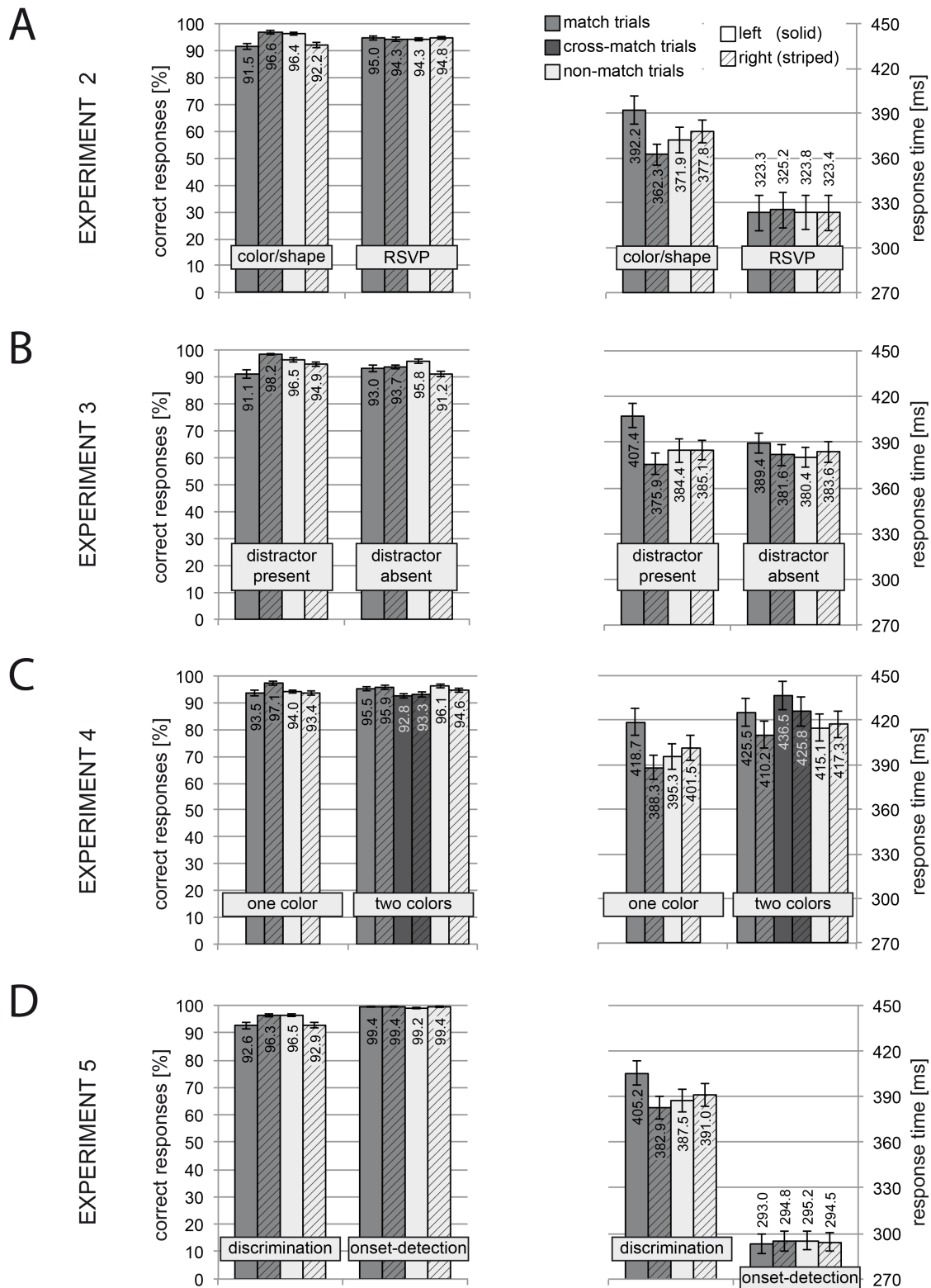
Figure S.3. Behavioral performance data of experiments 2-5 split into 'left' and 'right' responses. (A-D) The error bars reflect the standard error of the mean (SEM). As can be seen, all experimental conditions requiring a 'left/right' discrimination of the colored target – i.e., the color/shape task of experiment 2, the distractor-absent/present tasks of experiment 3, the one-/two-color tasks of experiment 4 and the discrimination task of experiment 5 – show the same response pattern reported for experiment 1 with slower and less accurate 'left' responses and faster and more accurate 'right' responses on match trials relative to non-match trials.

response time

		MATCH	SIDE	MATCH x SIDE	COLOR	COLOR x MATCH	COLOR x SIDE	COLOR x MATCH x SIDE	TASK	TASK x MATCH	TASK x SIDE	TASK x MATCH x SIDE
Experiment 1	df	1,20	1,20	1,20								
	F	29.7	24.8	129.0								
	p	***	***	***								
target color constant	df	1,20	1,20	1,20	2,19	2,19	2,19	2,19				
	F	28.9	25.0	129.4	4.4	2.3	6.6	3.4				
	p	***	***	***	*	n.s.	**	n.s.				
probe color constant	df	1,20	1,20	1,20	2,19	2,19	2,19	2,19				
	F	29.0	24.9	129.1	1.6	5.7	2.1	8.5				
	p	***	***	***	n.s.	*	n.s.	**				
Experiment 2	df	1,18	1,18	1,18					1,18	1,18	1,18	1,18
	F	3.9	8.5	47.1					16.8	0.8	16.9	50.9
	p	n.s.	**	***					***	n.s.	***	***
Experiment 3	df	1,21	1,21	1,21					1,21	1,21	1,21	1,21
	F	21.1	12.3	146.9					4.5	5.1	25.7	24.0
	p	***	**	***					*	*	***	***
Experiment 4 **one-color blocks**	df	1,24	1,24	1,24								
	F	18.8	14.7	119.4								
	p	***	***	***								
two-color blocks	df	2,23	1,24	2,23								
	F	30.2	6.6	29.6								
	p	***	*	***								
Experiment 5	df	1,19	1,19	1,19	1,19	1,19	1,19	1,19				
	F	6.9	7.6	48.9	233.9	10.8	9.2	64.5				
	p	*	*	***	***	**	**	***				

response accuracy

		MATCH	SIDE	MATCH x SIDE	COLOR	COLOR x MATCH	COLOR x SIDE	COLOR x MATCH x SIDE	TASK	TASK x MATCH	TASK x SIDE	TASK x MATCH x SIDE
Experiment 1	df	1,20	1,20	1,20								
	F	0.3	0.4	61.2								
	p	n.s.	n.s.	***								
target color constant	df	1,20	1,20	1,20	2,19	2,19	2,19	2,19				
	F	0.3	0.4	61.4	5.7	6.5	5.2	0.8				
	p	n.s.	n.s.	***	*	**	*	n.s.				
probe color constant	df	1,20	1,20	1,20	2,19	2,19	2,19	2,19				
	F	0.3	0.4	61.5	7.6	8.7	0.8	4.3				
	p	n.s.	n.s.	***	**	**	n.s.	*				
Experiment 2	df	1,18	1,18	1,18					1,18	1,18	1,18	1,18
	F	0.02	0.8	23.4					0.2	0.4	0.9	111.8
	p	n.s.	n.s.	***					n.s.	n.s.	n.s.	***
Experiment 3	df	1,21	1,21	1,21					1,21	1,21	1,21	1,21
	F	5.5	0.4	30.5					37.4	4.9	29.1	9.4
	p	*	n.s.	***					***	*	***	**
Experiment 4 **one-color blocks**	df	1,24	1,24	1,24								
	F	15.9	7.5	14.5								
	p	***	*	***								
two-color blocks	df	2,23	1,24	2,23								
	F	12.2	0.1	7.9								
	p	***	n.s.	**								
Experiment 5	df	1,19	1,19	1,19	1,19	1,19	1,19	1,19				
	F	0.03	0.04	34.6	46.9	0.45	0.003	25.9				
	p	n.s.	n.s.	***	***	n.s.	n.s.	***				

Table S.1. Results of the rANOVAs performed on the behavioral data of experiments 1-5. The significant MATCH x SIDE interactions (highlighted in light grey) indicate a dependence of 'left' and 'right' response patterns on the matching-condition throughout all experiments. *** $p \leq 0.001$; ** $p \leq 0.01$; * $p \leq 0.05$.

Measure	Experiment	Condition	M left vs. M right	M left vs. CM left	M left vs. NM left	M right vs. CM right	M right vs. NM right	CM left vs. NM left	CM left vs. NM right	CM right vs. NM right	NM left vs. NM right	CM left vs. CM right
response accuracy	Experiment 1	collapsed	***		***		***			***		
	red	target const.	***		***		***			***		
		probe const.	—"—		***		***			***		
	magenta	target const.	***		***		***			***		
		probe const.	—"—		***		***			***		
	blue	target const.	***		***		***			***		
		probe const.	—"—		***		***			***		
	Experiment 2	color/shape task	***		***		***			***		
		RSVP task	n.s.		n.s.		n.s.			n.s.		
	Experiment 3	distractor present	***		***		***			*		
		distractor absent	n.s.		***		***			***		
	Experiment 4	one-color	***		n.s.		***			n.s.		
		two-color	n.s.	***	n.s.	**	**	***	n.s.	*	*	n.s.
	Experiment 5	discrimination	**		***		***			***		
		onset-detection	n.s.		n.s.		n.s.			n.s.		
response time	Experiment 1	collapsed	***		***		***			n.s.		
	red	target const.	***		***		***			n.s.		
		probe const.	—"—		***		***			n.s.		
	magenta	target const.	***		***		***			n.s.		
		probe const.	—"—		***		***			n.s.		
	blue	target const.	***		***		***			n.s.		
		probe const.	—"—		***		***			*		
	Experiment 2	color/shape task	***		***		***			n.s.		
		RSVP task	n.s.		n.s.		n.s.			n.s.		
	Experiment 3	distractor present	***		***		***			n.s.		
		distractor absent	*		***		n.s.			n.s.		
	Experiment 4	one-color	***		***		***			n.s.		
		two-color	***	***	***	***	***	***	***	n.s.	n.s.	**
	Experiment 5	discrimination	***		***		***			n.s.		
		onset-detection	n.s.		n.s.		n.s.			n.s.		

Table S.2. P-values of the Student's t-tests for the behavioral data of experiments 1-5. 'Left' responses are compared with 'right' responses within and between the different matching-conditions. *** $p \leq 0.001$; ** $p \leq 0.01$; * $p \leq 0.05$.

S.2.2. ERMF responses

As described in the previous section (S.2.1), the significantly slower responses on match compared to non-match trials were caused by prolonged response times to target color half circles with the convexity facing to the left (left-facing targets; response: 'left', index finger). An important point to clarify is as to whether the slowing on left responses is somehow reflected by the early and/or late modulation of GCBA. To this end, the ERMF data of experiment 1 were separated into trials where the target half circle faced to the left (response: 'left', index finger) and trials where it faced to the right (response: 'right', middle finger). Figure S.4. replots the match minus non-match difference of experiment 1 ('all' responses, cf. 4.1.3) together with the data split up into 'left' and 'right' responses. While the early and the late modulation of GCBA arose for both 'left' and 'right' responses, the delayed third effect described under 4.1.3 (peaking at 346ms), could only be observed for 'left' responses. Source localization using the sLORETA approach (see Methods 3.4.2) revealed that the underlying current source originated in the region of the anterior cingulate cortex (ACC, located on the medial surface of the frontal lobes).

ACC activation indicates conflicts at the level of response selection

Previous studies showed that ACC activations can reflect the presence of conflicts at the level of response selection (e.g., van Veen et al., 2001; Weissman et al., 2003). For example, in the study of van Veen et al. (2001) subjects performed a version of the Eriksen flanker task (B. A. Eriksen & Eriksen, 1974), i.e., they had to discriminate a target letter that was surrounded by irrelevant distractor letters. The central target letter could be mapped on the same or a different response with respect to the distractor letters. If target and distractor letters were mapped on different responses (index vs. middle finger of the right hand), mean reaction times were slowed, which was accompanied by an increased activation of the ACC. An analogous issue may apply to the present experiments. Target color probes in the RVF could have prompted to a 'right' response (middle finger) thereby interfering with the response to left-facing targets requiring a response with the index finger (see detailed discussion in the previous section S.2.1). In fact, the ACC activation was observed only on trials with left-facing targets. Regarding the timing of the ACC activation, previous studies suggest that it should precede responses on correct trials while it should follow responses on error trials (Van Veen & Carter, 2002; Yeung et al., 2004). Since only stimuli followed by correct responses were analyzed for the ERMF data (see section 3.3), the ACC activation (peaking 346ms after stimulus onset) prior to the response (given around 390ms) perfectly fits that prediction.
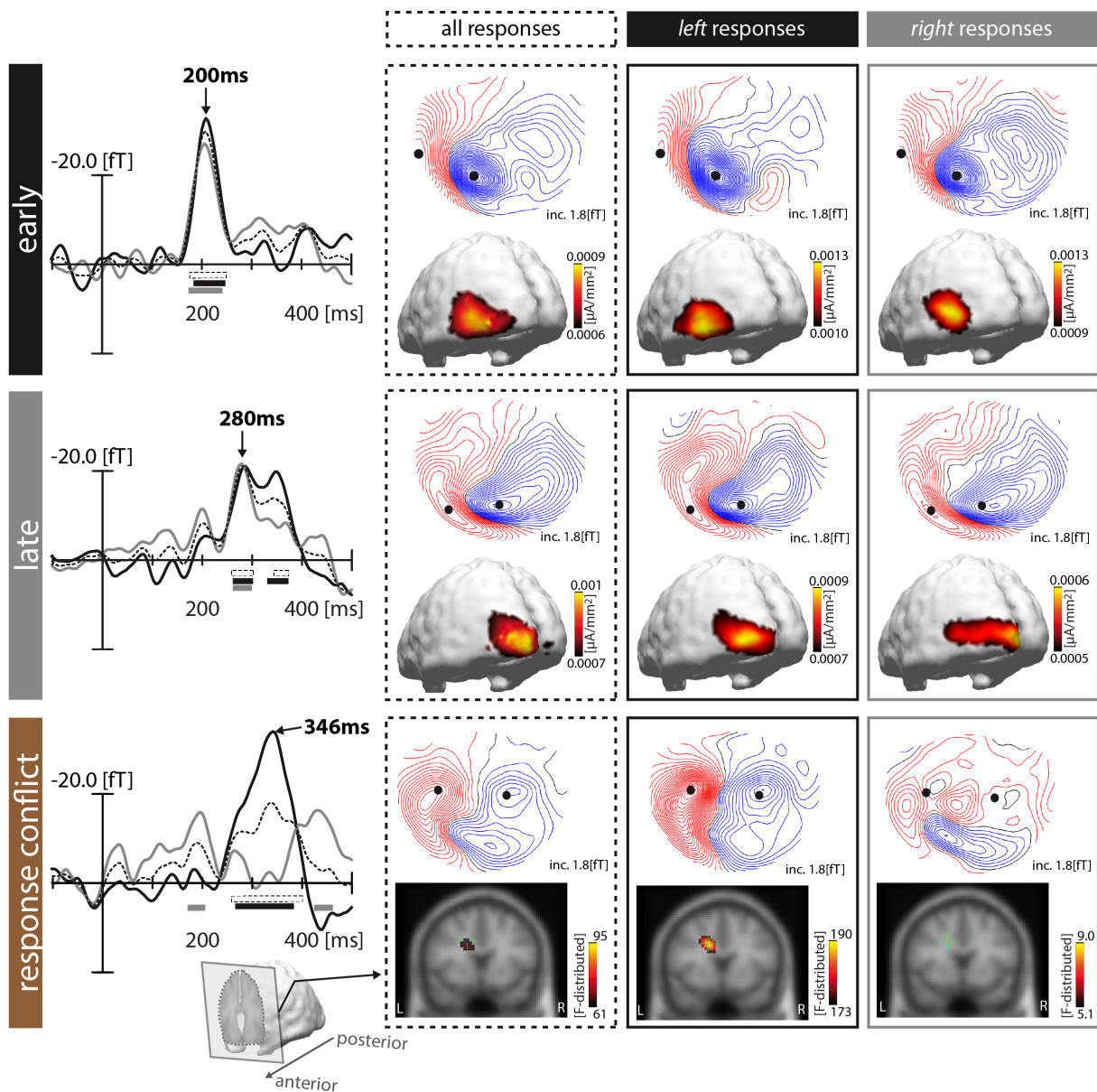
Figure S.4. ERMF responses of experiment 1 dissociating 'left' from 'right' responses. 'All' responses resembles the original data collapsed across 'left' and 'right' responses (cf. section 4.1.3). The field distributions and current source localizations are shown at time points of modulation maxima of the early and late phase of GCBA and the response conflict modulation. The corresponding waveforms (left column) show the ERMF responses of 'all' (dashed), 'left' (solid black) and 'right' (solid grey) responses at identical sensors sites (signal collapsed across sensors close to efflux (polarity reversed prior averaging) and influx maxima (black dots). Time points and sensor sites were chosen according to the 'all' response condition (early/late modulation) and to the 'left' response condition (response conflict modulation). The current source localization for the response conflict modulation was done with a sLORETA estimate (see 3.4.2). While the early and late modulations of GCBA could be oberserved for both 'left' and 'right' responses, the response conflict modulation arose solely on 'left' trials, presumably in the anterior cingulate cortex (ACC).
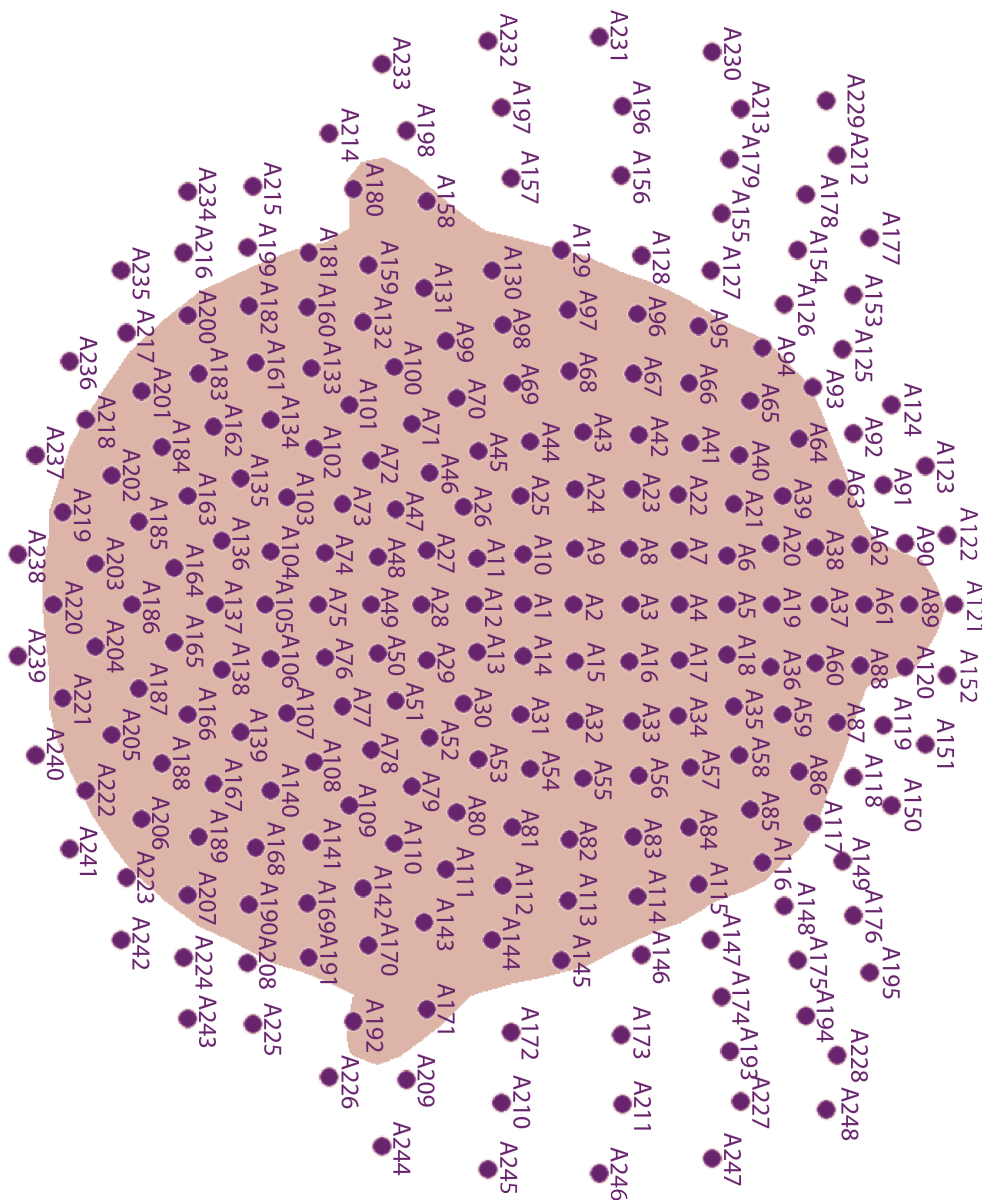
S.3. MEG sensor layout

Figure S.5. 2D map of the MEG sensor layout.

Bibliography

Alvarez, G.A., & Cavanagh, P. (2005). Independent resources for attentional tracking in the left and right visual hemifields. *Psychol. Sci., 16*(8), 637-643.

American Electroencephalographic Society. (1994). Guideline thirteen: guidelines for standard electrode position nomenclature. American Electroencephalographic Society. *J. Clin. Neurophysiol., 11*(1), 111-113.

Andersen, S.K., Müller, M.M., & Hillyard, S.A. (2009). Color-selective attention need not be mediated by spatial attention. *J. Vis., 9*(6), 2, 1-7.

Andersen, S.K., & Müller, M.M. (2010). Behavioral performance follows the time course of neural facilitation and suppression during cued shifts of feature-selective attention. *Proc. Natl. Acad. Sci. U. S. A., 107*(31), 13878-13882.

Andersen, S.K., Fuchs, S., & Müller, M.M. (2011). Effects of feature-selective and spatial attention at different stages of visual processing. *J. Cogn. Neurosci., 23*(1), 238-246.

Andersen, S.K., Hillyard, S.A., & Müller, M.M. (2013). Global facilitation of attended features is obligatory and restricts divided attention. *J. Neurosci., 33*(46), 18200-18207.

Anllo-Vento, L. (1995). Shifting attention in visual space: the effects of peripheral cueing on brain cortical potentials. *Int. J. Neurosci., 80*, 353-370.

Anllo-Vento, L., & Hillyard, S.A. (1996). Selective attention to the color and direction of moving stimuli: electrophysiological correlates of hierarchical feature selection. *Percept. Psychophys., 58*(2), 191-206.

Anllo-Vento, L., Luck, S.J., & Hillyard, S.A. (1998). Spatio-temporal dynamics of attention to color: evidence from human electrophysiology. *Hum. Brain Mapp., 6*(4), 216-238.

Arman, A.C., Ciaramitaro, V.M., & Boynton, G.M. (2006). Effects of feature-based attention on the motion aftereffect at remote locations. *Vision Res., 46*(18), 2968-2976.

Baas, J.M., Kenemans, J.L., & Mangun, G.R. (2002). Selective attention to spatial frequency: an ERP and source localization analysis. *Clin. Neurophysiol., 113*(11), 1840-1854.

Bartsch, M.V., Boehler, C.N., Stoppel, C.M., Merkel, C., Heinze, H.-J., Schoenfeld, M.A., & Hopf, J.-M. (2014). Determinants of Global Color-Based Selection in Human Visual Cortex. *Cereb. Cortex, Advance online publication. doi:10.1093/cercor/bhu078*.

Baylis, G.C., & Driver, J. (1993). Visual attention and objects: evidence for hierarchical coding of location. *J. Exp. Psychol. Hum. Percept. Perform., 19*(3), 451-470.

Beauchamp, M.S., Cox, R.W., & DeYoe, E.A. (1997). Graded effects of spatial and featural attention on human area MT and associated motion processing areas. *J. Neurophysiol., 78*(1), 516-520.

Beck, D.M., & Kastner, S. (2005). Stimulus context modulates competition in human extrastriate cortex. *Nat. Neurosci., 8*(8), 1110-1116.

Beck, D.M., & Kastner, S. (2009). Top-down and bottom-up mechanisms in biasing competition in the human brain. *Vision Res., 49*(10), 1154-1165.

Bichot, N.P., Rossi, A.F., & Desimone, R. (2005). Parallel and serial neural mechanisms for visual search in macaque area V4. *Science, 308*(5721), 529-534.

Blaser, E., Pylyshyn, Z.W., & Holcombe, A.O. (2000). Tracking an object through feature space. *Nature, 408*(6809), 196-199.

Boehler, C.N., Schoenfeld, M.A., Heinze, H.-J., & Hopf, J.-M. (2011). Object-based selection of irrelevant features is not confined to the attended object. *J. Cogn. Neurosci., 23*(9), 2231-2239.

Bondarenko, R., Boehler, C.N., Stoppel, C.M., Heinze, H.-J., Schoenfeld, M.A., & Hopf, J.-M. (2012). Separable mechanisms underlying global feature-based attention. *J. Neurosci., 32*(44), 15284-15295.

Brewer, A.A., Liu, J., Wade, A.R., & Wandell, B.A. (2005). Visual field maps and stimulus selectivity in human ventral occipital cortex. *Nat. Neurosci., 8*(8), 1102-1109.

Broadbent, D.E. (1958). Perception and Communication. *Oxford: Pergamon Press.*

Brouwer, G.J., & Heeger, D.J. (2009). Decoding and reconstructing color from responses in human visual cortex. *J. Neurosci., 29*(44), 13992-14003.

Bullier, J. (2001). Feedback connections and conscious vision. *Trends Cogn. Sci., 5*(9), 369-370.

Chawla, D., Rees, G., & Friston, K.J. (1999). The physiological basis of attentional modulation in extrastriate visual areas. *Nat. Neurosci., 2*(7), 671-676.

Chelazzi, L., Miller, E.K., Duncan, J., & Desimone, R. (1993). A neural basis for visual search in inferior temporal cortex. *Nature, 363*, 345-347.

Corbetta, M., Miezin, F.M., Dobmeyer, S., Shulman, G.L., & Petersen, S.E. (1990). Attentional modulation of neural processing of shape, color, and velocity in humans. *Science, 248*(4962), 1556-1559.

Corbetta, M., Miezin, F.M., Dobmeyer, S., Shulman, G.L., & Petersen, S.E. (1991). Selective and divided attention during visual discriminations of shape, color, and speed: functional anatomy by positron emission tomography. *J. Neurosci., 11*(8), 2383-2402.

Cornwell, B.R., Carver, F.W., Coppola, R., Johnson, L., Alvarez, R., & Grillon, C. (2008). Evoked amygdala responses to negative faces revealed by adaptive MEG beamformers. *Brain Res., 1244*, 103-112.

Creutzfeldt, O.D., & Houchin, J. (1974). Neuronal basis of EEG waves. In A. Rémond (Ed.), *Handbook of Electroencephalography and Clinical Neurophysiology* (Vol. 2, pt. C, pp. 5–55): Amsterdam: Elsevier.

Crick, F. (1984). Function of the thalamic reticular complex: the searchlight hypothesis. *Proc. Natl. Acad. Sci. U. S. A., 81*(14), 4586-4590.

de Munck, J.C., van Dijk, B.W., & Spekreijse, H. (1988). Mathematical dipoles are adequate to describe realistic generators of human brain activity. *IEEE Trans. Biomed. Eng., 35*(11), 960-966.

Desimone, R., & Duncan, J. (1995). Neural mechanisms of selective visual attention. *Annu. Rev. Neurosci., 18*, 193-222.

Deutsch, J.A., & Deutsch, D. (1963). Attention: some theoretical considerations. *Psychol. Rev., 70*, 80-90.

Di Lollo, V., Enns, J.T., & Rensink, R.A. (2000). Competition for consciousness among visual events: the psychophysics of reentrant visual processes. *J. Exp. Psychol. Gen., 129*(4), 481-507.

Di Russo, F., Martínez, A., & Hillyard, S.A. (2003). Source analysis of event-related cortical activity during visuo-spatial attention. *Cereb. Cortex, 13*(5), 486-499.

Downing, C.J., & Pinker, S. (1985). The spatial structure of visual attention. In M. I. Posner & O. S. M. Marin (Eds.), *Attention and Performance XI* (pp. 171-188). Hillsdale, NJ: Erlbaum.

Downing, C.J. (1988). Expectancy and visual-spatial attention: effects on perceptual quality. *J. Exp. Psychol. Hum. Percept. Perform., 14*(2), 188-202.

Driver, J. (1996). Attention and segmentation. *The Psychologist*, 119 - 123.

Driver, J., & Baylis, G.C. (1998). Attention and visual object segmentation. In R. Parasuraman (Ed.), *The attentive brain* (pp. 299 - 325). Cambridge, MA: MIT Press.

Duncan, J. (1984). Selective attention and the organization of visual information. *J. Exp. Psychol. Gen., 113*(4), 501-517.

Duncan, J., Humphreys, G., & Ward, R. (1997). Competitive brain activity in visual attention. *Curr. Opin. Neurobiol., 7*, 255-261.

Egly, R., Driver, J., & Rafal, R.D. (1994). Shifting visual attention between objects and locations: evidence from normal and parietal lesion subjects. *J. Exp. Psychol. Gen., 123*(2), 161-177.

Elbert, T. (1993). Slow cortical potentials reflect the regulation of cortical excitability. In W. C. McCallum & S. H. Curry (Eds.), *Slow potential changes in the human brain* (pp. 235-251). New York: Plenum Press.

Engel, S.A., Glover, G.H., & Wandell, B.A. (1997). Retinotopic organization in human visual cortex and the spatial precision of functional MRI. *Cereb. Cortex, 7*, 181-192.

Eriksen, B.A., & Eriksen, C.W. (1974). Effects of noise letters upon the identification of a target letter in a nonsearch task. *Percept. Psychophys., 16*(1), 143-149.

Eriksen, C.W., & St James, J.D. (1986). Visual attention within and around the field of focal attention: a zoom lens model. *Percept. Psychophys., 40*(4), 225-240.

Fallah, M., Stoner, G.R., & Reynolds, J.H. (2007). Stimulus-specific competitive selection in macaque extrastriate visual area V4. *Proc. Natl. Acad. Sci. U. S. A., 104*(10), 4165-4169.

Folk, C.L., Remington, R.W., & Johnston, J.C. (1992). Involuntary covert orienting is contingent on attentional control settings. *J. Exp. Psychol. Hum. Percept. Perform., 18*(4), 1030-1044.

Fuchs, M., Drenckhahn, R. , Wischmann, H.A., & Wagner, M. (1998). An improved boundary element method for realistic volume-conductor modeling. *IEEE Trans. Biomed. Eng., 45*(8), 980-997.

Fuchs, M., Wagner, M., Köhler, T., & Wischmann, H.A. (1999). Linear and nonlinear current density reconstructions. *J. Clin. Neurophysiol., 16*(3), 267-295.

Gegenfurtner, K.R. (2003). Cortical mechanisms of colour vision. *Nat. Rev. Neurosci., 4*(7), 563-572.

Gibson, B.S., & Kelsey, E.M. (1998). Stimulus-driven attentional capture is contingent on attentional set for displaywide visual features. *J. Exp. Psychol. Hum. Percept. Perform., 24*(3), 699-706.

Grill-Spector, K. (2003). The neural basis of object perception. *Curr. Opin. Neurobiol., 13*(2), 159-166.

Grill-Spector, K., & Malach, R. (2004). The human visual cortex. *Annu. Rev. Neurosci., 27*, 649-677.

Guthrie, D., & Buchwald, J. S. (1991). Significance testing of difference potentials. *Psychophysiology, 28*(2), 240-244.

Hadjikhani, N., Liu, A.K., Dale, A.M., Cavanagh, P., & Tootell, R.B.H. (1998). Retinotopy and color sensitivity in human visual cortical area V8. *Nat. Neurosci., 1*(3), 235-241.

Hämäläinen, M., Hari, R., Ilmoniemi, R.J., Knuutila, J., & Lounasmaa, O.V. (1993). Magnetoencephalography - theory, instrumentation, and applications to noninvasive studies of the working human brain. *Reviews of Modern Physics, 65*(2), 413-497.

Hämäläinen, M.S., & Ilmoniemi, R.J. (1984). Interpreting measured magnetic fields of the brain: estimates of current distributions. *Technical Report TKK-F-A559, Helsinki University of Technology, Finland.*

Hämäläinen, M.S., & Sarvas, J. (1989). Realistic conductivity geometry model of the human head for interpretation of neuromagnetic data. *IEEE Trans. Biomed. Eng., 36*(2), 165-171.

Harter, M.R., & Previc, F.H. (1978). Size-specific information channels and selective attention: visual evoked potential and behavioral measures. *Electroencephalogr. Clin. Neurophysiol., 45*(5), 628-640.

Harter, M.R., & Guido, W. (1980). Attention to pattern orientation: negative cortical potentials, reaction time, and the selection process. *Electroencephalogr. Clin. Neurophysiol., 49*(5-6), 461-475.

Heinze, H.J., Mangun, G.R., Burchert, W., Hinrichs, H., Scholz, M., Münte, T.F., Gös, A., Scherg, M., Johannes, S., Hundeshagen, H., Gazzaniga, M.S., & Hillyard, S.A. (1994). Combined spatial and temporal imaging of brain activity during visual selective attention in humans. *Nature, 372*, 543-546.

Helmholtz, H. (1853). Ueber einige Gesetze der Vertheilung elektrischer Ströme in körperlichen Leitern, mit Anwendung auf die thierisch-elektrischen Versuche. *Annalen der Physik und Chemie, Pogg. Ann. 89*, 211-233, 353-377.

Hickey, C., Di Lollo, V., & McDonald, J.J. (2009). Electrophysiological indices of target and distractor processing in visual search. *J. Cogn. Neurosci., 21*(4), 760-775.

Hillebrand, A., & Barnes, G.R. (2002). A quantitative assessment of the sensitivity of whole-head MEG to activity in the adult human cortex. *Neuroimage, 16*(3 Pt A), 638-650.

Hillyard, S.A., & Münte, T.F. (1984). Selective attention to color and location: an analysis with event-related brain potentials. *Percept. Psychophys., 36*(2), 185-198.

Hillyard, S.A., & Anllo-Vento, L. (1998). Event-related brain potentials in the study of visual selective attention. *Proc. Natl. Acad. Sci. U. S. A., 95*(3), 781-787.

Hillyard, S.A., Vogel, E.K., & Luck, S.J. (1998). Sensory gain control (amplification) as a mechanism of selective attention: electrophysiological and neuroimaging evidence. *Philos. Trans. R. Soc. Lond. B Biol. Sci., 353*(1373), 1257-1270.

Hochstein, S., & Ahissar, M. (2002). View from the top: hierarchies and reverse hierarchies in the visual system. *Neuron, 36*(5), 791-804.

Hopf, J.-M., Vogel, E., Woodman, G., Heinze, H.-J., & Luck, S.J. (2002). Localizing visual discrimination processes in time and space. *J. Neurophysiol., 88*(4), 2088-2095.

Hopf, J.-M., Boelmans, K., Schoenfeld, M.A., Luck, S.J., & Heinze, H.-J. (2004). Attention to features precedes attention to locations in visual search: evidence from electromagnetic brain responses in humans. *J. Neurosci., 24*(8), 1822-1832.

Hopf, J.-M., Boehler, C.N., Luck, S.J., Tsotsos, J.K., Heinze, H.-J., & Schoenfeld, M.A. (2006). Direct neurophysiological evidence for spatial suppression surrounding the focus of attention in vision. *Proc. Natl. Acad. Sci. U. S. A., 103*(4), 1053-1058.

Houtkamp, R., & Roelfsema, P.R. (2009). Matching of visual input to only one item at any one time. *Psychol. Res., 73*(3), 317-326.

Hubbard, J.I., Llinás, R., & Quastel, D.M.J. (1969). *Electrophysiological Analysis of Synaptic Transmission.* London: Edward Arnold Ltd.

Ipata, A.E., Gee, A.L., & Goldberg, M.E. (2012). Feature attention evokes task-specific pattern selectivity in V4 neurons. *Proc. Natl. Acad. Sci. U. S. A., 109*(42), 16778-16785.

Itti, L., Koch, C., & Niebur, E. (1998). A model of saliency-based visual attention for rapid scene analysis. *IEEE Transactions on Pattern Analysis and Machine Intelligence, 20*(11), 1254–1259.

Itti, L., & Koch, C. (2001). Computational modelling of visual attention. *Nat. Rev. Neurosci., 2*(3), 194-203.

James, W. (1890). *The Principles of Psychology* (Vol. 1). New York: Henry Holt.

Jehee, J.F., Brady, D.K., & Tong, F. (2011). Attention improves encoding of task-relevant features in the human visual cortex. *J. Neurosci., 31*(22), 8210-8219.

Kanwisher, N., & Driver, J. (1992). Objects, Attributes, and Visual Attention: Which, What, and Where. *Curr. Dir. Psychol. Sci., 1*(1), 26 - 31.

Katzner, S., Busse, L., & Treue, S. (2009). Attention to the Color of a Moving Stimulus Modulates Motion-Signal Processing in Macaque Area MT: Evidence for a Unified Attentional System. *Front. Syst. Neurosci., 3*, 12.

Kenemans, J.L., Kok, A., & Smulders, F.T. (1993). Event-related potentials to conjunctions of spatial frequency and orientation as a function of stimulus parameters and response requirements. *Electroencephalogr. Clin. Neurophysiol., 88*(1), 51-63.

Koch, C., & Ullman, S. (1985). Shifts in selective visual attention: towards the underlying neural circuitry. *Hum. Neurobiol., 4*(4), 219-227.

Kourtzi, Z., & Kanwisher, N. (2000). Cortical regions involved in perceiving object shape. *J. Neurosci., 20*(9), 3310-3318.

Kristjánsson, Á. (2006). Simultaneous priming along multiple feature dimensions in a visual search task. *Vision Res., 46*(16), 2554-2570.

Lamme, V.A.F., Supèr, H., & Spekreijse, H. (1998). Feedforward, horizontal, and feedback processing in the visual cortex. *Curr. Opin. Neurobiol., 8*(4), 529-535.

Lamme, V.A.F., & Roelfsema, P.R. (2000). The distinct modes of vision offered by feedforward and recurrent processing. *Trends Neurosci., 23*(11), 571-579.

Larsson, J., & Heeger, D.J. (2006). Two retinotopic visual areas in human lateral occipital cortex. *J. Neurosci., 26*(51), 13128-13142.

Lavie, N., & Tsal, Y. (1994). Perceptual load as a major determinant of the locus of selection in visual attention. *Percept. Psychophys., 56*(2), 183-197.

Lavie, N. (1995). Perceptual load as a necessary condition for selective attention. *J. Exp. Psychol. Hum. Percept. Perform., 21*(3), 451-468.

Lavie, N., & Driver, J. (1996). On the spatial extent of attention in object-based visual selection. *Percept. Psychophys., 58*(8), 1238-1251.

Lee, B.B., Martin, P.R., & Valberg, A. (1988). The physiological basis of heterochromatic flicker photometry demonstrated in the ganglion cells of the macaque retina. *J. Physiol., 404*, 323-347.

Lee, J., & Maunsell, J.H.R. (2010). Attentional modulation of MT neurons with single or multiple stimuli in their receptive fields. *J. Neurosci., 30*(8), 3058-3066.

Ling, S., Liu, T., & Carrasco, M. (2009). How spatial and feature-based attention affect the gain and tuning of population responses. *Vision Res., 49*(10), 1194-1204.

Liu, L., Ioannides, A.A., & Streit, M. (1999). Single trial analysis of neurophysiological correlates of the recognition of complex objects and facial expressions of emotion. *Brain Topogr., 11*(4), 291-303.

Liu, T., Stevens, S.T., & Carrasco, M. (2007). Comparing the time course and efficacy of spatial and feature-based attention. *Vision Res., 47*(1), 108-113.

Liu, T., & Hou, Y. (2011). Global feature-based attention to orientation. *J. Vis., 11*(10):8, 1-8.

Liu, T., & Mance, I. (2011). Constant spread of feature-based attention across the visual field. *Vision Res., 51*(1), 26-33.

Liu, T., Becker, M.W., & Jigo, M. (2013). Limited featured-based attention to multiple features. *Vision Res., 85*, 36-44.

Lorente de Nó, Rafael. (1947). Action potential of the motoneurons of the hypoglossus nucleus. *J. Cell. Comp. Physiol., 29*(3), 207-287.

Luck, S.J., Chelazzi, L., Hillyard, S.A., & Desimone, R. (1997). Neural mechanisms of spatial selective attention in areas V1, V2, and V4 of macaque visual cortex. *J. Neurophysiol., 77*(1), 24-42.

Luck, S.J., & Vogel, E.K. (1997). The capacity of visual working memory for features and conjunctions. *Nature, 390*(6657), 279-281.

Luck, S.J. (2005). *An Introduction to the Event-Related Potential Technique*. Cambridge, MA: The MIT Press.

MacKay, D.G. (1973). Aspects of the theory of comprehension, memory and attention. *Q. J. Exp. Psychol., 25*(1), 22-40.

Makeig, S., Bell, A.J., Jung, T.-P., & Sejnowski, T.J. (1996). Independent component analysis of electroencephalographic data. In D. Touretzky, M. Mozer & M. Hasselmo (Eds.), *Adv. Neural Inf. Process. Syst.* (Vol. 8, pp. 145-151). Cambridge, MA: MIT Press.

Maljkovic, V., & Nakayama, K. (1994). Priming of pop-out: I. Role of features. *Mem. Cognit., 22*(6), 657-672.

Mangun, G.R., Hansen, J.C., & Hillyard, S.A. (1987). The spatial orienting of attention: Sensory facilitation or response bias? In R. Johnson, Jr., J. W. Rohrbaugh & R. Parasuraman (Eds.), *Current Trends in Event-Related Potential Research* (pp. 118-124). Amsterdam: Elsevier.

Mangun, G.R., & Hillyard, S.A. (1991). Modulations of sensory-evoked brain potentials indicate changes in perceptual processing during visual-spatial priming. *J. Exp. Psychol. Hum. Percept. Perform., 17*(4), 1057-1074.

Mangun, G.R. (1995). Neural mechanisms of visual selective attention. *Psychophysiology, 32*(1), 4-18.

Mangun, G.R., Hopfinger, J.B., Kussmaul, C.L., Fletcher, E.M., & Heinze, H.-J. (1997). Covariations in ERP and PET measures of spatial selective attention in human extrastriate visual cortex. *Hum. Brain Mapp., 5*(4), 273-279.

Martínez, A., Teder-Sälejärvi, W., Vazquez, M., Molholm, S., Foxe, J.J., Javitt, D.C., Di Russo, F., Worden, M.S., & Hillyard, S.A. (2006). Objects are highlighted by spatial attention. *J. Cogn. Neurosci., 18*(2), 298-310.

Martinez-Trujillo, J.C., & Treue, S. (2004). Feature-based attention increases the selectivity of population responses in primate visual cortex. *Curr. Biol., 14*(9), 744-751.

Maunsell, J.H.R., & Treue, S. (2006). Feature-based attention in visual cortex. *Trends Neurosci., 29*(6), 317-322.

McAdams, C.J., & Maunsell, J.H.R. (2000). Attention to both space and feature modulates neuronal responses in macaque area V4. *J. Neurophysiol., 83*(3), 1751-1755.

McKeefry, D.J., & Zeki, S. (1997). The position and topography of the human colour centre as revealed by functional magnetic resonance imaging. *Brain, 120*(12), 2229-2242.

Mehta, A.D., Ulbert, I., & Schroeder, C.E. (2000a). Intermodal selective attention in monkeys. I: distribution and timing of effects across visual areas. *Cereb. Cortex, 10*(4), 343-358.

Mehta, A.D., Ulbert, I., & Schroeder, C.E. (2000b). Intermodal selective attention in monkeys. II: physiological mechanisms of modulation. *Cereb. Cortex, 10*(4), 359-370.

Melcher, D., Papathomas, T.V., & Vidnyánszky, Z. (2005). Implicit attentional selection of bound visual features. *Neuron, 46*(5), 723-729.

Moher, J., Lakshmanan, B.M., Egeth, H.E., & Ewen, J.B. (2014). Inhibition drives early feature-based attention. *Psychol. Sci., 25*(2), 315-324.

Moore, C.M., & Egeth, H. (1998). How does feature-based attention affect visual processing? *J. Exp. Psychol. Hum. Percept. Perform., 24*(4), 1296-1310.

Moore, C.M., Yantis, S., & Vaughan, B. (1998). Object-based visual selection: Evidence from perceptual completion. *Psychol. Sci., 9*(2), 104-110.

Moran, J., & Desimone, R. (1985). Selective attention gates visual processing in the extrastriate cortex. *Science, 229*(4715), 782-784.

Motter, B.C. (1994). Neural correlates of attentive selection for color or luminance in extrastriate area V4. *J. Neurosci., 14*(4), 2178-2189.

Müller, M.M., Teder-Sälejärvi, W., & Hillyard, S.A. (1998). The time course of cortical facilitation during cued shifts of spatial attention. *Nat. Neurosci., 1*(7), 631-634.

Murakami, S., & Okada, Y. (2006). Contributions of principal neocortical neurons to magnetoencephalography and electroencephalography signals. *J. Physiol., 575*(3), 925-936.

Nicoletti, R., Anzola, G.P., Luppino, G., Rizzolatti, G., & Umiltà, C. (1982). Spatial compatibility effects on the same side of the body midline. *J. Exp. Psychol. Hum. Percept. Perform., 8*(5), 664-673.

Nicoletti, R., Umiltà, C., & Ladavas, E. (1984). Compatibility due to the coding of the relative position of the effectors. *Acta Psychol. (Amst.), 57*(2), 133-143.

Nicoletti, R., & Umiltà, C. (1994). Attention shifts produce spatial stimulus codes. *Psychol. Res., 56*(3), 144-150.

Niebur, E., & Koch, C. (1996). Control of selective visual attention: modeling the "where" pathway. In D. S. Touretzky, M. C. Mozer & M. E. Hasselmo (Eds.), *Adv. Neural Inf. Process. Syst.* (Vol. 8, pp. 802-808). Cambridge, MA: MIT Press.

Norman, D.A. (1968). Toward a theory of memory and attention. *Psychol. Rev., 75*, 522-536.

Nunez, P.L. (1981). *Electric fields of the brain: The neurophysics of EEG* (1st ed.). New York: Oxford University Press.

O'Craven, K.M., Rosen, B.R., Kwong, K.K., Treisman, A., & Savoy, R.L. (1997). Voluntary attention modulates fMRI activity in human MT-MST. *Neuron, 18*(4), 591-598.

O'Craven, K.M., Downing, P.E., & Kanwisher, N. (1999). fMRI evidence for objects as the units of attentional selection. *Nature, 401*(6753), 584-587.

Okada, Y.C. (1982). Neurogenesis of evoked magnetic fields. In S. J. Williamson, G.-L. Romani, L. Kaufman & I. Modena (Eds.), *Biomagnetism: an interdisciplinary approach* (pp. 399-408). New York and London: Plenum Press.

Onton, J., & Makeig, S. (2006). Information-based modeling of event-related brain dynamics. *Prog. Brain Res., 159*, 99-120.

Pascual-Marqui, R.D. (2002). Standardized low-resolution brain electromagnetic tomography (sLORETA): technical details. *Methods Find. Exp. Clin. Pharmacol., 24*(Suppl. D), 5-12.

Posner, M.I. (1980). Orienting of attention. *Q. J. Exp. Psychol., 32*(1), 3-25.

Posner, M.I., Snyder, C.R., & Davidson, B.J. (1980). Attention and the detection of signals. *J. Exp. Psychol., 109*(2), 160-174.

Posner, M.I., & Cohen, Y. (1984). Components of visual orienting. In H. Bouma & D. G. Bouwhuis (Eds.), *Attention and performance X* (pp. 531-556). Hillsdale, N.J.: Lawrence Erlbaum Associates.

Regan, D. (1989). The Visual Pathway *Human brain electrophysiology: Evoked potentials and evoked magnetic fields in science and medicine* (pp. 302-470). New York: Elsevier Science Publishing Co., Inc.

Remington, R., & Pierce, L. (1984). Moving attention: evidence for time-invariant shifts of visual selective attention. *Percept. Psychophys., 35*(4), 393-399.

Reynolds, J.H., Chelazzi, L., & Desimone, R. (1999). Competitive mechanisms subserve attention in macaque areas V2 and V4. *J. Neurosci., 19*(5), 1736-1753.

Reynolds, J.H., & Chelazzi, L. (2004). Attentional modulation of visual processing. *Annu. Rev. Neurosci., 27*, 611-647.

Ribary, U., Ioannides, A.A., Singh, K.D., Hasson, R., Bolton, J.P.R., Lado, F., Mogilner, A., & Llinás, R. (1991). Magnetic field tomography of coherent thalamocortical 40-Hz oscillations in humans. *Proc. Natl. Acad. Sci. U. S. A., 88*(24), 11037-11041.

Riggs, L., Moses, S.N., Bardouille, T., Herdman, A.T., Ross, B., & Ryan, J.D. (2009). A complementary analytic approach to examining medial temporal lobe sources using magnetoencephalography. *Neuroimage, 45*(2), 627-642.

Robinson, S.E. (1989). Environmental noise cancellation for biomagnetic measurements. In S. J. Williamson, M. Hoke, G. Stroink & M. Kotani (Eds.), *Advances in Biomagnetism* (pp. 721-724). New York: Plenum Press.

Roelfsema, P.R., Lamme, V.A.F., & Spekreijse, H. (1998). Object-based attention in the primary visual cortex of the macaque monkey. *Nature, 395*(6700), 376-381.

Rossi, A.F., & Paradiso, M.A. (1995). Feature-specific effects of selective visual attention. *Vision Res., 35*(5), 621-634.

Saenz, M., Buracas, G.T., & Boynton, G.M. (2002). Global effects of feature-based attention in human visual cortex. *Nat. Neurosci., 5*(7), 631-632.

Sàenz, M., Buracas, G.T., & Boynton, G.M. (2003). Global feature-based attention for motion and color. *Vision Res., 43*(6), 629-637.

Sarvas, J. (1987). Basic mathematical and electromagnetic concepts of the biomagnetic inverse problem. *Phys. Med. Biol., 32*(1), 11-22.

Sawaki, R., & Luck, S.J. (2010). Capture versus suppression of attention by salient singletons: electrophysiological evidence for an automatic attend-to-me signal. *Atten. Percept. Psychophys., 72*(6), 1455-1470.

Sawaki, R., & Luck, S.J. (2011). Active suppression of distractors that match the contents of visual working memory. *Vis. cogn., 19*(7), 956-972.

Schoenfeld, M.A., Tempelmann, C., Martinez, A., Hopf, J.-M., Sattler, C., Heinze, H.-J., & Hillyard, S.A. (2003). Dynamics of feature binding during object-selective attention. *Proc. Natl. Acad. Sci. U. S. A., 100*(20), 11806-11811.

Schoenfeld, M.A., Hopf, J.-M., Merkel, C., Heinze, H.-J., & Hillyard, S.A. (2014). Object-based attention involves the sequential activation of feature-specific cortical modules. *Nat. Neurosci., 17*(4), 619-624.

Scholl, B.J. (2001). Objects and attention: the state of the art. *Cognition, 80*(1-2), 1-46.

Serences, J.T., & Boynton, G.M. (2007). Feature-based attentional modulations in the absence of direct visual stimulation. *Neuron, 55*(2), 301-312.

Sereno, M.I., Dale, A.M., Reppas, J.B., Kwong, K.K., Belliveau, J.W., Brady, T.J., Rosen, B.R., & Tootell, R.B. (1995). Borders of multiple visual areas in humans revealed by functional magnetic resonance imaging. *Science, 268*(5212), 889-893.

Shih, S.-I., & Sperling, G. (1996). Is there feature-based attentional selection in visual search? *J. Exp. Psychol. Hum. Percept. Perform., 22*(3), 758-779.

Shulman, G.L., Remington, R.W., & McLean, J.P. (1979). Moving attention through visual space. *J. Exp. Psychol. Hum. Percept. Perform., 5*(3), 522-526.

Sohn, W., Chong, S.C., Papathomas, T.V., & Vidnyánszky, Z. (2005). Cross-feature spread of global attentional modulation in human area MT+. *Neuroreport, 16*(12), 1389-1393.

Spratling, M.W., & Johnson, M.H. (2004). A feedback model of visual attention. *J. Cogn. Neurosci., 16*(2), 219-237.

Stoppel, C.M., Boehler, C.N., Strumpf, H., Krebs, R.M., Heinze, H.-J., Hopf, J.-M., & Schoenfeld, M.A. (2012). Spatiotemporal dynamics of feature-based attention spread: evidence from combined electroencephalographic and magnetoencephalographic recordings. *J. Neurosci., 32*(28), 9671-9676.

Tesche, C.D. (1997). Non-invasive detection of ongoing neuronal population activity in normal human hippocampus. *Brain Res., 749*(1), 53-60.

Theeuwes, J. (2013). Feature-based attention: it is all bottom-up priming. *Philos. Trans. R. Soc. Lond. B Biol. Sci., 368*(1628), 20130055.

Timmermann, L., Gross, J., Dirks, M., Volkmann, J., Freund, H.-J., & Schnitzler, A. (2003). The cerebral oscillatory network of parkinsonian resting tremor. *Brain, 126*(1), 199-212.

Tootell, R.B.H., Hadjikhani, N., Hall, E.K., Marrett, S., Vanduffel, W., Vaughan, J.T., & Dale, A.M. (1998). The retinotopy of visual spatial attention. *Neuron, 21*(6), 1409-1422.

Treisman, A.M. (1969). Strategies and models of selective attention. *Psychol. Rev., 76*(3), 282-299.

Treue, S., & Martínez Trujillo, J.C. (1999). Feature-based attention influences motion processing gain in macaque visual cortex. *Nature, 399*(6736), 575-579.

Treue, S., & Maunsell, J.H.R. (1999). Effects of attention on the processing of motion in macaque middle temporal and medial superior temporal visual cortical areas. *J. Neurosci., 19*(17), 7591-7602.

Tsotsos, J.K. (2011). *A Computational Perspective on Visual Attention.* Cambridge, MA: The MIT Press.

Valdes-Sosa, M., Cobo, A., & Pinilla, T. (1998). Transparent motion and object-based attention. *Cognition, 66*(2), B13-B23.

Van Essen, D.C. (2004). Organization of visual areas in macaque and human cerebral cortex. In L. M. Chalupa & J. S. Werner (Eds.), *The Visual Neurosciences* (Vol. 1, pp. 507–521). Cambridge, MA: MIT Press.

van Veen, V., Cohen, J.D., Botvinick, M.M., Stenger, V.A., & Carter, C.S. (2001). Anterior cingulate cortex, conflict monitoring, and levels of processing. *Neuroimage, 14*(6), 1302-1308.

Van Veen, V., & Carter, C.S. (2002). The timing of action-monitoring processes in the anterior cingulate cortex. *J. Cogn. Neurosci., 14*(4), 593-602.

Vaughan, H.G., Jr. (1969). The relationship of brain activity to scalp recordings of event-related potentials. In E. Donchin & D. B. Lindsley (Eds.), *Average Evoked Potentials: Methods, Results, and Evaluations* (pp. 45-75). Washington, D.C.: U.S. Government Printing Office.

Vogel, E.K., & Luck, S.J. (2000). The visual N1 component as an index of a discrimination process. *Psychophysiology, 37*(2), 190-203.

Volkmann, J., Joliot, M., Mogilner, A., Ioannides, A.A., Lado, F., Fazzini, E., Ribary, U., & Llinás, R. (1996). Central motor loop oscillations in parkinsonian resting tremor revealed by magnetoencephalography. *Neurology, 46*(5), 1359-1370.

von Helmholtz, H. (1896). *Handbuch der Physiologischen Optik.* Hamburg und Leipzig: Verlag von Leopold Voss.

Wade, A., Augath, M., Logothetis, N., & Wandell, B. (2008). fMRI measurements of color in macaque and human. *J. Vis., 8*(10):6, 1-19.

Wade, A.R., Brewer, A.A., Rieger, J.W., & Wandell, B.A. (2002). Functional measurements of human ventral occipital cortex: retinotopy and colour. *Philos. Trans. R. Soc. Lond. B Biol. Sci., 357*(1424), 963-973.

Wandell, B.A., Dumoulin, S.O., & Brewer, A.A. (2007). Visual field maps in human cortex. *Neuron, 56*(2), 366-383.

Wannig, A., Rodríguez, V., & Freiwald, W.A. (2007). Attention to surfaces modulates motion processing in extrastriate area MT. *Neuron, 54*(4), 639-651.

Weber, T.A., Kramer, A.F., & Miller, G.A. (1997). Selective processing of superimposed objects: an electrophysiological analysis of object-based attentional selection. *Biol. Psychol., 45*(1-3), 159-182.

Weissman, D.H., Giesbrecht, B., Song, A.W., Mangun, G.R., & Woldorff, M.G. (2003). Conflict monitoring in the human anterior cingulate cortex during selective attention to global and local object features. *Neuroimage, 19*(4), 1361-1368.

White, A.L., & Carrasco, M. (2011). Feature-based attention involuntarily and simultaneously improves visual performance across locations. *J. Vis., 11*(6):15, 1-10.

Wijers, A.A., Lamain, W., Slopsema, J.S., Mulder, G., & Mulder, L.J.M. (1989). An electrophysiological investigation of the spatial distribution of attention to colored stimuli in focused and divided attention conditions. *Biol. Psychol., 29*(3), 213-245.

Wolfe, J.M., & Horowitz, T.S. (2004). What attributes guide the deployment of visual attention and how do they do it? *Nat. Rev. Neurosci., 5*(6), 495-501.

Yamamoto, T., Williamson, S.J., Kaufman, L., Nicholson, C., & Llinás, R. (1988). Magnetic localization of neuronal activity in the human brain. *Proc. Natl. Acad. Sci. U. S. A., 85*(22), 8732-8736.

Yeung, N., Botvinick, M.M., & Cohen, J.D. (2004). The neural basis of error detection: conflict monitoring and the error-related negativity. *Psychol. Rev., 111*(4), 931-959.

Zeki, S., Watson, J.D.G., Lueck, C.J., Friston, K.J., Kennard, C., & Frackowiak, R.S.J. (1991). A direct demonstration of functional specialization in human visual cortex. *J. Neurosci., 11*(3), 641-649.

Zhang, W., & Luck, S.J. (2009). Feature-based attention modulates feedforward visual processing. *Nat. Neurosci., 12*(1), 24-25.

Zimmerman, J.E., Thiene, P., & Harding, J.T. (1970). Design and operation of stable rf-biased superconducting point-contact quantum devices, and a note on the properties of perfectly clean metal contacts. *J. Appl. Phys., 41*, 1572-1580.

Zirnsak, M., & Hamker, F.H. (2010). Attention alters feature space in motion processing. *J. Neurosci., 30*(20), 6882-6890.

Mandy Bartsch

Hellestr. 2

39112 Magdeburg

Erklärung

Hiermit erkläre ich, dass ich die von mir eingereichte Dissertation zu dem Thema

"**Determinants of global color-based attention: insights
from electromagnetic brain recordings in humans**"

selbständig verfasst, nicht schon als Dissertation verwendet habe und die benutzten Hilfsmittel und Quellen vollständig angegeben wurden.

Weiterhin erkläre ich, dass ich weder diese noch eine andere Arbeit zur Erlangung des akademischen Grades *doctor rerum naturalium* (Dr. rer. nat.) an anderen Einrichtungen eingereicht habe.

Magdeburg, den 15.12.2014

_____

(Mandy Bartsch)